EXPERIMENTAL STUDY ON THE MOBILITY OF LIGHTWEIGHT VEHICLES ON SAND

by

Marilyn Elizabeth Worley

Thesis submitted to the Faculty of the Virginia Polytechnic Institute and State University in partial fulfillment of the requirements for the degree of Master of Science in Mechanical Engineering

Approved:

Corina Sandu, Chairperson

Dennis Hong

J.P. Morgan

29 June 2007

Blacksburg, Virginia

Keywords: Lightweight vehicles, robotic ground vehicles, novel locomotion, mobility, off-road vehicle performance, coastal terrain

EXPERIMENTAL STUDY ON THE MOBILITY OF LIGHTWEIGHT VEHICLES ON SAND

by

Marilyn E. Worley

Corina Sandu, Chairperson
Mechanical Engineering

Abstract

This study focuses on developing a better comprehension of the mobility of lightweight autonomous vehicles with varying locomotion platforms on sand. This research involves four segments.

The first segment is a review of military criteria for the development of lightweight unmanned ground vehicles, followed by a review a review of current methodologies for evaluating the terramechanic (vehicle-ground interaction) mobility measures of heavyweight wheeled and tracked vehicles, and ending with a review of the defining properties of deformable terrain with specific emphasis on sand. These present a basis for understanding what currently defines mobility and how mobility is quantified for traditional heavyweight wheeled and tracked vehicles, as well as an understanding of the environment of operation (sandy terrain) for the lightweight vehicles in this study.

The second segment involves the identification of key properties associated with the mobility and operation of lightweight vehicles on sand as related to given mission criteria, so as to form a quantitative assessment system to compare lightweight vehicles of varying locomotion platforms. A table based on the House of Quality shows the relationships—high, low, or adverse—between mission profile requirements and general performance measures and geometries of vehicles under consideration for use. This table,

when combined with known values for vehicle metrics, provides information for an index formula used to quantitatively compare the mobility of a user-chosen set of vehicles, regardless of their methods of locomotion. This table identifies several important or fundamental terramechanics properties that necessitate model development for robots with novel locomotion platforms and testing for lightweight wheeled and tracked vehicles so as to consider the adaptation of counterpart heavyweight terramechanics models for use.

The third segment is a study of robots utilizing novel forms of locomotion, emphasizing the kinematics of locomotion (gait and foot placement) and proposed starting points for the development of terramechanics models so as to compare their mobility and performance with more traditional wheeled and tracked vehicles. In this study several new autonomous vehicles—bipedal, self-excited dynamic tripedal, active spoke-wheel—that are currently under development are explored.

The final segment involves experimentation of several lightweight vehicles and robots on sand. A preliminary experimentation was performed evaluating a lightweight autonomous tracked vehicle for its performance and operation on sand. A bipedal robot was then tested to study the foot-ground interaction with and sinkage into a medium-grade sand, utilizing a one of the first-developed walking gaits. Finally, a comprehensive set of experiments was performed on a lightweight wheeled vehicle. While the terramechanics properties of wheeled and tracked vehicles, such as the contact patch pressure distribution, have been understood and models have been developed for heavy vehicles, the feasibility of extrapolating them to the analysis of light vehicles is still under analysis. A wheeled all-terrain vehicle was tested for effects of sand gradation, vehicle speed, and vehicle payload on measures of pressure and sinkage in the contact patch, and preliminary analysis is presented on the sinkage of the wheeled all-terrain vehicle.

These four segments—review of properties of sandy terrain and measures of and criteria for the mobility of lightweight vehicles operating on sandy terrain, the development of the comparison matrix and indexing function, modeling and development of novel forms of locomotion, and physical experimentation of lightweight tracked and wheeled vehicles

as well as a bipedal robot—combine to give an overall picture of mobility that spans across different forms of locomotion.

Acknowledgments

This project was partially sponsored by the United States Office of Naval Research.

Thank you to Dr. Corina Sandu, for being the best advisor I could have ever hoped for: To whom no question was to simple, no problem to big, and no phone call too late, including one at 4:00am when I locked myself out of the office.

Thank you to Dr. Dennis Hong, for supplying the robotic knowledge and the MAC-based encouragement, to Ping Ren for his assistance in the development of the Mobility Metrics Matrix, and to Dr. J.P. Morgan for all of the experiment design and statistical analysis assistance, not to mention putting up with the last-minute changes.

Special thanks to the members of my CVeSS family:

To those who froze in the field studies in Winter 2006, and worked under the blazing sun with the imminent threat of lightening in Spring/Summer 2007 including (in no particular order): Brent Ballew (fo' shizzle), Sarah O'Neil (who never wants to see sand again), Sturges Wheeler, Ray Craft, Jon Ziegenmeyer, Erin Hissong (who loves sand), Lin Li (who can really drive), Brendan Chan (who will always at least try to know a little more than me, and most often succeeds), Jenn Steets (who took breaks with me between countless hours of thesophizing), Emmanuel Blanchard (who always jumps off the high rocks), Brian Templeton (who makes great bread), and Mohammad Rastgaar (who now knows the meaning of "schmooze").

To Florin Marcu for his countless and tireless efforts to keep the office running, and for teaching me how to ski.

To the faculty of CVeSS, including Dr. Mehdi Ahmadian, Dr. John Ferris (for letting me slack on grading when needed), and Dr. Steve Southward, who all taught me more than I ever wanted to know.

To the folks in Danville including Shannon, Josh, Scott for good times at Pigs in the Park and SPIE in Orlando.

To Jeff Biggans and Brian Southern for their supply of and lessons in driving the ATVs used for this study, and for the eggs and pool games, respectively.

To Sue Teel and Charlie Weil, without whom nothing could have possibly gone right.

I am very proud to be a part of this lab. I wish I could be Social Director forever.

Thanks to members of JOUSTER for their support and loan of MATILDA and pretty much everything else used in the field, specifically Shane Barnett, Jon Weekly, and Ruel Faruque. Thanks to Karl Muecke and Mark Showalter for their assistance in tests of robots under development in RoMeLa.

Thanks to the PhD comic strip, for getting graduate life in engineering completely right.

Thanks to Dr. Thomas L. Brandon and Dr. Naraine Persaud for their assistance in understanding the complexities of sand.

Thanks to my awesome roommies Maggie Headly (for always being ready with a hug), and Ellery Hanlin (for amazing me on a regular basis and with an awesome laugh), for the laughs, for the cool furniture I got to use, for putting up with me when I got stressed, and for taking me out when I needed it!

Thanks to the future Dr. Megan Stobart for being a million times better than WebMD.com, and the countless Pokie Sticks consumed throughout our friendship thusfar.

Thanks to Bekah Macko for teaching me how to make llamas with my hand, for never making me feel more insane than necessary, and for smacking me with common sense when I needed some.

Thanks to Katherine Eriksson for making me smarter by association, for ranting with me when needed, and for being an awesome friend for the past six years.

Thanks to Jon Ziegenmeyer, for making sure that I ate and slept and exercised when I otherwise might have forgotten to, for taking me out to the mountains for some clarity, and for keeping me laughing, sane, happy and supported. Always worth the 250-mile round-trip.

Dedicated to my parents, Sue and Craig Worley, for their endless encouragement and undergraduate tuition payments, and my sister Jenn, for going through all of this first and providing me with advice and comic relief.

TABLE OF CONTENTS

LIST OF FIGURES AND TABLES

1 INTRODUCTION

Vehicle mobility is defined by the Department of Defense as the "overall capacity of a vehicle to move from place to place while retaining its ability to perform its primary mission" [1]. Traditionally, the term has been used to assess the capability of a manned ground vehicle, with predilection for large wheeled or tracked military vehicles. Several semi-empirical methods have been developed to analyze the mobility of such vehicles, for example Bekker's methodology [2-4] and the Cone Penetrometer Technique [5]. With the recent development of lightweight military and space exploration ground vehicles, and vehicles that use new locomotion strategies including legs and spoke-wheels, the meaning of vehicle mobility must be viewed in a larger context, and the evaluation tools have to be expanded.

This study focuses on analyzing the mobility of lightweight ground vehicles that use different means of locomotion on sand. An overview of the research elements involved in this analysis is illustrated in Figure 1-1. This study investigates the mobility of four categories of autonomous ground vehicles, as defined by the vehicle locomotion method: Vehicles are categorized as wheeled, tracked, legged, or spoke-wheeled. The challenges in evaluating the mobility of these vehicles stem from the characteristics of the soil and terrain profile, vehicle performance during obstacle negotiation maneuvers, operational environmental conditions, insufficient experimental data to evaluate performance metrics, and the availability of vehicles that use legs or spoke-wheels for modeling and testing. Existing methods to predict the mobility of heavy vehicles cannot be directly applied to light/robotic vehicles or vehicles that use alternative locomotion methods such as legs or spoke-wheels. Moreover, the task to compare the mobility of two vehicles from different categories is hampered by the lack of common applicable evaluation criteria.

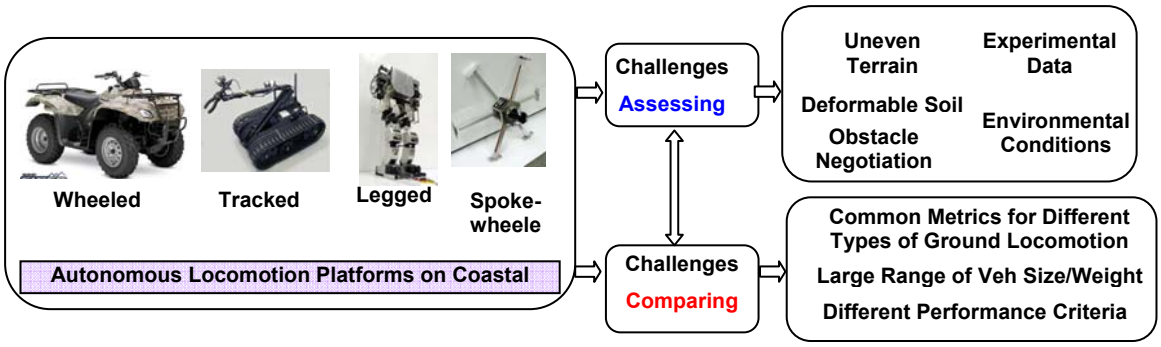

Figure 1-1: Research Components for Lightweight Vehicle Locomotion on Coastal Terrain

The work presented in this thesis started as part of a project for the United States Office of Naval Research to analyze the mobility of unmanned ground vehicles on coastal terrain.

1.1 Motivation

Robotic technology in development today often is focused on the development of vehicles suited for dull, dirty and dangerous missions. From scientific exploration of remote areas of land difficult for humans to traverse, to military missions presenting safety threats to personnel, to rescue missions deep into mines or otherwise unstable lands, to planetary exploration, construction and soil sampling, the need for mobile lightweight vehicle technology with special emphasis on off-road conditions is great. In order to frame the development of this technology, a basic level of understanding of the things that define and the challenges presented in assessing off-road mobility of lightweight vehicles is needed.

1.2 Objectives

The objectives of the present work are to: (1) Identify a common set of metrics that will allow a quantitative comparison of the mobility of legged, wheeled, and tracked vehicles on coastal terrain. (2) Evaluate the use of alternative locomotion platforms that make discontinuous contact with the surface such as such as legged or spoke-wheeled vehicles. (3) Study the interaction of each vehicle with the coastal terrain and analyze basic parameters essential for the mobility of each category of vehicle. Due to limited

availability of lightweight tracked, legged and spoke-wheeled vehicles, the experimental study concentrated on lightweight wheeled vehicles.

1.3 Research Approach

The research for this study was conducted in the theoretical formation of a system to compare lightweight autonomous vehicles on sand, and in the practical experimentation of different vehicles on sand, with a particularly detailed study of lightweight wheeled vehicles under different speed and payload requirements and on dry and wet sand.

Important mission performance parameters were identified for lightweight autonomous ground vehicles were identified using military standards. Elements of current heavyweight models for traditional wheeled and tracked vehicle terrain interaction characteristics were reviewed to select appropriate vehicle design and vehicle-ground interaction parameters connected to important mission parameters. Strength characteristics of sand were studied to identify potential mission environments, as well as assist in the setup and later interpretation of results of experimental work. The combination of these three literature studies presented the basis for the formation of the Mobility Metrics Matrix (MMM), used to quantitatively compare vehicles on their expected performance of mission parameters.

To study the development of robots with novel locomotion platforms, such as bipedal, tripedal, and spoke-wheeled, prototypes for three robots under development in the Robotics & Mechanisms Laboratory (RoMeLa) in the Department of Mechanical Engineering at Virginia Tech were observed for properties in or related to vehicle parameters in the MMM. Specific emphasis was placed on the foot shape and expected ground interaction.

Preliminary tests were conducted in this study to further the understanding of vehicle-ground interaction for a lightweight tracked vehicle and a bipedal walking robot. Tests conducted on the lightweight tracked vehicle were performed using an experiment design that was left incomplete due to vehicle damage, however observational analysis was performed. An observational study was also performed for the bipedal walking robot to

test the form and synthesis of the foot-ground interaction, the sinkage into the sand, and the maximum speeds moving across the sand.

The most in-depth experimentation was done on a lightweight wheeled vehicle to study the effect of sand moisture, sand grain size, vehicle speed, and vehicle payload on the sinkage into the sand, and on elements of vehicle sinkage into the ground and of the pressure distribution in the contact patch of the sand. This study was done in two phases. The first phase involved preliminary testing using an experiment design concurrent with that of the lightweight tracked vehicle, performed on dry sand only. This first study provided guidance for the revisions of procedures and the experimental setting for a more in-depth study involving a larger quantity of data collection taken under a new experiment design, adapted for two levels of sand moisture content. Data from this study was statistically analyzed to reveal the relative importance of each parameter on the response variables of sinkage and elements of pressure distribution in the contact patch.

One last experiment was performed on the lightweight wheeled vehicle to partially mimic a common multiple-pass experiment used to assess the mobility of traditional manned, heavyweight wheeled vehicles. This data is presented with comments on trends in the sinkage of the vehicle and the elements of the pressure distribution in the contact patch over the course of 100 runs across the sand (running over the same tracks.)

1.4 Summary of Chapters

Chapter 2 presents a review of literature on the topics of current models for vehicle/ground interaction of traditional heavyweight wheeled and tracked vehicles, current systems in use to assess mobility, and classification of sand.

Chapter 3 presents the development and proposed use of the Mobility Metrics Matrix (MMM). The matrix of mobility metrics identifies pertinent measurable mobility performance criteria to form an assessment tool to compare vehicles of different locomotion platforms for their mission suitability.

Chapters 4-7 present the study of different locomotion platforms including novel locomotion platforms currently in the development/prototyping stage and traditional wheeled and tracked vehicles.

Chapter 4 presents the technology development of robots with alternative locomotion platforms. The locomotion platform, walking mechanism and foot specification of each robot is presented. By examination of the shape of the robot feet and proposed ground interaction paths, preliminary directions for future foot-ground interaction are presented.

Chapter 5 discusses the design of experiments for the four sets of tests performed for this study. Descriptions of the experiment objectives, the parameters varied and studied in the tests, and the sampling methodologies for data collection are presented. In each of these tests vehicle-ground interaction parameters were studied.

Chapter 6 describes the main equipment used during the primary vehicle tests, the physical experiment sites and field conditions, and the daily operations for data collection. This chapter serves as a record of actions taken during the testing and a manual for future work.

Chapter 7 presents the qualifications and quantifications of the results found from the experiments on lightweight tracked and wheeled vehicles, as well as those tests performed on the prototype of a bipedal robot as a part of the preliminary study of the performance of robots with novel locomotion platforms.

Chapter 8 presents a summary of the work completed in this study as well as recommendations for future work.

2 REVIEW OF LITERATURE

The review of literature focuses on current models for vehicle/ground interaction of traditional heavyweight wheeled and tracked vehicles, current systems in use to assess vehicle mobility, and classification of sand.

2.1 Military Criteria for the Development of Unmanned Ground Vehicles

The United States Marine Corps Tactical Unmanned Ground Vehicle (TUGV) Desired Operational Characteristics, rev. 2001, provides standards for TUGV mobility measures. TUGVs must be designed for operations such as information or package delivery, reconnaissance and rescue where mission profiles are estimated to include 50% of robot operation time traveling cross-country at speeds of 0-6mh with sprints up to 12mph in a range of operating conditions including temperatures ranging from -25 degrees Fahrenheit to 125 degrees Fahrenheit.

Mission Essential Functions, or MEFs, define the basic characteristics that are required for military robotic development. Besides the aforementioned speeds, there are standards for vertical obstacle negotiation of 16 inches (threshold) and 24 inches (objective), a turning radius of 3 meters (threshold), payload capacities of 150lbs (threshold) and 300lbs (objective), ground inclination climbing abilities of 40% slide-slopes (threshold) and 60% up/down slopes (threshold). One more notable MEF is the level ground composition standard stating that a TUGV must be able to operate on 12 inches of mud, snow, or sand [6].

2.2 Measures of and Current Systems in Use to Assess Mobility of Traditional Heavyweight Vehicles

Three predominant vehicle-ground interaction assessment systems exist in order to predict the performance of heavyweight vehicles operating on off-road conditions. Bekker's Derived Terramechanics Model (BDTM) relates important vehicle-ground interaction parameters through seven empirically defined soil strength properties, providing the basis to predict vehicle performance and traction characteristics on soil [2-4, 7, 8]. The Cone Index, a single measure of soil strength, is utilized to characterize the

soil for the NATO Reference Mobility Model (software used to predict on- and off-road vehicle performance on a go/no go basis) and to use with the vehicle Mobility Index to predict the performance potential of vehicles [5, 9]. Lastly, finite element methods examine the soil on a microscopic level in order to study vehicle-ground interaction. These first two methods are reviewed briefly in this study.

Bekker's Derived Terramechanics Model, developed in the 1960's by M.G. Bekker, involves semi-empirical (partly based on scientific law, and partly from observational data) relationships to characterize the vehicle-ground interaction. BDTM involves the pressure-sinkage relationship existing in the vehicle-ground contact patch, and the slip-shear phenomenon experienced during vehicle operation.

The BDTM pressure-sinkage relationship uses two soil properties, k_ϕ as related to the frictional properties of the soil and k_c as related to the cohesive properties of the soil, to define the relationship between normal pressure p exerted by the vehicle and the sinkage depth z as

$$p = \left(\frac{k_c}{b} + k_\phi \right) z^n \tag{1.1}$$

where k_ϕ and k_c must be found empirically, and b is a measurement of the characteristic length of the wheel or track geometry.

The slip-shear relationship, formulating the shear stress developed in the contact patch while a vehicle locomotion platform undergoes slip (the difference in forward velocity and gear train velocity) as

$$\tau = A_1 e^{(-K_2 + \sqrt{K_2^2 - 1})K_1 j} + A_2 e^{(-K_2 - \sqrt{K_2^2 - 1})K_1 j} \tag{1.2}$$

where K_1 and K_2 are soil parameters found empirically.

These relationships can be expanded to formulate other measures of predicted heavy vehicle performance including the prediction of compaction resistance force imparted by the soil as a reaction to vehicle impact, the tractive effort developed at the running gears.

The original work of M.G. Bekker to derive these formulas made use of a machine called a bevameter, shown in Figure 2-1. The bevameter created the pressure-sinkage curve by driving stiff metal plates into soil using a constant rate of increasing normal force (up to this range of magnitude) [2-4]. This model does not explore the various contributions to normal pressure in the vehicle contact patch, nor the dynamic changes in soft soil strength parameters under dynamic loading. Further, it has been shown that for one-dimensional compression of dry sand, at low pressures sand is relatively incompressible, while at high pressure there can be considerable volume change due to the crushing of the sand grains [10]. The slip-shear relations were found empirically driving a large ring into the ground and rotating it at constant angular velocity, measuring the torque required to maintain that velocity. As such, these empirical relationships developed for large weight and large geometry wheeled and tracked vehicles may not be directly applicable to lightweight vehicles.

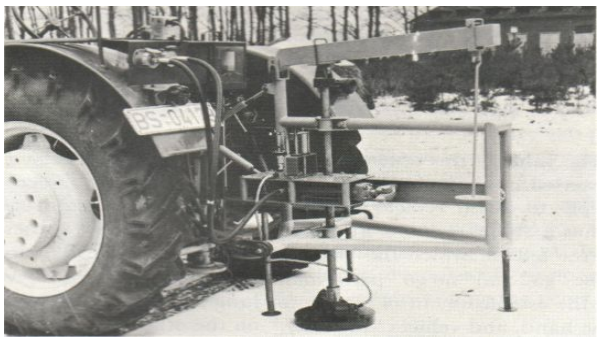

Figure 2-1: Vehicle-Mounted Bekker's Values Meter (Bevameter) in Use on Snow [3]

As a further hindrance, the cyclic loading effects on undrained soils (soils containing moisture) have been shown to be dramatically different from those effects in which the stress or strain is increased progressively to failure [11]. Bekker's pressure-sinkage relationship is the direct result of a progressively caused failure.

The Cone Index, a value found empirically through the use of a cone penetrometer such as the one shown in Figure 2-2, is a measure of ground resistance to normal pressure. The cone penetrometer is driven vertically into the sand while the resistance force is measured. This force is divided by the surface area of the tip of the cone to form the CI

value for the soil. The level to which a soil can be compacted is dependent mostly upon three factors: the amount of compactive effort (load) on the soil, the water content in the soil, and the type of soil as classified by its cohesiveness and plasticity [12]. The Cone Index has been empirically related to the values k_ϕ and k_c used in Bekker's computations. The CI is utilized by both NRMM software and empirical relationships involving the calculation of the vehicle Mobility Index [8].

Figure 2-2: Cone Penetrometer with Digital Depth and Pressure Reading

NATO Reference Mobility Model software uses the CI as its main input classification to characterize the strength of soft terrain (one of five inputs to the terrain scenario). CI readings of terrains around the world have been stored in a database for the software user to select as a part of the mission scenario. It is by CI value that the potential sinkage of the vehicle is measured, and can result in one of the "no go" outputs if it is computed that the vehicle does not have enough power to overcome the computed sinkage. NRMM also involves input of weather conditions, obstacle geometries and specific vehicle characteristics. The software in NRMM makes a qualitative analysis of all the input characteristics to define a go/no go mobility potential based on stored data from three decades of experimental work [8].

NRMM was developed entirely from empirical data for vehicles heavyweight vehicles weighing ¾ of a ton or more and is primarily geared toward vehicles weighing within a range of 1-70tons. NRMM bases some "no go" calculations on the potential impact to and abilities of a driver. This factor is not present in the failure of autonomous vehicles [8].

An attempt to test a lightweight (45lb) autonomous tracked vehicle, PACKBOT, in NRMM showed that, when the terrain profile inputs were scaled to include those that would affect a robot with small geometries, showed the potential for a successful "snapshot" of a PACKBOT's capabilities. The authors, however, note that certain complicated decisions had to be made about input factors. There are no small-scale terrains defined appropriately for assessing lightweight vehicle performance. Further, NRMM is only suited for wheeled and tracked vehicles, and not for robots of any other mobility platform [8].

The vehicle Mobility Index was developed for heavyweight tracked and wheeled vehicles to compute the Vehicle Cone Index, a numeric equivalent of the Cone Index used to directly compare the vehicle's potential impact on the ground with the resistance force of the ground. The VCI is calculated for the impact of running a vehicle once, 50 times and 100 times over soil, so as to represent the proper level of usage of a given off-road path. The VCI is calculated from the MI by a series of multiplied "factors" to increase or decrease the nominal pressure at the contact patch (vehicle weight divided by contact area) based on geometries of the running gear, power of the engine, and type of transmission. The difference between the VCI and the CI can be used to empirically predict vehicle performance via drawbar pull. Drawbar pull is a evaluated as of the difference between the tractive effort developed by the running gear (related to vehicle slip) and the total of resistance force on the vehicle, and is thus a measure a vehicle's ability to push or pull a certain weight. While heavyweight vehicles create a significant amount of compaction, lightweight vehicles do not, which may hamper the ability of the VCI to be appropriately adapted to lightweight vehicles [8].

2.3 Sand Terrain

Soils can be well described at the basic level by a checklist of seventeen parameters that can be field-identified or tested with precise equipment. Most of the relative levels presented as low, medium, etc. can be determined through field examinations, and can be refined with laboratory tests as necessary [13, 14].

The first two criteria, (1) Group name and (1) symbol, identify the soil as a clay, gravel, sand, etc. The next three criteria refine the former into a more precise description of the size of grains contained in the soil using (3) percent of cobbles or boulders by volume, (4) percent of gravel, sand, or fines, or all three by dry weight, and (5) particle size range, which sub-divides the group name of "sand" into fine, medium, and coarse. If the soil is sand, there will be zero percent cobbles or boulders, and limited gravel or fines in the sample.

The next three criteria describe the size and shape of the grains of soil including (6) particle angularity as angular, subangular, subrounded, or rounded, (7) Particle shape as flat, elongated, or flat and elongated, if appropriate, and (8) maximum particle size or dimension.

The next five criteria are all related to strength including (9) hardness (resistance to indentation or scratching) of coarse sand and larger particles, (10) plasticity of fines as non-plastic, low, medium or high, (11) the dry strength (maximum stress which a material can resist without failing for any given type of loading) as none, low, medium, high or very high, (12) the dilantancy (volume increase under loading) as none, slow or rapid, and (13) toughness (indexed as the ratio of the plasticity index to the flow index) as low, medium, or high. These criteria can be further studied in the lab for more precise classification using strength parameters.

The last of the criteria are the observable and include (14) color, (15) odor (if organic or unusual soil), (16) moisture as dry, moist, or wet, and (17) Reaction with HCl (to identify presence of the cementing agent calcium carbonate) as none, weak, or strong [13, 14].

In general, sand is classified as an inorganic soil comprised of small particles of rock, and less than 5% fines. Sand particles may have any of the four listed angularities and three listed shapes. The acceptable particle diameter range is 0.0029-0.187inch (0.1-2mm). Sand is considered to have no plasticity (which leads to very low toughness), no to very low interparticle cohesion, high interparticle friction, very low compressibility, and an immediate rate of compression. Sand is also noted to have low porosity/void ratio and high permeability [12-15].

2.3.1 Sand Size and Texture Classification Systems

Sorting

The United States Unified Soil Classification System, as utilized/approved by the American Society of Testing and Measurements (ASTM) Standards, classifies sand as fine aggregate comprised of particles each with a diameter greater than 0.0029 inch, but less than 0.187 inch (0.1-2 mm). The diameter is referred to as the grain size. Within this range sand is further categorized as coarse, medium, or fine. Coarse sand particles have diameters within a range of 0.0787 to 0.187 inch, medium 0.0165 to 0.0787 inch, and fine 0.0029 to 0.0165 inch [12, 14, 15].

In order to sort sand into these categories, sieve analysis is performed wherein samples of sand are sorted from the highest mesh openings to the lowest, so that particles will pass through meshes having openings larger than the grain diameter, and be retained in sieves having mesh openings smaller or very close to the grain diameter. U.S. Standard Sieves, are numbered according to the number of mesh openings per inch, so that U.S. Sieve No. 4 has four openings per inch, and U.S. Sieve No. 200 has 200 openings per inch. The former represents a sieve with mesh openings the size of a large diameter coarse sand particle, the latter a small diameter fine sand particle. Coarse sand is thus defined as that sand which, during sieve analysis, passes through U.S. Sieve No. 4, and retained in or above U.S. Sieve No. 10. Medium sand is that which passes through U.S. Sieve No. 10, and retained in U.S. Sieve No. 40. Fine sand is that which passes through U.S. Sieve No. 40, and retained in U.S. Sieve No. 200 [12, 14]. The No. 200 sieve is about the smallest particle size visible to the naked eye [16].

Grain size distribution, represented by a gradation curve, shows the proportions by mass of a sand distributed in specified particle size ranges (abundance versus grain size). The results of sieve analysis can be represented in a semi-log gradation curve, or a plot of the cumulative particle size distribution. To form this curve, calculations from the sieve analysis are used to create a plot of percentage of sand finer vs. grain size. The percent finer axis shows the amount of sand that passes through a certain sieve, thus the amount of sand having a diameter finer than the mesh openings or grain sizes presented in the grain diameter axis. These curves show the level of sorting that a sample of sand has, where poorly graded (well-sorted) sand has a small range of grain sizes, and a well-graded (poorly sorted) sand has a large range of grain sizes that are well distributed [12, 16]. Figure 2-3 shows the gradation curves for the five sands used for this study.

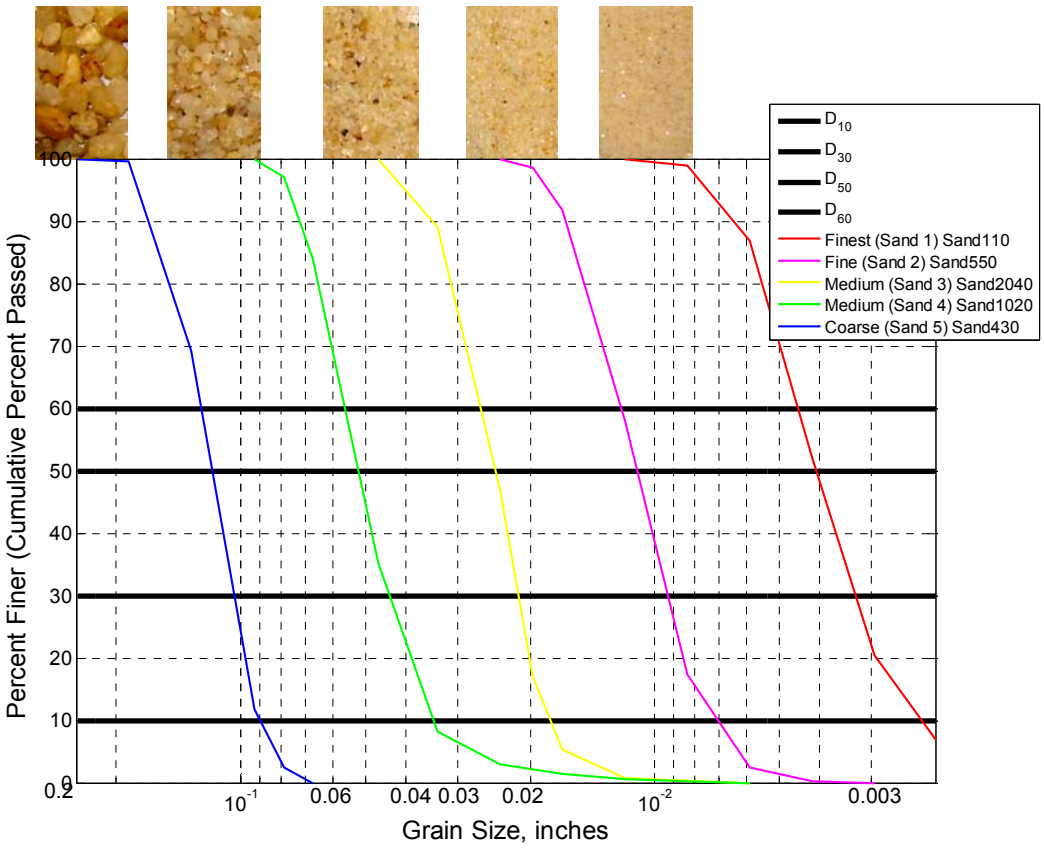

Figure 2-3: Gradation (Sorting) Curves for Sands Used in Experimental Study

The coefficient of curvature, C_c, represents the smoothness and shape of the curve. Very high or very low values indicate an irregular curve. The coefficient of uniformity, C_u,

indicates the degree to which the particles are of the same size. Increasing values of C_u indicate an increasingly wide range of particle size differences, or a higher level of sorting. If all of the particles of a soil were to have the same size (indicating the extreme of poorly graded or well sorted), then the coefficient of curvature and the coefficient of uniformity for that soil's gradation curve would both be at a minimum value of one [12, 16]. Together these values represent the sorting of the soil, and thus an indication of the ability of the soil to be compacted [12].

The values C_c and C_u are calculated using three values obtained from the gradation curve. The value D_n is equal to the maximum particle size in the n^{th} finer percentage, so that D_{60}, D_{30}, and D_{10} correspond to diameter sizes where 60%, 30% and 10% of the particles in the sand have a finer grain size than the D-value, respectively, on the cumulative particle-size distribution curve. The coefficient of curvature is calculated as

$$C_u = \frac{D_{60}}{D_{10}} \tag{2.3}$$

and the coefficient of uniformity is calculated as

$$C_c = \frac{(D_{30})^2}{D_{60} \cdot D_{10}} \tag{2.4}$$

which are used to classify sand into the primary grading categories of the Unified Soil Classification System. D_{10} is referred to as the effective grain size, and D_{50}, marking the diameter for which 50% of the sand particles are finer, is referred to as the mean grain size [12, 13, 15].

If a soil is well graded (poorly sorted), having a flat or slightly concave curve, then the coefficient of curvature C_c will typically have a value within the range of 0.5-2.0. A value of the coefficient of uniformity C_u less than three indicates more uniform grading (poor grading), while a value greater than five indicates a well-graded soil [12].

The grading properties for the sands used in this study are summarized in Table 2-1. The values for the characteristic diameters were read from the cumulative distribution chart, and rounded to the nearest thousandth of an inch. The values for C_u and C_c are rounded to

the nearest tenth decimal place. As can be seen in this table, the sands are graded almost the same, so that the main difference between the sands is their average grain size.

Table 2-1: Sand Size and Texture Classifications

Sand	Cc	Cu	D_{10}, in	D_{30}, in	D_{50}, in	D_{60}, in
Fine 110	2.0	1.1	0.002	0.003	0.004	0.004
Fine 550	1.7	1.0	0.007	0.009	0.011	0.012
Med 2040	1.5	1.0	0.018	0.021	0.024	0.026
Med 1020	1.6	1.0	0.034	0.044	0.052	0.056
Coarse 430	1.4	1.0	0.090	0.104	0.117	0.124

While the mineralogy of a sand particle is attributed to the source or parent rock, particle textural parameters are chiefly affected by the mode of transportation of the particle and the energy conditions of the transporting medium. Beach sands are typically poorly graded, meaning the particles have high uniformity, much like the sands used in this study [17-19].

Shape effects (Roundness/Angularity, Sphericity, Smoothness)

Particle shape can be described using the angularity (roundedness), sphericity (eccentricity or platiness), and smoothness (roughness) of the grains.

The angularity of particles describes the scale of major surface features, which are typically one order of magnitude smaller than the particle size (appearance of edges). Angularity is quantified as the average radius of curvature of the surface features relative to the radius of the maximum sphere that can be inscribed in the particle [20]. The angularity/roundness of sand particles can be described as angular, subangular, subrounded, rounded, or a range between any of the two consecutive classifications. Angular granules are those which have sharp or well-defined edges formed at the intersection of unpolished, roughly planar surfaces. Subangular particles are similar to angular grains but have rounded edges. Subrounded particles have nearly planar sides but have well-rounded edges and corners. Rounded grains have smoothly curved sides and no edges [14]. All sands but the finest sand available for this study are listed as having a roundness of 0.8 indicating that the surface edges are more rounded than angular [21].

Particle sphericity describes the similarity between a particle's length, width, and height, as well as the overall form of the particle (is the particle closer to a sphere or a rectangular solid). Sphericity is quantified as the diameter of the largest inscribed sphere of a grain to the diameter of the smallest circumscribed sphere [3]. Particle sphericity can be qualified as flat, elongated, or flat and elongated, if appropriate. If the particle does not fit any of these descriptions, the qualification is not given [14]. All sands but the finest sand available for this study are listed as having a sphericity of 0.8, implying that the sand particles do not exhibit flatness or elongation and have more uniform lengths, widths, and heights [21].

Smoothness (roughness) qualifies the particle's surface texture relative to the radius of the particle [14, 15, 20].

Particle shape, affecting particle-level interactions, has been shown to affect the macroscale behaviors of packing density, stiffness, and strength, of the overall sand mass [20].

Void, in sand, is any space in the soil mass that is not occupied by solid mineral matter, and may be occupied by a gaseous or liquid material. A void ratio describes the ratio of the column of a void space to the volume of solid particles in a given soil mass [15]. Larger void ratios imply a looser packing of the sand. Decreased angularity (increased roundedness) has been shown to produce an decrease in the critical (maximum and minimum) void ratios, used to express the packing of the sand [20].

Regularity of sand particles refers to the average of the values of roundness/angularity and sphericity. Increased particle irregularity has been shown to cause a decrease in sand bulk stiffness yet a heightened sensitivity to the state of stress; an increase in compressibility under zero-lateral strain loading; and an increase in the critical state friction angle [20]. This property in part discussed in the next section of this literature review.

Packing Density and Water Content

Related to the grain size distribution and particle shapes of a sample of sand, the maximum and minimum relative densities of sand, ρ_{max} and ρ_{min}, define the packing limits of a sand. Relative density of a sand is defined as the proportion of the sand's current density to the value of ρ_{max} for that sand, with 0% being the loosest a sand can be while still considered a bulk aggregate, and 100% being the densest a sand will pack [12]. Sands typically do not compact much within the top twelve inches of the layer, unless forced by measures often taken during building construction. The sands used during testing for this study can be approximated as having a 40% relative density [19]. This packing density will have a direct effect on the amount of water retained in the top twelve inches of the sand, and in the total of the sand pit.

Water (or any other gaseous or liquid matter) will occupy spaces in sands referred to as voids. A void is simply a space in a soil or rock mass not occupied by solid mineral matter. The void ratio of a sand is the ratio of (1) the column of a void space to (2) the volume of solid particles in a given soil mass. Water content is defined as the ratio of the mass of water contained in the pore spaces of soil or rock material, to the solid mass of particles in that material, expressed as a percentage [15], and is sometimes referred to as the gravimetric water content.

Water that fills the void ratios without liquefying the sand creates a surface tension that bonds the particles together. The measured angle of friction of undrained sand can also vary from that of drained sand depending on the chosen failure criterion

2.3.2 Sand Strength and Geotechnical Engineering Properties

Friction Properties

Soil strength is generally classified using two shear strength parameters—the cohesion, *c*, and the internal friction angle, ϕ, based on Mohr-Coulomb failure criteria using Coulomb's equation

$$\tau = \underbrace{c}_{\text{Cohesion}} + \underbrace{\sigma \tan(\phi)}_{\text{Internal Friction}} \qquad 2.5$$

where τ is the shear stress, and σ is the normal pressure. This relationship is graphically represented in Figure 2-4, where shear stress is plotted against normal stress [12]. Both of these values represent interparticle interactions. Mohr's theory states that materials will fail from a critical combination of normal stress and shearing stress. To form this Mohr-Coulomb failure, shear tests are performed on the sand to find the critical values of normal pressure that overcome applied axial pressure.

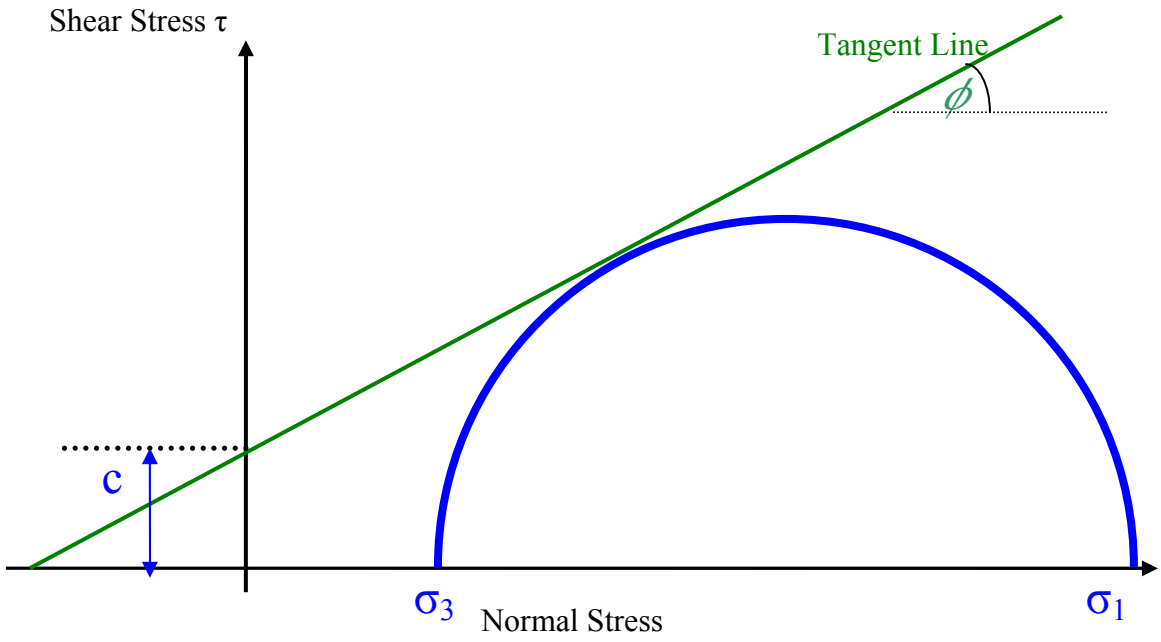

Figure 2-4: Mohr's Circle used to find cohesion and friction angle for a soil.

The coefficient of cohesion, *c*, also known as the apparent cohesion of the material, quantifies the bond between particles of the soil irrespective of the normal pressure exerted by one particle upon the other [5], or the level to which the particles will stay together (shear resistance) under zero normal force [15]. Simply, if the particles are naturally inclined to stick together, the soil possesses cohesion [12]. This value (in force per unit area) is the shear stress offset of the Mohr-Coulomb representation of shear stress versus normal (compressive) stress. Cohesive soils are those soils which have considerable strength when unconfined and significant cohesion when submerged. Cohesionless soils are those soils that when unconfined and air-dried have little or no strength and that have little or no cohesion when submerged [12, 22]. Sand is generally

accepted as a cohesionless soil, even when wet. As such, to calculate the angle of internal friction, c was set to zero for all sands [19].

Internal friction or shear resistance, measured in force per unit area, is the resistance attributed to the interlocking of the soil grains and the resistance to sliding between the grains [22]. When a normal load is applied to sand, the shear resistance defines how much the sand will displace perpendicular to the application of the load [5]. The angle of internal friction, ϕ, also known as the angle of internal shearing resistance, defines the slope of the Mohr-Coulomb failure envelope as the angle, in degrees, between the axis of normal stress and the tangent to the Mohr-Coulomb envelope at a point representing a given failure-stress condition [12, 22]. As such, the angle of internal friction can be thought of as a measure of the angularity of the soil particles to resist rolling. The tangent of the angle of internal friction/shear resistance is the coefficient of internal friction, μ [22].

Confined Drained Triaxial Shear Tests

Confined drained triaxial shear tests were performed on each of the five sands available for this study in order to find their angles of internal friction. For these tests, roughly 7.5-inch tall, 2.7-inch diameter cylinders of sand were formed in a flexible membrane. This membrane applied user-set radial confinement pressures of roughly 5inHg, 10inHg, and 15inHg to the sand. A load cell was used to apply increasing, uniformly distributed normal pressure (or deviator stress), σ_D, at the top face of the cylinder. This experimental setup is shown in Figure 2-5a. This force was applied until the cylinder of sand experienced 12-15% strain in height. As the force increased, the sand particles went into shear failure and the radius of the cylinder nonuniformly increased as pictured in Figure 2-5b. The data acquisition system recorded coded (in voltage) values of the force applied by the load cell and the position of the load cell force applicator.

Figure 2-5: Triaxial Shear Test (a) Apparatus and (b) Failure Mode

Three calculations were performed to process the raw force and load cell displacement data. First, the incremental axial strain was calculated for each step as

$$\varepsilon_{axial} = \frac{\Delta H}{H_0} \tag{2.6}$$

where the change in height, ΔH, is the displacement of the load cell from its original placement on top of the cylinder of sand, and H_0 is the original height of the cylinder of sand prior to deformation. From this, an incremental corrected cylinder face area $A_{corrected}$ was calculated to compensate for the changing size of the cylinder during shear deformation as

$$A_{Corrected} = \frac{A_0}{1 - \varepsilon_{axial}} \tag{2.7}$$

where A_0 is the original face area of the cylinder, prior to axial loading, and ε_{axial} is the axial strain.

To calculate the normal pressure increasingly applied to the cylinder of sand, each incremental force F recorded by the load cell was divided by the corrected cylinder face areas as

$$\sigma_D = \frac{F}{A_{Corrected}} \tag{2.8}$$

to define the deviator stress, which is the difference between the major and minor principle stresses in a triaxial test.

For each confining stress, the values found for deviator stress and axial strain were plotted as shown in Figure 2-6, picturing the failure tests for the coarsest sand in the study. The maximum deviator stress, σ_{Dmax}, for each confining pressure is circled in green. These values occur just before failure, when the cylinder becomes highly deformed during testing.

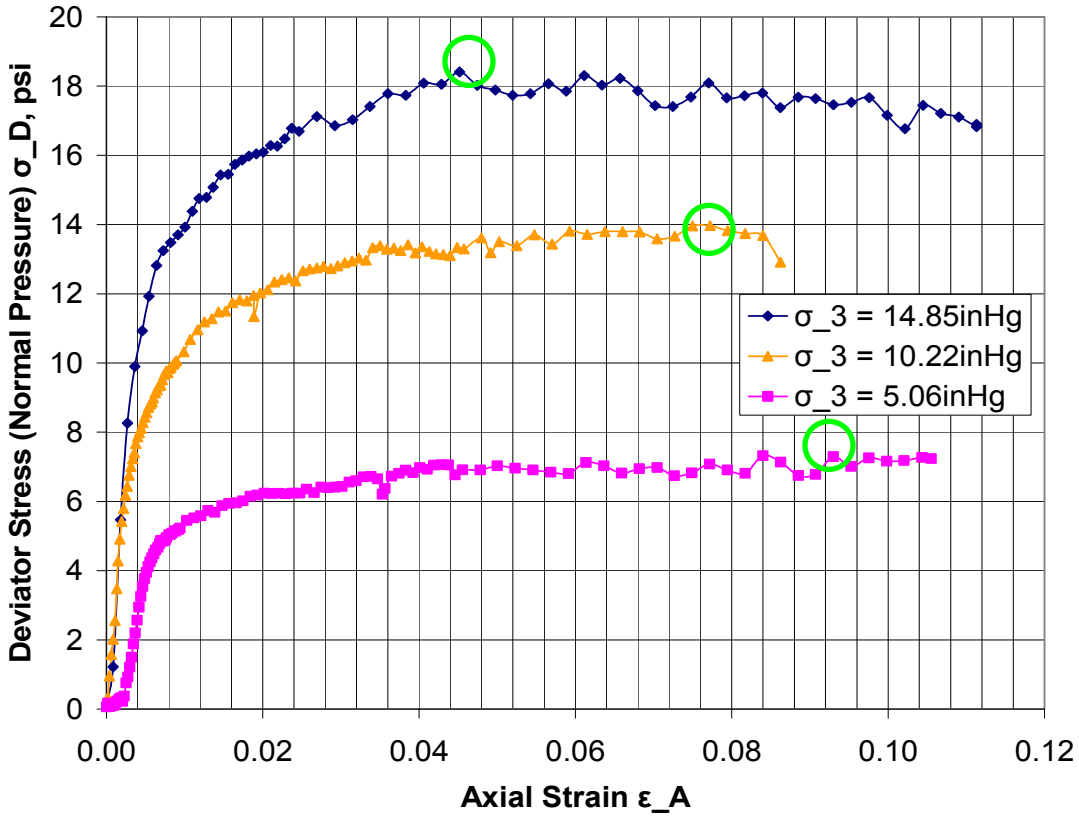

Figure 2-6: Drained consolidated triaxial shear test data for Coarse Sand 430.

From these tests, three Mohr's circles are formed for each sand and used to find the friction angle. Each confining pressure is defined as σ_3, and has a corresponding maximum deviator stress σ_{Dmax}. This value σ_{Dmax} defines the diameter of Mohr's circle as the distance between two points on the normal stress axis (x-axis), the first of which is the confining pressure σ_3, and the second of which is defined as

$$\sigma_1 = \sigma_3 + \sigma_{D\max} \qquad 2.9$$

forming a circle such as the one shown in Figure 2-7.When a series of Mohr's failure circles are plotted for a given sand, where the value of cohesion *c* is zero, the results are plotted as shown in Figure 2-7. In this plot a tangent line to all three failure circles is drawn at the friction angle ϕ to the normal stress axis. A second line that crosses through the height of each circle, defined by half of the maximum deviator stress, is drawn at an angle of θ to the normal stress axis.

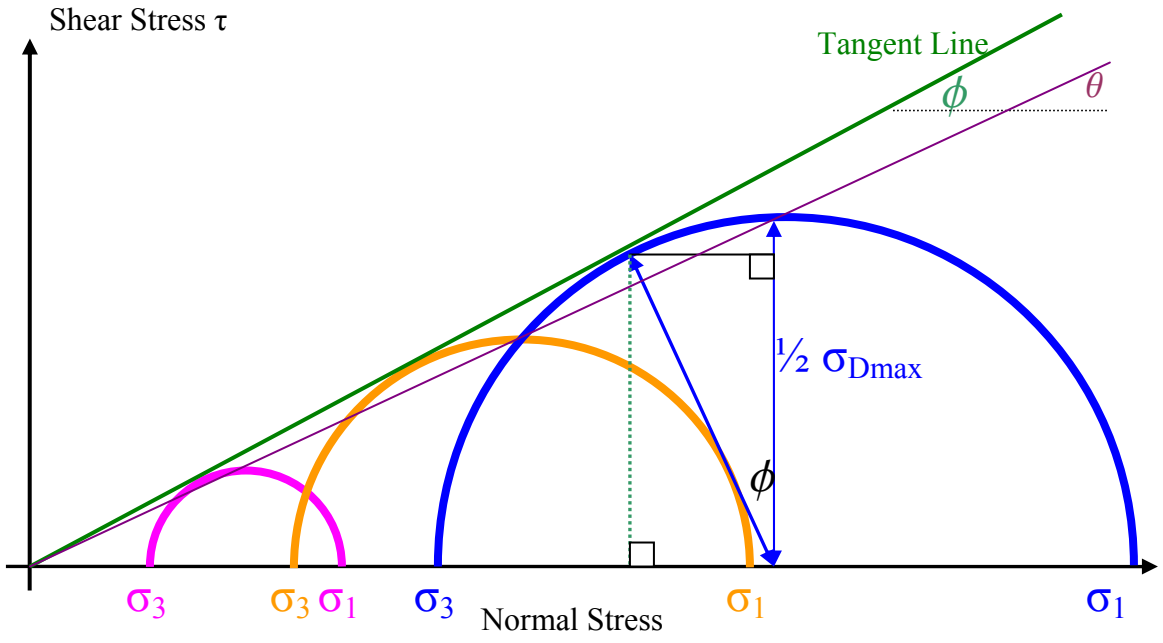

Figure 2-7: Mohr's Diagram (cohesionless sand) used to find the value of the friction angle.

Observing the Mohr's diagram pictured in Figure 2-7, the friction angle ϕ can be calculated as

$$\frac{\sigma_1}{\sigma_3} = \tan^2\left(45° + \phi/2\right) \qquad 2.10$$

through geometric relations. The friction angles for sands used in this study are shown in Table 2-2. The close values of the friction angles can be attributed to the similar grading characteristics [12, 19]..

Table 2-2: Friction Angles for Sands Used in the Study

Sand	ϕ (degrees)
Fine 110	34.5
Fine 550	30.7
Med 2040	33.9
Med 1020	32.9
Coarse 430	34.7

Plasticity

Plasticity is the ability of a soil to take and retain a new shape when compressed or molded. Plastic soils can be quickly identified as those soils that can be easily molded without cracking. Sands are considered non-plastic when dry [12, 19].

3 MOBILITY METRICS MATRIX

The Matrix of Mobility Matrix (MMM) identifies pertinent measurable mobility performance criteria to form an assessment tool to compare vehicles of different locomotion platforms for their mission suitability [23]. This tool presumes that all vehicles being ranked against each other meet the basic needs of the mission. This entails that, once mission needs and subsequent dependent vehicle performance parameters have been identified (via the matrix), all vehicles meet the minimum operating criteria. For instance, if there is a limited vehicle path, all vehicles have allowable dimensions for this path. Once viable mission candidates have been identified, they can be compared using the indexing function so as to rank the vehicles against each other in an intuitive and quick manner. Thus, this system can be used to quickly narrow down a wide pool of mission candidates for those vehicles best suited for a given mission. A further benefit of this system is that it is adaptable to user needs. Performance parameters and mission criteria can be added to expand the system for unforeseen specifications. Figure 3-1 shows a template for the mobility metrics matrix, which can be further expanded, as needed.

A = Adverse
L = Low Positive
H = High Positive

	Terrain Characteristics and Mission Requirements	TRI	Tractive Effort/Soil Thrust (per veh.)	Compaction Resistance (per veh.)	Safe Weight	Sinkage	Slippage	Weight (Nominal)	Contact Area	Weight/Contact Area (High)	Ground Clearance*	Payload Support Area	Length (Longitudinal)	Width (Lateral)	Height	Vehicle Speed Range** (Low)	Vehicle Speed Range** (High)	Turning Radius (Minimum)	Slope Climbing Capability (Longitudinal)	Slope Traversing Capability (Lateral)	Energy Consumption	Payload Capacity (High)	Tow Capacity/Drawbar Pull	Jumping Ability	Vibration	Temperature	Light	Impact	Moisture
			Vehicle-Terrain Param.: Interaction					Vehicle Parameters: Geom.								Vehicle Parameters: Performance									Vehicle Parameters: Instrument Sensitivity				
Interaction	Non-Disturbance Of Terrain			L	L	H	H			L	L																		
Interaction	Non-Impact of Terrain				L	H																							
Interaction	Rough/Uneven Terrain		H	L		L	L		H	L	L														H				
Interaction	Soft/Non-Cohesive Terrain		H	H	L	H	L																						
Interaction	Hard/Cohesive Terrain		H	H	L	H	L																						
Geom.	Water Hazards								L	L	H																		H
Geom.	Confined Travel Path Area								L				H	H	H			H	L	L			L						
Geom.	Obstacle Avoidance										H							H	L	L			H						
Performance	Distance of Travel															H	H				L								
Performance	Confrontation/Evasion																H										L		
Performance	Discontinuous Movement		H	L			H			H			L	L	L	L	L												
Performance	Rescue/Recovery											H										H	H						
Performance	Agility		L				A	A								H	H	H	H	H				H					
Performance	Time Limitations															H	H				A								
Performance	Daytime/Nighttime Mission																									H	H		

Figure 3-1: Mobility Metrics Matrix

3.1 The Relationship Between Mission Needs and Vehicle Parameters and Performance Measurements

The House of Quality (HOQ) is a tool used in business practice and product development to match product specifications to relevant consumer needs in order to develop a marketable and useful product. The core of the HOQ is a matrix structure listing consumer needs in rows and product specifications in columns, marking the relations between the two in the matrix body. Each need is rated with the relative importance of the need to the consumer. The HOQ can be expanded with a "roof" that creates links between product specifications to mark tradeoffs or direct links between them. This roof allows for a detailed study of what features might take precedence over others depending on the importance noted for each consumer need [24].

The main matrix of the House of Quality (HOQ) structure is used to tabulate the relationship between user-defined mission criteria and pertinent vehicle parameters and performance measurements. Mission criteria consist of desired vehicle-ground interactions, existing geometric terrain properties, and mission performance needs/purposes. For each category of mission criteria there is a vehicle metric category counterpart (interactions, geometries, and performances, respectively). Vehicle-terrain interactions refer to terramechanic measures of vehicle performance. Vehicle performance metrics refer to measures of vehicle power. A fourth vehicle metric category is comprised of instrumentation sensitivities to accommodate special mission needs specific to autonomous vehicles. As designed, the majority of identified relationships fall within like categories of metrics. Logically the geometry of the terrain imposes direct limitations on the geometry of the vehicle. The matrix reveals cross-category relationships that may otherwise be overlooked.

3.1.1 Interaction Measures

Mission requirements for vehicle-ground interaction are selected for sensitive mission details or important terrain composition properties. Improvised Explosive Device (IED) and mine management each involve careful consideration of the vehicle's disturbance of the threat device via non-impact of the terrain. Habitats involving sensitive balance of nature may require that vegetation or wildlife not be destroyed during the mission.

Mission involving such habitats would require non-disturbance of the terrain Soft or less cohesive sand requires some different formulations than the hard or cohesive ground.

Vehicle parameters of interaction are those measurements of vehicle-ground interaction that establish the forces necessary for vehicle propulsion and the subsequent effects on the terrain, and are thus dependent on both the soil and the vehicle properties. Empirical relationships for these measures have been established in the work of M.G. Bekker and J.Y. Wong based on soil characteristics as outlined in Whitlow's *Basic Soil Mechanics* [2-5, 12]. These formulas allow for the adverse or positive effect of locomotion type to be accounted for in the overall vehicle operation rating. Tracked vehicles can have advantageously lower ground pressures than wheeled vehicles, while wheeled vehicles can have lower values of slip and soil disturbance in the contact patch. Specific recommendations for the development of robot equivalent vehicle-ground interaction parameters are suggested later.

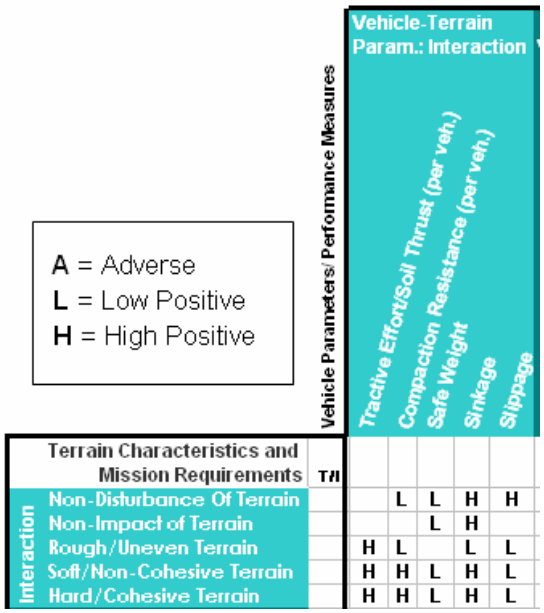

Figure 3-2: Vehicle-Terrain Interaction Mission Requirements and Vehicle Parameters for MMM

3.1.2 Geometries

Terrain geometries refer to measures of the soil and operation area to be traversed. Path limitations including size and obstacles limit the basic area of operation. Soil classifications identifying the granulation, cohesion, and friction properties of the terrain are used to identify desirable vehicle parameters for successful missions. Soft terrain requires lower ground pressure for vehicle performance. Vehicle geometries are basic physical measurements of the vehicle including weight, ground contact area size, overall vehicle size, and payload support area.

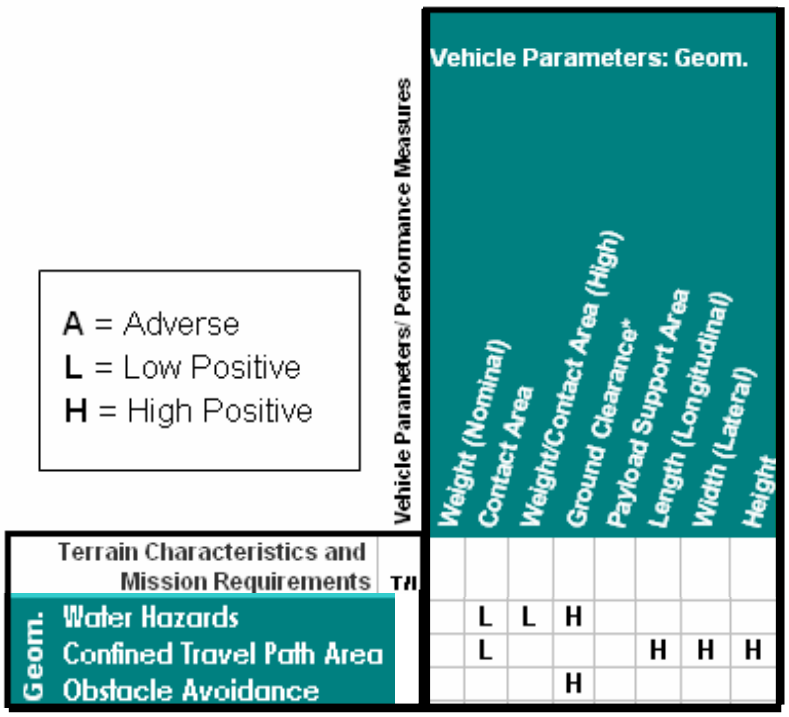

Figure 3-3: Geometric Mission Requirements and Vehicle Parameters for MMM

3.1.3 Performance

Mission performance criteria provide the basic functions that the unmanned ground vehicle (UGV) must fulfill or perform. Broad categories are given so that the user can define the importance or threat level associated with these functions. Vehicle performance metrics correspond to actions that the UGV may have to take to complete its mission. Some criterion have multiple levels, indicating that for certain missions low

speed levels may be desired, for stability perhaps, and for other missions high speed ranges may be critical for mission performance.

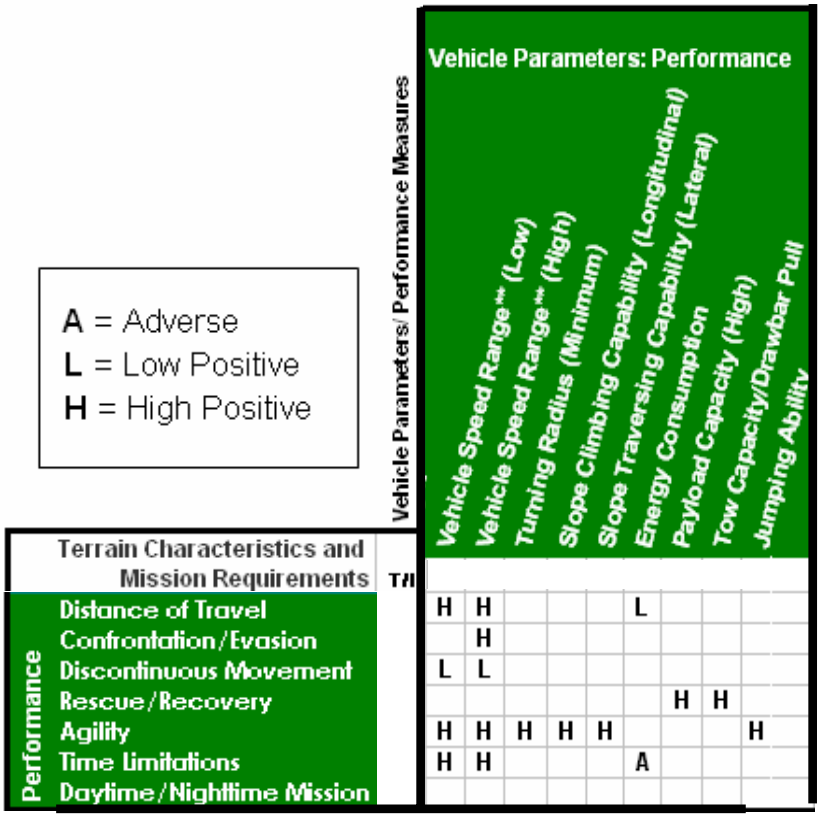

Figure 3-4: Performance Mission Requirements and Vehicle Parameters for MMM

3.1.4 Sensitivity

Sensitivity relations are those that describe instrument sensitivities to mission criteria. An overview of the critical equipment for operation will show any vibration, temperature or other sensitivity considerations that must be accounted for during a mission. These vehicle sensitivities correlate to mission requirements in all three categories.

3.2 Vehicle Ranking for Mission Suitability

Within the matrix each mission category is assigned (by the user) a level of importance to allow mission customization. Each connection between a mission need and a vehicle parameter identified using a high, lower, or negative impact marker. To avoid compounding the effect of a vehicle parameter, in cases where vehicle parameters

overlap (tractive effort and vehicle weight, for instance) precedence is given to the parameter that encompasses the other (tractive effort, in this case.) Once these relationships are identified a simple indexing function is used to judge vehicles for mission suitability. Vehicles are rated against each other to create a relative score (for which there is purposefully no universal scale or range). From this relative score a large number of vehicles identified for mission deployment can be judged for relative predicted performance, dramatically reducing the candidate pool.

3.2.1 Impact Markers

General levels of weighting between mission parameters and vehicle parameters represent how strongly effects of the latter are felt on the former during mission performance, or the level of impact that the former has on the calculation of the latter. A high or strong positive marker (H) represents a beneficial, direct, or high dependency. This could indicate that the vehicle parameter is critical to the mission criteria, that the mission criteria creates a greater need for a better performance of the vehicle parameter, or that the mission criteria directly affects the need for or method of calculation of the vehicle parameter. A low positive marker (L) represents a beneficial relationship where the relationship is either indirect or not of great enough importance to warrant a stronger status. Correlation exists, but may be as an intermediate calculation. A negative or adverse marker (A) represents a situation where the vehicle parameter, no matter the level, will adversely affect the mission parameter. For soft soils there is a much higher level of sensitivity to or effect of compaction resistance than with harder terrains in terms of effect on mission performance. Agility has an adverse relationship with sinkage and slippage, but a strong positive correlation with turning radius and jumping ability. Energy consumption has an adverse relationship to mission time limitations. Markers provide for some tradeoff compensation between mission criteria. Each marker category is assigned a specific weighting for use in the indexing function. This methodology is based in part on Quality Function Deployment, and indexing function associated with the House of Quality [24].

3.2.2 Indexing Function

The various ratings in the mobility metrics matrix provide for a computational approach to comparing vehicles of different mobility platforms. Mission parameters are divided into T groups by their user-defined Threat/Importance (T/I) levels, $\ell_{T/I}$. Within the k^{th} T/I group, vehicles are rated for mission suitability first by the importance of each vehicle metric to the mission criteria, then by their comparative abilities to fulfill each vehicle metric category.

Table 3-1: Index Function Symbol Guide

	T/I Level	Vehicle Parameter	Vehicle
Value	$\ell_{T/I}$	p	None
Index	k	j	i
Range	T	M	V

In order to rate vehicles against each other, values of vehicle metrics must be normalized so as not to introduce unwanted effects of units and ranges imposed between unrelated parameters. As such, this indexing function rates vehicles against each other with an intuitive zero-to-ten relative rank. For the j^{th} vehicle metric (of those connected to the k^{th} group of mission criteria of equal $\ell_{T/I,k}$) the user selects an ideal or "best" vehicle candidate of the group. The "best" candidate can be chosen using military standards such as U.S. Marine Corps UGV Standards [6], or according to tested experience with the vehicle, but is always chosen for the maximum performance in that category, including cases where the metric has been identified in an adverse relationship to a mission criteria. Each i^{th} vehicle is scored for its performance level for the j^{th} metric—$p_{i,j}$—in comparison to the best level of performance of all V vehicles for that metric, or $p_{best(V),j}$. This ranking factor is a pure measure of relative vehicle performance where the normalization dictates that the "best" vehicle for that metric receives a default score of 10. This rank is computed as

$$rank_{i,j(k)} = \frac{p_{i,j}}{p_{best(V),j(k)} \big/ 10}. \qquad 3.1$$

To give weight to the amount of connection of parameter p_j to a given mission T/I group two factors are used. The factors $n_{j,l}$, $n_{j,h}$, $n_{j,a}$ are equal to number of times a metric j is shown in the HOQ to be related to the k^{th} group of mission needs by a high, low, or adverse relationship, respectively. Each n-factor is combined with its respective weighting factor—w_h, w_l, *or* w_a—that provides a boost or penalty for each vehicle metric's level of relation to a given mission need. This combination factor of $wn_{j(k)}$ is a pure measure of the importance of the j^{th} metric to the mission parameter, as

$$imp_{j(k)} = (w_l n_{j(k),l} + w_h n_{j(k),h} + w_a n_{j(k),a}) . \qquad 3.2$$

The values for the weighting factors are left to be defined by the user based on, for example, experience with a given mission, the number of vehicles to be compared and the level to which the vehicles must be differentiated from each other and/or eliminated from the general pool of vehicles. The exception is that the adverse relationship must always have a negative weighting factor to match with the formulations in this study. In product development there are no established methods of applying the values of relationship markers so as to allow each company to tailor its system to its market and experience. The larger the spread of values for these weighting factors, the larger the computed value for comparison emphasizes the differences between strong positive, weak positive, and adverse relationships, while a smaller scale will discriminate between these relationships more evenly. An example of the first set of values, as has been used in industry product development, would be 9 = strong positive, 3 = weak positive, -3 = medium adverse. An example of the second set of values would be 5 = strong positive, 3 = weak positive, -1 = adverse. The MMM can be adapted to include more or fewer levels of relationships between mission criteria and vehicle metrics [24].

The use of the level of Threat/Importance $\ell_{T/I,k}$ provides a pure measure of the importance of the mission parameter to the overall mission, and the final link between mission needs and vehicle performance. This mission T/I category weighting is used in combination with the impact marker weights to form a cumulative value by which to rank a vehicle directly against others in the population of vehicles under consideration. Rank of vehicle i is computed by

$$Q_i = \sum_{k=1}^{T} 1_{T/I,k} \sum_{j=1}^{M} \left\{ (w_l n_{j(k),l} + w_h n_{j(k),h}) \left(\frac{p_{i,j}}{p_{best(V),j(k)} / 10} \right) + w_a n_{j(k),a} \left(11 - \frac{p_{i,j}}{p_{best(V),j(k)} / 10} \right) \right\} \quad .3.3$$

The adversarial effects are computed such that the vehicle with the best performance of a vehicle parameter is the least penalized of the group. For instance, if time limitations are identified in mission criteria, the vehicle with the best (or lowest) energy consumption rate will be penalized the least in comparison with competing vehicles with higher consumption rates. Each score Q_i will be a mission-specific rank of the i^{th} vehicle's mission suitability as compared to all V vehicles.

4 TECHNOLOGY DEVELOPMENT OF ROBOTS WITH WALKING LOCOMOTION

In the following sections, three types of robots with novel locomotion—a bipedal, a self-excited dynamic tripedal and an active spoke-wheel—are introduced. These locomotion platforms are unique in their complexity of dynamic interaction with the ground, which may include several phases such as the initial penetration into the soil, the power stroke in the soil and the withdrawal out of the soil [25]. When possible, theoretical work is presented to provide the basis for future robotic foot-ground interaction study to aid in developing equivalent vehicle-ground interaction parameters to use in the mobility metrics matrix and thus the understanding of the dynamics of novel locomotion platforms operating on deformable terrain.

Considering the complicated environments such as coastal terrain and the growing use of autonomous vehicles in dull, dirty, and dangerous applications [26], the development of novel robots with alternative locomotion strategies becomes necessary. Compared with lightweight tracked and wheeled autonomous vehicles, legged robots are more adaptable in the actuation of their locomotion platforms, and may therefore have the potential of greater agility in certain rough terrains and unstructured environments. Note that the legged locomotion discussed in this chapter is equivalent locomotion with discontinuous contact with the ground.

As suggested in [25], any proposed theory for mathematical models will require specific adaptation to small-scale applications such as walking robots, and further require physical testing and validation. Models and prototypes of these and other robots are under development at the Robotics & Mechanisms Laboratory (RoMeLa) in the Department of Mechanical Engineering of Virginia Tech. A summary of some basic specifications of current working prototypes is shown in Table 4-1.

Table 4-1: Basic Specifications of Selected Current RoMeLa Robot Prototypes

Robot	Foot Geometry	# of Feet	Foot Dimensions L x W x T	Unloaded Weight	Max. Velocity	L x W x H	Approx. Turning Capacity (per step)
DARwIn	Rectangular Plate	2	4.44in x 2.75in x 0.75in	4lbs	0.23m/s (0.50mph)	4"x9"x18"	45 degrees
STriDER	Cylindrical Spear	3	1-inch diam., 51.25inch long	10lbs	0.5m/s (1.10mph)	25" x25"x70 "	45 degrees
IMPASS	Two center-hinged curved rectangular plates	6/w heel	4.5in x 1.75in x0.15in (plate thickness)	Body Incomp.	1m/s (2.25mph)	32.5 inches Eff. Wheel diameter	30 degrees

4.1 DARwIn (Dynamic Anthropomorphic Robot with Intelligence)

DARwIn, Dynamic Anthropomorphic Robot with Intelligence as shown in Figure 4-1, is a humanoid robot capable of bipedal walking and performing human-like motions. DARwIn is a 21 degree-of-freedom (DOF) system with each joint actuated by cordless DC motors. Implementing a computer vision system on the head and multiple force sensors on the foot, DARwIn can execute human-like gaits while navigating obstacles and traversing uneven terrain [27].

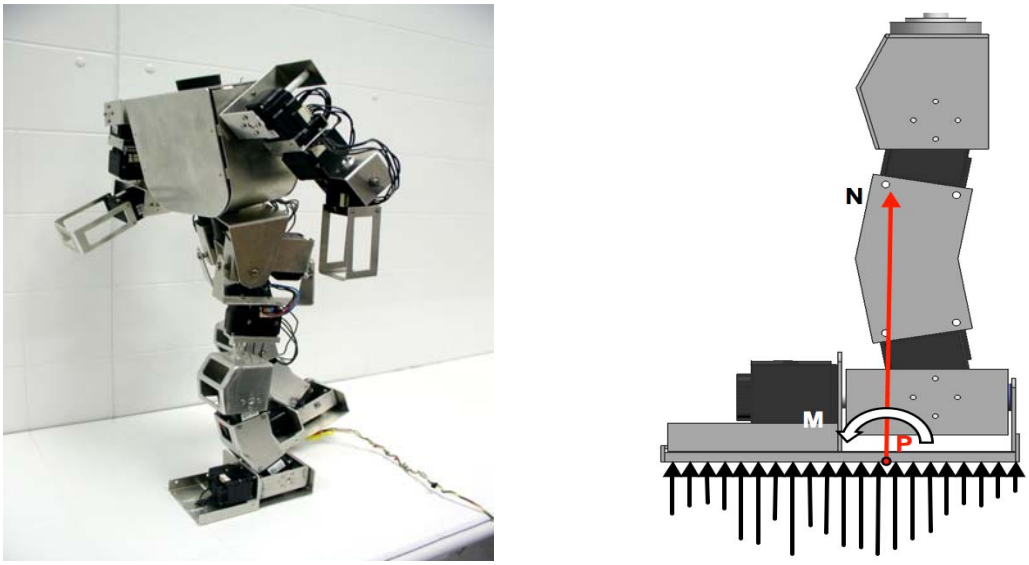

Figure 4-1: DARwIn prototype and foot with controlled force distribution.

The bipedal gait of DARwIn and the interaction between the robotic foot and the ground is dynamically controlled using a Zero Moment Point (ZMP) control. Ground interaction is similar to human walking. The rectangular foot is placed heal first, a rotation at an ankle joint presses the foot flat against the ground, and weight is transferred to this stance foot. Vertical force sensors on the stance foot feed measurements into a control algorithm

to create a reactive robot stance, varying the vertical force distribution to keep the ZMP under the stance foot. An example of such a controlled force distribution is shown in Figure 4-1. Once the second foot is planted, the stance foot is lifted. Vertical force distribution is only considered in the profile shown in Figure 4-1, as forces lateral to the direction of robot path are not measured [27].

The dynamic loading process of robotic feet has been studied by Ingvast, addressing issues of horizontal deflection and contributing forces, as well as dynamic vertical force-deflection interaction that is specific to walking robots [28]. To model the foot-ground interaction during loading and unloading (placement, weight shift, and lift of the foot), some models are proposed in differential forms to describe the relationships of soil deflection and changing force. It is assumed in [28] that the contact area does not change, the orientation of the pad of the foot does not change (no tipping or rotating about an ankle joint), and that ground interactions with the horizontal surface (such as from pileups of soil) are ignored. Based on Bekker's theory, a vertical deflection-force model and a horizontal deflection-force model for plastic soil are formulated, shown as Equations 4.1 and 4.2, as well as a one-dimensional horizontal deflection-force model for plastic elastic soils shown as Equation 4.3, which lay the foundation for further analysis of the vertical pressure-sinkage relationship, and the quantification of walking robot thrust as,

$$dF_z = \begin{cases} Az^{n-1}k_z dz, & z \geq z_{\max} \\ Ak_r dz, & z < z_{\max} \text{ and } F_z > 0 \end{cases} \tag{4.1}$$

$$dF_x = \frac{1}{K_p}\left(F_{\max}\, dx - F_x \left|d_x\right|\right) \tag{4.2}$$

$$dF_x = \begin{cases} \frac{1}{K_p}\left(F_{\max} - \left|F_x\right|\right)d_x, & F_x dx \geq 0 \\ k_e dx, & otherwise \end{cases} \tag{4.3}$$

In these equations z denotes vertical deflection and direction, x denotes horizontal direction, F represents a force vector in the given direction, A is the value of contact area, k_z and k_r are coefficients of ground stiffness in the vertical direction during load and

during unloading/reloading, respectively, K_p is the modulus for lateral deformation for plastic soils, $F_{\max}$ is the maximum horizontal force based on vertical force and soil friction, and k_e as the elasticity constant for a plastic-elastic soil. Horizontal forces refer to those in the direction of robot travel. Motion in the y-direction (perpendicular to the travel path and to the normal force) is assumed to be zero. Models that do not make this assumption are also presented in [28].

Limitations on using the models include that the contact area of DARwIn is smaller than that assumed in the framework of Bekker's classical model, which assumes a rectangular contact area with a preferred width no less than 4 inches [2-4], and that DARwIn's ZMP control provides a special case where the vertical force distribution is dynamically controlled instead of passively utilized. More information on the fundamentals of compaction and propulsion of walking robots is presented in [25].

4.2 STriDER (Self-excited Tripedal Dynamic Experimental Robot)

STriDER, Self-excited Tripedal Dynamic Experimental Robot, as shown in is a novel three-legged walking machine that exploits the concept of actuated passive dynamic locomotion to walk with high energy efficiency and minimal control. Unlike other passive dynamic walking machines, this unique tripedal locomotion robot is inherently stable with its tripod stance and can change directions while walking [29].

Figure 4-2: STriDER prototype model and foot

To initiate a step, the legs are oriented to push the center of gravity outside of the stance legs. As the body of the robot falls forward, the swing leg naturally swings in between the two stance legs and catches the fall. Once all three legs are in contact with the ground, the robot regains its stability and the posture of the robot is then reset in preparation for the next step. The foot can be regarded as the end of the leg close to the ground. Each time a leg is placed, the foot will sink into the ground at its placement angle. During swing, stance feet will likely sink farther into the soft ground due to increased weight distribution. These stance feet will tilt as the body tilts, and thus any portion of the foot that is sunk into the ground will cut through soft soil. When a swing foot is initially lifted off the ground it will have tilted with the body, and will drag through soft soils until it is freed. As an example of adaptability, controls may be developed in the future to prevent some of this dragging effect.

Given that STriDER's feet are like spears, basic models for ground interaction may be based on theory behind the cone penetrometer's ground interaction as presented in [9]. This work presents formulations connecting the vertical force that must be exerted on the penetrometer's shaft in order to penetrate the soil to a given depth for plastic-elastic soils, and could be used to create an equivalent pressure-sinkage measurement for STriDER. Some technical reports concerning the effect that an upward flow of soil that results from ground penetration are also made, and this shearing flow effect may assist in the formulation of an equivalent for compaction resistance. If it cannot be avoided using controls, the dragging motion will have to be studied more when prototypes are further developed for testing, but also has potential links to blade cutting as studied in the agricultural field [30].

4.3 IMPASS (Intelligent Mobility Platform with Active Spoke System)

IMPASS, Intelligent Mobility Platform with Active Spoke System, as shown in Figure 5, utilizes rimless wheels with individually actuated spokes to follow the contour of uneven surfaces and step over large obstacles. To move the wheel can rotate as a whole, much like a conventional wheel, and/or each spoke in the wheel can stretch in and out to push against the soil. As shown in Figure 4-3, foot consists of two rectangular plates hinged together at the center, with a curve of each blade up from the ground, formed at the end away from the hinge. During rolling, the foot can flex at its center hinge to react to the ground, and will dig into the ground starting at the curve of the blade, as necessary to create motion/thrust. When a spoke is actuated the applied pressure on the foot will "flex" the foot about its center hinge and/or sink the foot into soft soil.

Figure 4-3: IMPASS Virtual Model, Spoke-Wheel Prototype and Foot

The shape of the feet of IMPASS lends itself to the bulldozer blade studied in the work of Bekker and Wong [2-5].Models developed for the resultant force acting on the blade per unit width, caused by passive earth pressure and related to cutting depth, soil density, and soil friction, may provide a good measure for compaction thrust imposed upon IMPASS during the cutting of the foot into the soft soil. Pressure-sinkage relationships may be developed based upon the original work of Bekker, where rectangular plates were driven vertically into soft soil to impose a sinkage [2-4].

5 DESIGN OF EXPERIMENTS

This chapter discusses the design of experiments for the four sets of tests performed for this study. Descriptions of the experiment objectives, the parameters varied and studied in the tests, and the sampling methodologies for data collection are presented. In each of these tests vehicle-ground interaction parameters were studied.

The vehicle-terrain interaction parameters used in the presented mobility metrics matrix relate to one or both of two basic off-road vehicle characteristics—normal ground pressure in the vehicle-ground contact patch and vehicle locomotion platform sinkage into the ground. For this reason, these are the most intensively studied characteristics.

In Winter 2006 preliminary tests of a lightweight robotic tracked vehicle and a lightweight manned wheeled vehicle were performed and served as a learning experience in testing procedures. In Spring/Summer 2007 these tests were performed with a higher number of collected data points and more accurate procedures than the Winter 2007 tests. These Spring/Summer 2007 tests were performed with a lightweight wheeled all-terrain vehicle and focused on testing the effect of multiple levels of vehicle speed, vehicle payload, sand grain size, and sand moisture content on the sinkage of the vehicle into the ground and the normal pressures exerted by the vehicle on the ground in the contact patch. Secondary tests in Summer 2007 were conducted for the 100-pass performance of the lightweight wheeled ATV on two of the sands, emphasizing the cumulative run effect on the vehicle's sinkage into the ground and the pressure in the contact patch (mimicking, for instance, the effects of running a convoy of vehicles across a stretch of unimproved terrain). Preliminary tests on two of the robotic vehicles with novel walking locomotion platforms were also performed in Summer 2007 to study the robots basic vehicle-ground interaction. Observations on how the robotic feet interacted with the soft ground during stepping serve to better the direction of future foot-ground interaction modeling.

5.1 Experiment Objectives

The vehicle-terrain interaction parameters used in the presented mobility metrics matrix relate to one or both of two basic off-road vehicle characteristics—normal ground

pressure in the vehicle-ground contact patch and vehicle locomotion platform sinkage into the ground. Terrain composition and vehicle gross weight are considered in popular models for pressure vs. sinkage as static contributions, while vehicle speed is not often considered for its dynamic effect on these contact patch properties. Existing models were originally attained for heavyweight wheeled and tracked vehicles, and still require validation for their lightweight autonomous vehicle counterparts. To study the contact patch pressure and the sinkage of lightweight wheeled and tracked vehicles a series of preliminary and primary experiments have been designed to test for effects of sand gradation, moisture content, on-board payload, and vehicle speed.

5.2 Parameters Selected for Lightweight Wheeled and Tracked Vehicles Experimental Study

5.2.1 Vehicles

Two vehicle locomotion platforms were used in the experiments conducted for this portion of the study: wheeled and tracked. The tracked vehicle testing began in November 2006 and was left incomplete due to vehicle failure. These tests were conducted using MATILDA (Mesa Associates' Tactical Integrated Light-force Deployment Agent), a lightweight autonomous tracked vehicle developed by MESA Robotics and modified by the JOUSTER laboratory at Virginia Tech. Each wheeled vehicle test was conducted using one of two four-wheel all-terrain vehicle (ATVs). A 2004 Suzuki Eiger was used in the preliminary examination of wheeled vehicles, conducted in November/December 2006 (Winter 2006). Following this, a 2004 Honda Rancher was used in April-June 2007 (Spring 2007) experiments including more extensive dry sand testing, wet sand testing and 100-pass testing. Each of these vehicles was chosen for predicted ability to operate on sand and for the fit of some performance characteristics outlined in the 2000 U.S. Marine Corps TUGV Standards [6]. Some basic parameters for each vehicle are presented in Table 5-1.

Table 5-1: Basic Parameters of Vehicles Used in Experiment

Vehicle	Unloaded Weight	Payload Capacity	Estimated Vel. Range	L x W x H	Locomotion Platform Size	Estimated Turn Radius
MATILDA (tracked)	61lbs	125 lbs	0-2 mph	30" x 20" x 12"	20 inch contact length, 3 inch width each track	Omnidirectional (turns in place)
ATV Suzuki (wheeled)	577lbs (unmanned, dry)	200 lbs (Rear Rack)	0-35mph	85.6" x 44.1"x 50.0"	25 x 8-12 (Front) 25 x 10-12 (Rear)	9ft.
ATV Honda (wheeled)	511lbs (unmanned, dry)	150lbs (Rear Rack)	0-35mph	78.1" x 45.0" x 44.1", 49.3" wheelbase	24 x 8-12 (Front) 25 x 11-10 (Rear)	8.5ft

The MATILDA used in this study, shown in Figure 5-1 has an overall size of 30-inch length, 20-inch width, and 12-inch height during operation in the Winter 2006 experiments. Each of the two tracks is driven by one primary wheel that is configured angled up from the ground. Two main 5-inch diameter wheels at either end of MATILDA's length (separated by twenty inches from center to center) keep the 6 feet of 3-inch wide track moving and in tension, while three 1.5-inch diameter wheels exist between the two main wheels to keep the track in contact with the ground. The tread height is 0.3125 inch.

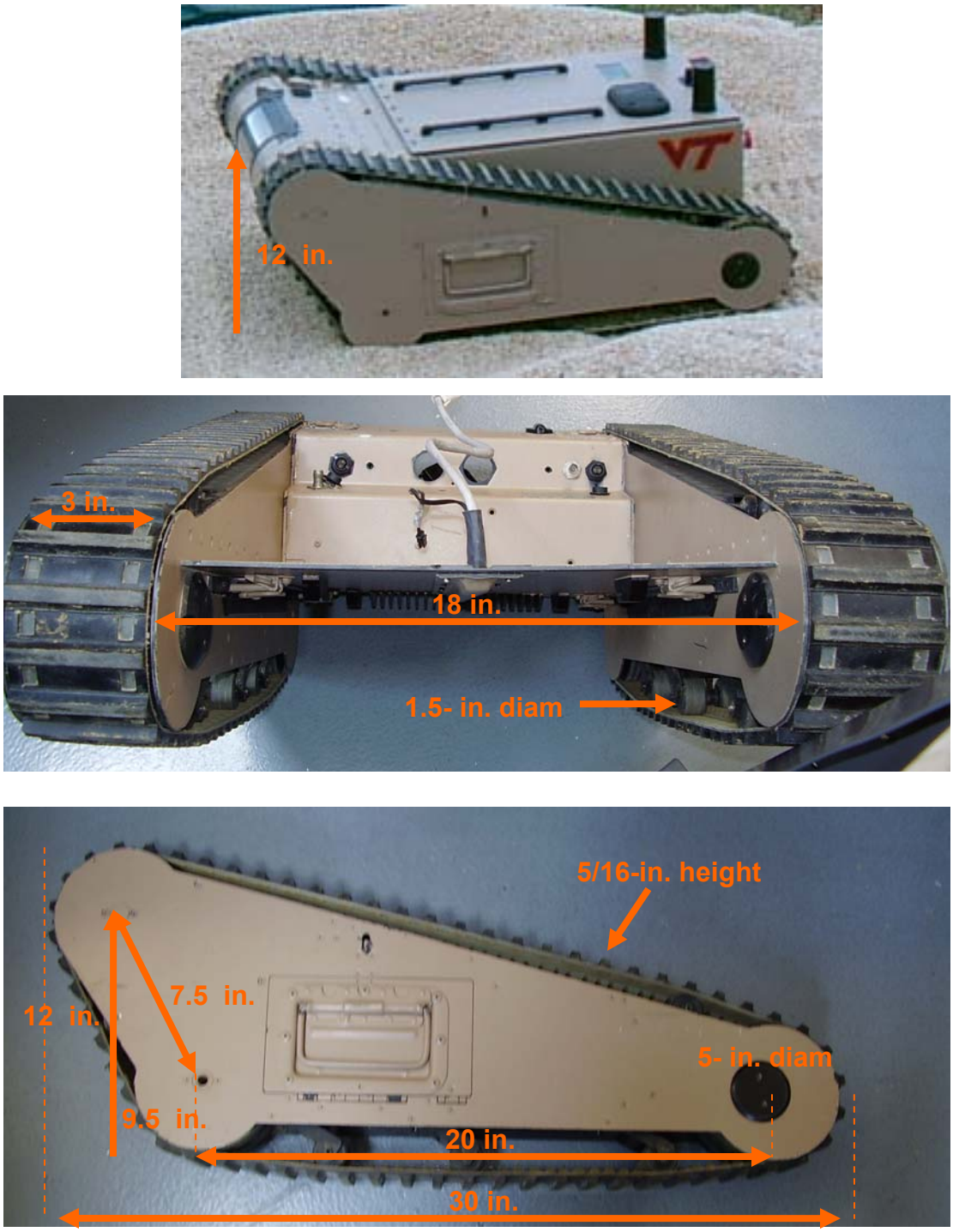

Figure 5-1: MATILDA Robot Used in Winter 2006 Study

The Suzuki Eiger measures 85.6 inches in length, defined by the direction of vehicle travel, 44.1 inches wide, and 50.0 inches tall with a wheelbase of 49.3 inches. The front tires are 25 x 8-12 inflated to 4-5psi, and the rear tires are 25 x 10-12 inflated to 4-5psi.

The tread depth is roughly 0.75 inch. The Eiger is powered by a carbureted 376cc single-cylinder four-stroke engine. The transmission is a foot pedal-shifting five-speed with an automatic clutch. The Eiger operates with a direct rear driveshaft in two-wheel drive mode. The rear suspension is an oil-damped swingarm. The ground clearance is 9.3 inches when unloaded. The front display, mounted between the handles, has an analogue speed display. The Suzuki Eiger is pictured in Figure 5-2.

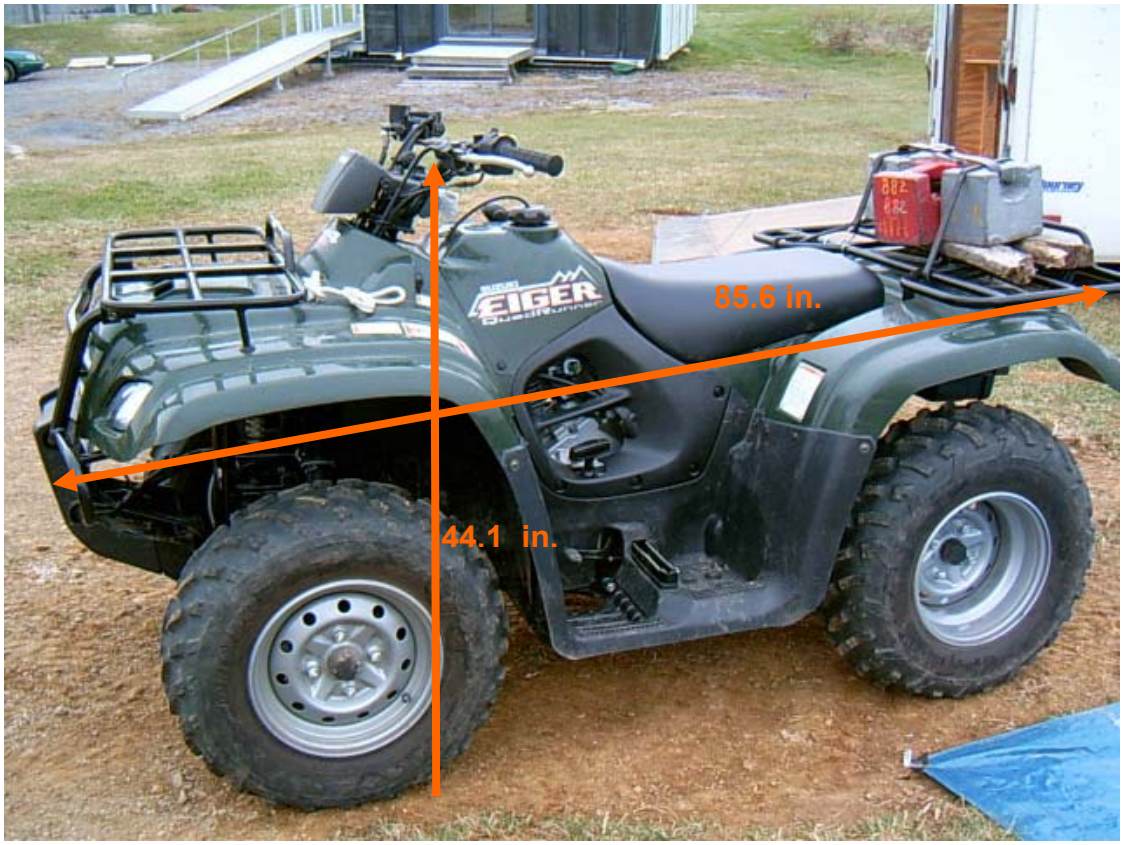

Figure 5-2: Suzuki ATV used in Winter 2006 Preliminary Study

The Honda Rancher measures 78.1 inches in length, defined by the direction of vehicle travel, 45.0 inches wide, and 44.1 inches tall with a wheelbase of 49.3 inches. Each of the tires is stock Dunlop Tracker CLs. The tread depth is roughly 0.5 inch. The front tires are 24 x 8-12 inflated to 3.5 psi, and the rear tires are 25 x 11-10 inflated to 3.5 psi. The Rancher is powered by a carbureted 329cc longitudinally-mounted, single-cylinder four-stroke engine fueled by a 3.43 US gallon tank. The transmission is an electric-shifting five-speed with an automatic clutch. The Rancher operates with a direct rear driveshaft in

two-wheel drive mode. The rear suspension is a swingarm with a single hydraulic shock and 5.9-inch travel. The ground clearance is 7.3 inches when unloaded. The wheels have a 7-degree caster angle. The front display, mounted between the handles, has a digital speed and gear display [31]. The Honda Rancher is pictured in Figure 5-3.

Figure 5-3: 2004 Honda ATV used in Spring/Summer 2007 Tests [31]

Both wheeled vehicles have a 5-speed manual transmission (the Suzuki has a foot shift, and the Honda has an electronic shift), and were operated in rear-wheel drive mode.

5.2.2 Sand

In all, five sands were used in this study, chosen according to their sand gradations and standards of purity. These five sands represent a range of average grain size. Each of the five sands is classified as fine, medium, or coarse according to the Unified Soil Classification System These five samples were chosen such that the bulk of the gradation (70% or more) fit between two standard U.S. sieves, so as to ensure the most uniform conditions. The coarsest sand (Best Sand 430) is close to classification as a gravel, having approximately 87% of the gradation by weight between 0.093-inch and 0.187-inch

diameter (passing U.S. Standard Mesh 4 and retained within either U.S. Standard Mesh 6 or Mesh 8). One of the midgrade sands (Best Sand 1020) has 71% of the sand granules having diameters between 0.0334 inch and 0.066 inch. The finest sand (Best Sand 110) is close to classification as clay, with 71% of the sand within a 0.029-0.059 inch diameter range. All sands have a sphericity of 0.8 and roundness of 0.8 [21]. The sands used for testing are shown in Figure 5-4. Each square grid is 0.20 inch on each side.

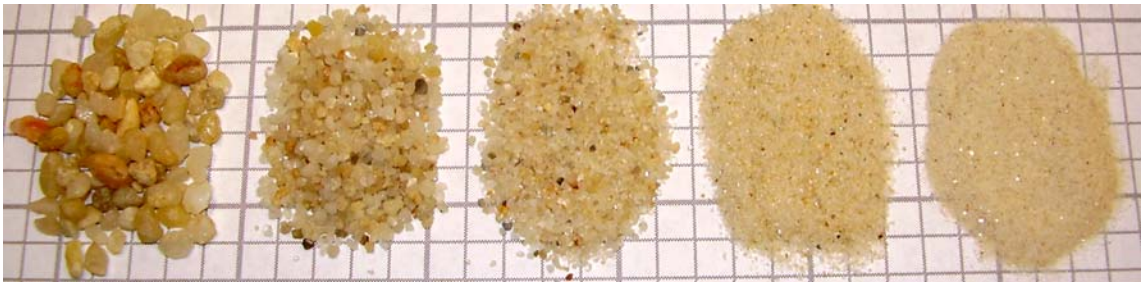

Figure 5-4: Sand from Experiments (Coarsest to Finest)

For the Winter 2006 all five sands were used. For the Spring 2007 extensive dry and wet sand experiments, all except for the finest sand was used. The finest sand was exposed to water during a storm and was not able to be dried sufficiently for the extensive dry testing. For the Spring 2007 extensive wet sand experiments, the same four sands from the dry experiment design were used. For the 100-pass tests, the second-most fine sand (Best Sand 550) and the coarsest sand (Best Sand 430) were used.

5.2.3 Moisture Content

In December 2006 preliminary tests all experiments were conducted at 0% moisture content. In April-June 2007 the dry sand tests were conducted with the sand at 0% moisture content. In May-June 2007 tests were also conducted on each of the sands at a 5-10% moisture content (by volume) throughout the sand pit, with the exception of occasional added moisture content at the bottom of the pit that was observed using the SMR probe. It is most likely that this heightened moisture content reading was a result of the probe being partially embedded in the soft soil surroundings, which were consistently wet. The bottom of each sand pit was visually inspected to ensure that no water pooled up at the bottom of the sand pit before testing. Most often the sand moisture content was between 5-8%, with a consistent 5-6% in the top 12-18 inches of sand. The 5-10%

moisture content level was chosen because it was observed to be the sands' natural water retention.

5.2.4 Payload

The United States Marine Corps TUGV standards set a threshold payload capacity of 150lbs, and a goal payload capacity of 300 lbs. As such, whenever possible, these payloads are included in the experiment design. For the Winter 2006 and Spring 2007 dry and wet sand tests, each vehicle had three payload settings, one of which was unloaded (with the exception of operator weight on the manned vehicles). The use of three payload settings allowed for detection of curvature in the experimental data, giving more insight into possible trends.

In Winter 2006 MATILDA carried 0 lb, 25 lbs, and 50 lbs. While MATILDA has a listed payload capacity of 125 lbs, after some preliminary testing at MATILDA's three expected operating speeds, the maximum payload was set at 50lbs to ensure movement at the lowest throttle power used for testing. In both the Winter 2006 preliminary ATV tests and the Spring 2007 extensive dry and wet sand tests the respective ATV carried payloads of with 0 lb, 75 lbs, and 150 lbs to accommodate the capacity of rear racks on the ATVs and meet the threshold TUGV standard [6]. Payload on the ATVs refers to weight added to the vehicle beyond the weight of the operator. The 100-pass test using the 2004 Honda Rancher was conducted with a 150 lb payload.

5.2.5 Speed

For all tests, with the exception of the 100-pass ATV tests, each vehicle operated with three speed settings. The use of three speed settings allowed for detection of curvature in the experimental data, giving more insight into possible trends.

In Winter 2006, MATILDA's mechanical controls allowed for a maximum speed of roughly 2 mph. Speed control was set in the computer control unit for levels of 50%, 75% and 100% throttle power. In Winter 2006 preliminary dry tests, the Suzuki Eiger minimum speed was set at 2 mph, incremented at 2 mph to the maximum speed of 6 mph. This maximum speed was set for driver safety. The Spring 2007 extensive dry and wet experimentations were conducted at a different location, allowing for the 2004 Honda

Rancher to be operated at 2 mph, 6 mph, and 10 mph. This maximum speed surpasses the TUGV standards for autonomous vehicle speed on secondary roads and cross-country terrain [6]. The 100-pass tests, conducted with the 2004 Honda Rancher, were performed at a 6mph speed.

5.3 Characteristics for Measurement

For all tests in this study two sets of data were collected. A Tekscan I-Scan 3150 pressure sensor embedded in the sand was used to record dynamic measurements of the contact patch pressure distribution as the vehicle ran over the pressure pad. This video reveals characteristics such as shape and distribution of pressure, peak pressure and its location, and average pressure. For all wheeled vehicle tests, the ATVs were operated in two-wheel drive mode with power at the rear wheels of the vehicle, so measurements of the pressure distribution were observed for the rear right wheel of the vehicle. For the preliminary experiments on MATILDA, measurements of the left track characteristics were taken. After each run measurements of center-track sinkage were taken within an area of sand over the embedded pressure sensor. These two features were studied because of their contribution to the basic measures of vehicle mobility.

5.4 Sampling Methodologies

5.4.1 Winter 2006 Preliminary Experiments of Wheeled and Tracked Vehicles

Each vehicle—MATILDA and the Suzuki Eiger—in this study represents a separate (independent) experiment. The general, the experiment guideline for each vehicle is a special case of the split plot design [32], with one blocking factor, one whole-plot factor applied as a balanced incomplete block design (BIBD), and two treatments for consideration, applied as split-plot factors using the randomized complete block design (RCBD), so that the overall design is characterized as SPD (BIBD,RCBD) [23]. The blocking factor is the day of experimentation, involving five levels or days. The whole-plot factor is the sand gradation, where each of the five gradations of sand was randomly assigned to a space of land, with four sand gradations tested per day. The split-plot factors were grouped such that the two effects of speed and payload were combined into

nine settings, representing all low-high-medium combinations (such as maximum speed with minimum payload). For a given day and sand gradation, the nine treatment groupings were randomly ordered to assign treatments to the sand. Each day of experimentation consisted of 72 unique runs (36 for each vehicle) for a total of 360 experimental runs in five days. For this first set of experiments the sands were dry.

5.4.2 Spring/Summer 2007 Extensive Wheeled Vehicle Tests on Dry and Wet Sand

In Spring 2007 the 2004 Honda Rancher wheeled ATV was tested on four of the available sands—the second finest through the coarsest—with two levels of sand moisture (dry and wet). The design for this test was significantly revised from the December 2006 design to add more data using a simpler design. The overall experiment design was a split-plot design with two whole plot factors of sand gradation (four levels) and moisture content (two levels), and two split-plot factors of speed (three levels) and payload (three levels). Within the split-plot experiment design there were two experiment designs—one at the whole-plot level and one at the split-plot level—to provide appropriate randomization to the factors at each level.

The culmination of this design was eight rounds of data collection, with most rounds completed within a single day of work. Each day, in a random order, four sand gradations were tested. For the first five days these sand gradations were dry and for the last three days these sand gradations were wet. On any given day, for each sand gradation 18 "runs" were made across the sandpit at one of nine speed-payload combinations, so that all nine combinations were used twice per sand pit per day.

In a split-plot design, whole plot factors are the factors applied to, in this case, whole physical plots of land. Whole plots are physical entities that are reused in combination with other factors within the experiment design to minimize the need for multiple samples [33]. In this design, whole plot factors are the sand grain size and the sand moisture level. The method of ordering the test sequence of grain size and moisture level is the whole-plot level design. Subplot factors are those treatments applied to the whole-plot factors in an order as dictated by a sub-plot level design [33].

The whole-plot level design had eight rounds of data collection. These rounds can be conceptualized as a blocking factor, and applied as random effect. This conceptual blocking provided for a daily schedule. This is a non-standard whole-plot level design, as the first five rounds of data collection had all sands tested under dry conditions, and the last three had all sands tested under wet conditions. This deviates from a standard design where both dry and wet conditions would be tested within the same round, and wet and dry levels would be tested evenly. Due to practical constraints of testing the sand, namely the incapability for the sand to be wet and dried between tests, this non-standard design was needed. The imbalance between dry testing days and wet testing days was also caused by time constraints. Because the rounds only represent a conceptual statistical block, they do not appear as a block in the data model.

At the whole-plot level, for each round of data collection the level of moisture (dry or wet) was assigned so that all dry sand data collection would be complete before wet sand data collection commenced. Within each round of data collection the order of which the sand gradations were tested was randomized.

The split-plot level experiment design involving the assignment of speed and payload treatments to each sand/moisture content combination within a given round, is a Generalized Randomized Complete Block Design or GRCBD. A Randomized Complete Design with two treatments (speed and payload) having three levels each creates the randomization of the order of the nine possible combinations of the treatments. The split-plot level design involves two replicates of the RCD, which is what makes it generalized. These two replicates are applied to each sand gradation/moisture content "round" on the whole-plot level (which can be thought of as a block for the RCD).

5.4.3 Multiple-Pass Experimentation of a Wheeled Vehicle

A second experiment was designed to look at the effects of compound vehicle loading on the contact patch pressure distribution and on the vehicle sinkage. The ATV was run with 150lb payload (non-vehicle weight additional to driver weight) at the maximum Spring 2007 speed of 10mph for 100 runs over four of the sands. At increments of ten runs, pressure data was taken during the run, and sinkage data after the run.

5.4.4 Preliminary Testing of Novel Locomotion Platforms

In Summer 2007 some preliminary tests were conducted on DARwIn, the bipedal robot under development at the Robotics & Mechanisms Laboratory (RoMeLa) at Virginia Tech, to examine the foot-ground interaction. The robot was tested three times on the middle medium grade sand, taking as many steps as possible before changing direction and going to the width-edge of the sand container or before the RoMeLa representative present during testing stopped the stepping to prevent DARwIn from falling.

6 EXPERIMENTAL SETTING

This chapter describes the main equipment used during the primary vehicle tests, the physical experiment sites and field conditions, and the daily operations for data collection. This chapter serves as a record of actions taken during the testing and a manual for future work.

6.1 Equipment and Calibration

6.1.1 Tekscan I-Scan Tire Footprint Pressure System

In order to record the pressure distribution in the contact patch of each of the vehicles, a Tekscan I-Scan 3150 pressure sensor was embedded into the sand during experimentation. The depth of embedding the sensor was used to offset any effect that the sensor would have on contact patch properties. The depth of embedment was several times greater than the sinkage seen in the data.

The pressure sensor can detect a maximum pressure of 125 psi. The roughly 5mills-thick pressure pad, shown in Figure 6-1 has an overall area of 20 inches x 19.65 inches, incorporating the 17.16 inches x 14.12 inches sensing region, housing a 52 x 44 grid of sensing lines to create 2288 sensels. There are roughly 9 sensels per square inch of sensing area. The pressure pad is secured to a 24-inches x 23-inches x 0.25-inch black plastic support, used to prevent scrunching of the sensor when embedded into the sand. There is a thin piece of copper weave fabric between the sensing pad and the black plastic support. On top of the sensor there is a thin sheet of plastic to prevent shearing damage to the sensor.

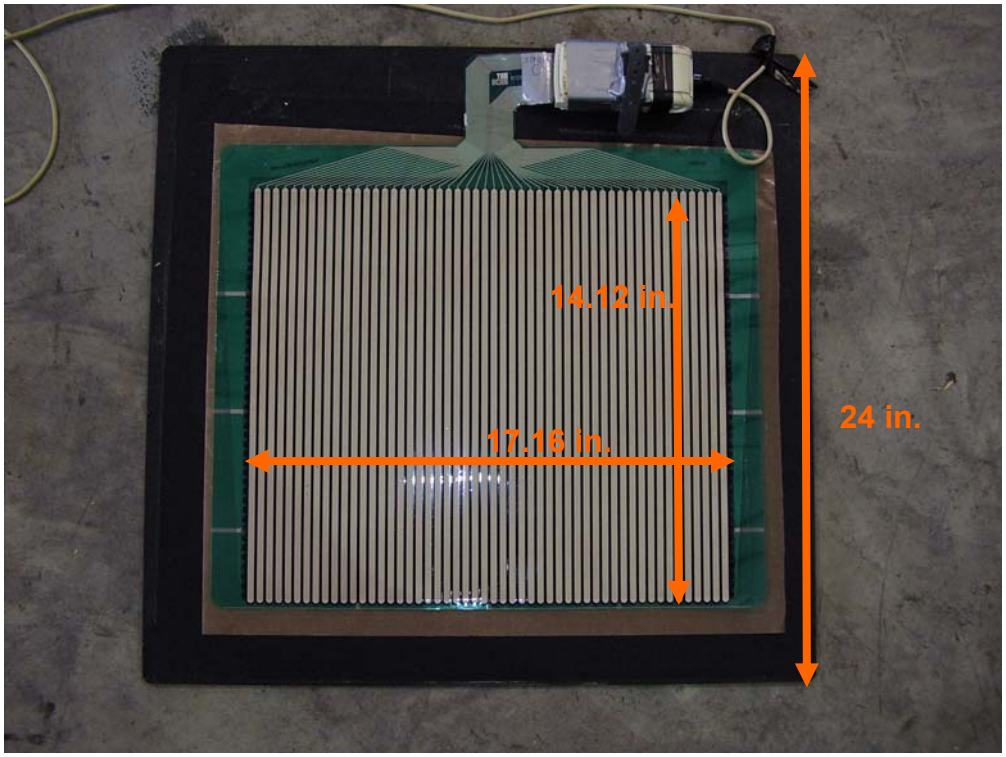

Figure 6-1: Tekscan I-Scan 3150 Pressure Sensor

In order to further protect from shear force damage (and, in turn, isolate the normal pressure in the sand from any shear force between the sensor and the sand) as well as to protect the pressure sensor from water, the unit was enclosed in a large plastic bag that was sealed at the top.

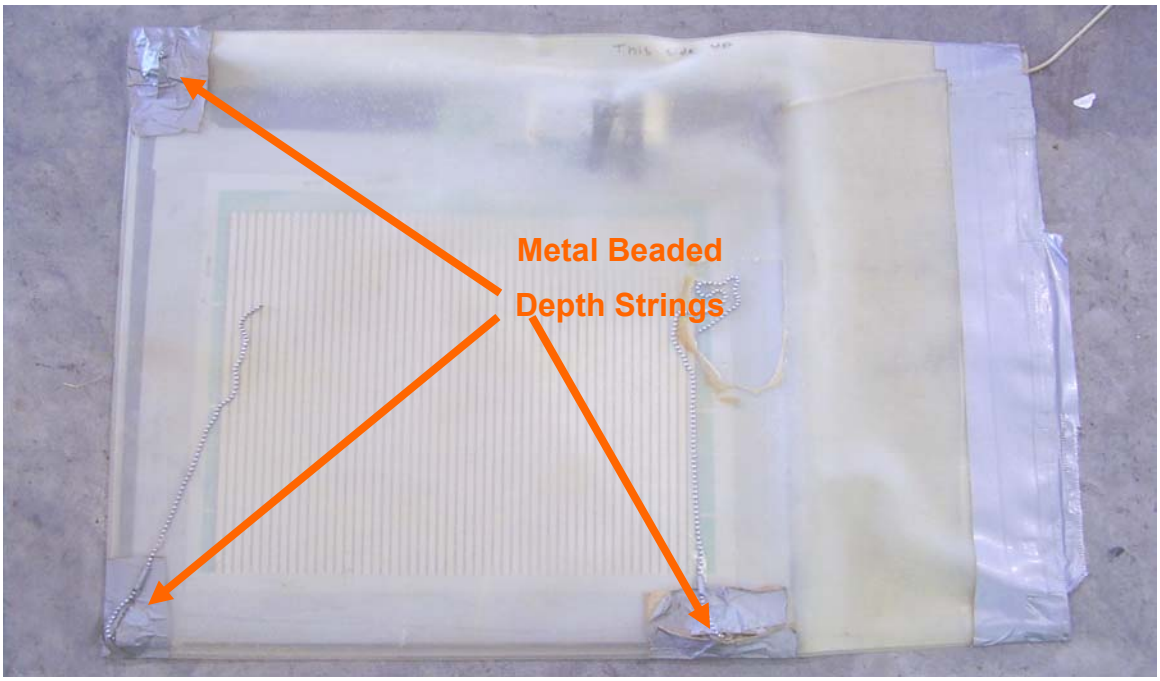

Figure 6-2: Tekscan Iscan 3150 Pressure Sensor in Protective Bladder

Equilibration was performed on the pressure sensor prior to calibration in order to ensure that all sensels reacted to a uniform pressure with a uniform reading.

In order to properly calibrate the pressure sensor for the Spring/Summer 2007 tests, the corner weights, or weights under each of the four tires, of 2004 Honda Rancher were measured using Longacre racing scales using the same loading conditions as in the field. These corner weights are summarized in Table 6-1. The focus for calibration was on the rear right tire. The ATV gas tank was between ¾ full and full. As can be seen in the corner weights, adding weight to the rear rack tilts the entire ATV back, so that the front tires are lifted and the rear tires carry more of the load. The difference between the 0-lb payload and the 150-lbs payload per the weight on the rear right tire is almost 100 lbs.

Table 6-1: Corner Weights of the 2004 Honda Rancher under Field Loading Conditions

Condition	Left Front Tire	Right Front Tire	Left Rear Tire	Right Rear Tire
Unloaded	124	136	138	135
Driver + 0lb	153	163	185	184
Driver + 75lbs	138	152	231	228
Driver + 150lbs	126	140	284	283

The Tekscan I-Scan manual includes a recommendation that the sensor be calibrated using two points representing 20% and 80% of the maximum expected test load. As the sensor is embedded in the soft ground, and as the vehicle is in motion during testing, the test load at the sensor location during experimentation does not reach the corner weights shown in Table 6-1 for a given payload scenario. The maximum rear wheel weight shown in Table 6-1, 283 lbs, corresponds to the 150-lbs payload. Because a 283 lbs payload spread over a significant portion of the sensor area represents sensel pressures already at the lower end of the capacity of the sensor, this weight was used to guide calibration. The two-point calibration was done using 38 lbs and 225 lbs to represent roughly 20% and 80% of the 150-lbs payload rear wheel weight from Table 6-1.

The pressure sensor was calibrated using sand weights created from the coarsest sand used in experimentation. This ensured that the weight on the sensor was distributed so as to avoid saturating any sensels and severely reducing the accuracy of the sensor.

6.1.2 Vertek Cone Penetrometer with Soil Moisture Sensor

An Applied Research Associates-Vertek DCP-1500 dynamic cone penetrometer with SMR probe was used to monitor moisture content in the sand during the wheeled and tracked vehicle experimentations. This probe records depth into the ground using a string potentiometer that was periodically calibrated as instructed in the manual. At the start of measurement the probe rests with the conical tip above ground, which corresponds to a negative depth reading. As the soil moisture bands, pictured in Figure 6-3, are driven under the surface of the sand the depth reading goes to zero, and then above zero to represent displacement into the ground. As the probe is driven into the sand, volumetric (% water present in sample by volume) moisture content readings are recorded and charted against depth into the ground. Temperature readings are simultaneously recorded.

Figure 6-3: Soil Moisture Resistivity Probe Used in the Field Experiments

Compaction was not recorded with the DCP-1500 due to the looseness of the sand. It can be expected that, unless specifically treated during a process like construction, sand in the top 12 inches of a site will be loose, showing a low relative density (the difference between in situ density and maximum possible density) [19].

6.1.3 Sinkage Measurement Instruments

Sinkage measurements were taken using a millimeter scale ruler measuring from the bottom of the tire implant up to a horizontal engineering scale (extending from the sand surrounding the tread to the area over the tread, perpendicular to the direction of vehicle travel). This technique is shown in Figure 6-4. During the Spring/Summer 2007 wheeled and tracked vehicle tests, the engineering scale was balanced on an Earth-level 4ft-long 2 inches x 4 inches plywood board embedded in the side of each sand pit, lengthwise to the direction of vehicle travel. This board was used during the grooming process so that the top of the board represents the height of the sand after grooming and prior to any vehicle

interaction with the sand. Sinkage was thus measured as the difference from the original height of sand and the height of sand after vehicle interference.

Figure 6-4: Sinkage Measurement Technique Employed in Spring/Summer 2007 Tests

6.2 Field Conditions

6.2.1 Winter 2006 Preliminary Experiments of Wheeled and Tracked Vehicles Experimentation Site

In Winter 2006 the site of the preliminary wheeled and tracked vehicle tests was a reasonably flat, grassy outdoor field in the Appalachian mountains of Blacksburg, Virginia. Space was limited so that the pits were stacked close together and speeds were reduced from what was originally envisioned. Approximately 4.5 tons of each of the five sand types was put into a hole dug into soft ground. Soft surroundings prevent interference that would exist with any hard supportive surface, such as concrete. Each hole was approximately 5-ft. wide, 7-ft. long (in the direction of vehicle travel) and 2.5 ft. deep, as can be viewed in the site dig presented in Figure 6-5.

Figure 6-5: Winter 2006 Test Site (Under Construction)

The weather varied with temperatures between approximately 20 and 50 degrees Fahrenheit, and cloudy, sunny, and windy weather. Testing did not occur during rain or snow. The field was not used if it was determined to be too muddy to provide adequate vehicle and personal traction, so as to avoid damaging the land or the sand pits.

6.2.2 Spring/Summer 2007 Site

In Spring/Summer 2007 the site of the extensive dry and wet sand wheeled vehicle tests was moved from the Winter 2006 site to a slightly sloped, grassy outdoor field in the Appalachian mountains of Blacksburg, Virginia. Five pits Approximately 4.5 tons of each of the five sand types was put into a hole dug into soft ground. Soft surroundings prevent interference that would exist with any hard supportive surface, such as concrete. Each hole was approximately 5.5-feet wide, 8-feet long (in the direction of vehicle travel) and 2-2.5 feet deep. To accommodate for the slope of the ground, extra length along the direction of vehicle travel was leveled by displacing or replacing excess dirt. This ensured that the vehicle approached the sand pits on a reasonably flat path, was perfectly flat upon entry and travel over the pit, and had a reasonably flat exit. If the exit could not be perfectly flush with the sand pit, the location of the exit bump up confirmed to be

placed so that the vehicle went on a tilt after the rear wheel was clear of the embedded pressure sensor.

Figure 6-6: Spring/Summer 2007 Test Site (In Use)

The weather varied with temperatures between approximately 60 and 90 degrees Fahrenheit, and cloudy, sunny, and windy weather. During dry sand tests, testing did not occur during rain. During wet sand tests, if the rain was only a light sprinkle, it was used as an advantage to combat moisture seepage into the sand pit (and away from the top layer of sand.). The field was not used if it was determined to be too muddy to provide adequate vehicle and personal traction, so as to avoid damaging the land or the sand pits.

During dry testing, if the sand did not appear dry to touch or sight, the sand was tested using the Vertek Soil Moisture Resistivity (SMR) probe to ensure dry sand in the top half or more of the sand pit. In the event that the sand was damp, it was air and sun dried until it was ready for testing.

During multiple-pass testing of the wheeled ATV, the sand moisture was measured prior to testing but not altered. This testing was done after the Summer 2007 extensive wet sand testing.

6.2.3 Preliminary Testing of Novel Locomotion Platforms

DARwIn, the bipedal walking robot, was tested indoors using a sandbox environment pictured in Figure 6-7. A roughly 14-inch wide, 4-feet long, and 5-inch thick cardboard box resting on concrete was used to contain a five-inch depth of the medium-grade sand. The lengths of the box were supported by plywood to avoid the edges warping and affecting the packing density of the sand. The sand was groomed flat to the edges of the container before each trial.

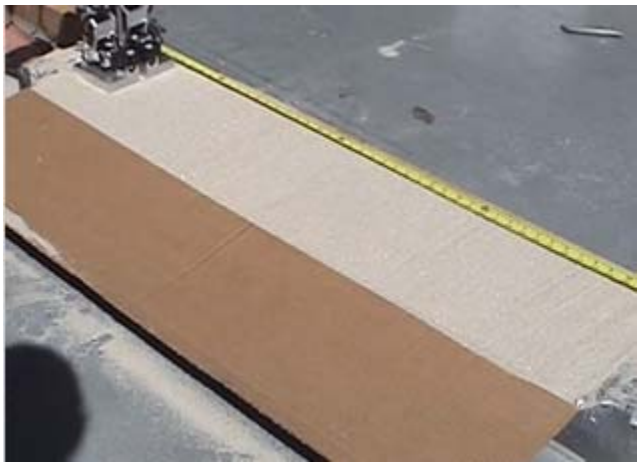

Figure 6-7: DARwIn Test Sand Container

6.3 Daily Operations and Data Collection

6.3.1 Winter 2006 Preliminary Experiments of Wheeled and Tracked Vehicles Testing Operations

In Winter 2006 preliminary tests of a lightweight wheeled 2004 Suzuki Eiger ATV and a lightweight tracked autonomous robot (MATILDA) were performed to study the effects of vehicle speed, payload, and sand gradation on the vehicle's sinkage and on the pressure distribution in the vehicle-ground contact patch. These tests are referred to as preliminary because they served as a learning experience for field operations and data collection. Ultimately the data collected from these tests showed a high level of

inconsistent variability for the studied parameters, and thus new, significantly revamped tests were performed in Spring/Summer 2007.

Land Preparation (Sensor Burial)

Simple, and later shown to be unreliable, methods were used to bury the pressure sensor at the desired depth during testing. This pressure pad was embedded six inches deep to record data for the ATV, and two inches deep to record data for MATILDA. In order to bury the sensor the hole in the sand was first groomed as flat for the senor to have an even surface on which to rest. For the ATV, a hole, approximately 6 inches deep, was dug into one corner of the sand pit. The sensor was placed in the hole and checked to be well-supported (no flexing when force was applied.) A 7-inch long right-angle triangle (speed square) was placed with one edge flat and flush against the sensor, close to the handle, and with the ruler extending upward. Sand was then piled onto the sensor up to the desired level (6 inches of sand for the ATV and 2 inches of sand for MATILDA). This method of burial occasionally resulted in folds in the protective bladder around the sensor, and therefore a loss of pressure distribution data.

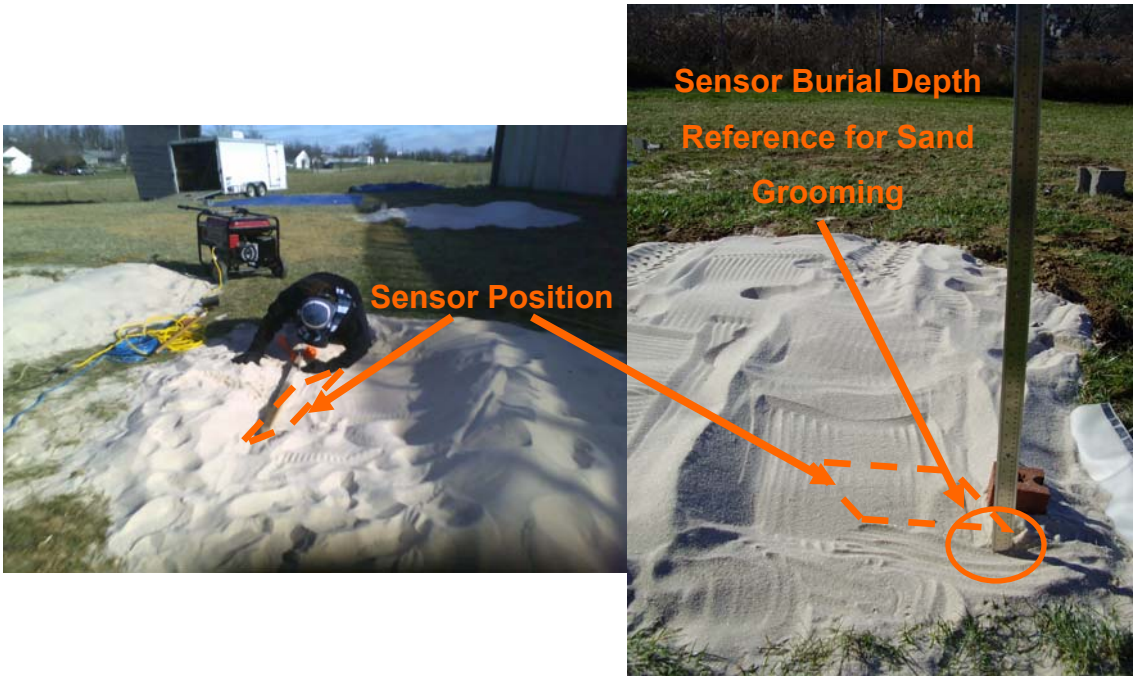

Figure 6-8: Winter 2006 Technique to Bury the Sensor and Monitor the Depth of Sensor Burial After Grooming

Pre-run Grooming Procedures

Prior to each run the sand pits were raked to dig up any compaction from crew members or previous vehicle runs. The sand was then smoothed over, flat to eyesight. For the MATILDA vehicle runs, a path was dug in the sand so that MATILDA could ramp down from the edge of the pit down to the area over the 2-inch embedded sensor. This ramping was possibly inconsistent from day to day, resulting in some variability in MATILDA's speed. MATILDA was horizontal when traveling over the pressure sensor.

For the ATV, combinations of 5 lbs, 10 lbs, and 50 lbs weights were secured to the rear rack to comprise the payload. For MATILDA, combinations of these same weights were added to on top of MATILDA's main body, isolated from the body using a lightweight postal packing cushion to prevent damage to the sensors below the weights.

Run Procedures

For this set of experiments the wheeled ATV was set in two-wheel drive mode, with power to the rear wheels. Speed was monitored by the driver using an onboard analogue

speedometer. The approach lane for the ATV to enter the sand pits was short relative to the maximum 6mph speed required for this set of experiments. The driver attempted to ramp up to the appropriate speed as far back from the sand pit as possible to ensure a consistent run over the sand pit. This was observably inaccurate at times, when the driver was forced to brake or accelerate right up to, and occasionally during entry to or run over the sand pit.

Figure 6-9: Winter 2006 Driver Gets Bearings on Driving the ATV over Targeted Sensor Area

The MATILDA tracked robot was computer operated for direction of vehicle travel and speed of vehicle travel in terms of percentage of available power to the throttle motors. MATILDA was set outside of the sand pit and put into motion at the exact desired percentage of power to the throttles (no ramp up to throttle power, but some ramp up to speed). If this failed, the power to MATILDA's throttles was increased until motion occurred, and then quickly reduced to the desired level. MATILDA was stopped when it ran into the soft edge of the pit.

Pressure for the ATV was measured for the rear right-side tire. Pressure for the MATILDA robot was observed for the front of the left track where one major support wheel exists. Occasionally the sensor was placed such that when MATILDA ran into the edge of the pit, the rear support wheel of the left track was not yet over the pressure sensor.

Post-Run Measurement Procedures

Three sinkage measurements were taken for each ATV and MATILDA run. These measurements were all taken in the tread or grouser imprint of the tread pattern. The data sinkage was taken above the pressure pad and in the center of the width of the tread pattern. Measurements were taken either by one person where he or she placed one lightweight engineering scale across the width of the tread pattern and on top of the crowning, or by two people spanning a meter stick over the crown of the travel pattern, with one person using an engineering scale to read the depth from the crossing bar down into the tread pattern. If the crowning was uneven, then the most average representative crowning spot was chosen. These techniques are demonstrated in Figure 6-10. For the ATV, the measurements were taken at the tip of the center-line tread arrow, spaced one tread arrow apart. For MATILDA the measurements were taken in the center of the rectangular grouser imprint, and spaced two grousers apart.

Figure 6-10: Winter 2007 Sinkage Measurement Techniques

Moisture Maintenance

The experiments to test the MATILDA robot and ATV in Winter 2006 were all performed on dry sand, as monitored using the ARA-Vertek SMR probe.

6.3.2 Spring/Summer 2007 Extensive Wheeled Vehicle Tests on Dry and Wet Sand Operations

The basic sensors remained constant between the November/December 2006 tests and the Spring/Summer 2007 wheeled tests. Advancements in daily operations in Spring/Summer 2007 were put in place to increase accuracy while decreasing run time from the Winter 2006 trials.

Land Preparation (Sensor Burial)

In each of the five sand pits, located uphill from the December 2006 site, two 4ft-long 2 inches x 4 inches plywood boards were embedded lengthwise in the direction of the vehicle travel, with one end of each board contacting the rear edge of the pit (rear being defined as the edge of vehicle entry during operation). Each time a sand pit was used for testing the embedded boards were checked to be level to the Earth and level with each other. These boards served three purposes: Reference for pressure sensor burial, assistance with sand grooming before each trial, and reference for sinkage measurements. A picture of this setup is shown as Figure 6-11.

Figure 6-11: Embedded Boards Used in Sand Pits in Spring/Summer 2007 Tests

The pressure sensor was buried so that the rear edge was 7-10 inches from the rear of the sand pit, and so that the handle edge was flat against the right-side board. This ensured that the sensor was placed in the same location each time. Two right-angle triangles (speed squares) were placed on top of the right-side board so that the ruler pointed downward. A long board was placed across the pit resting on the two side boards. Based on these rulers, a rectangular hole was dug 4.25 inches from the top of the board, so that when the sensor, secured to a 0.25-inch thick square plastic support, was placed in the hole, there was a four inch gap to from the top of the sensor to the top of the boards as marked by the longboard. The sensor was checked to be well supported (no flexing when pressure was applied), and level to the Earth (and therefore level to the boards). This burial step is pictured in Figure 6-12. After this preparation, sand was placed on top of the sensor up to the top of the side boards. To ensure that there were no wrinkles or air bubbles in the protective bag, a small layer of sand was smoothed from one side of the sensor toward the opening of the bag. The sensor was then tested for folds, and then fully covered.

Figure 6-12: Pressure Sensor Burial Using Level and Measured Height to Top of Sand (Used in Spring/Summer 2007 Tests)

Three beaded chains attached added to three points (corresponding to three corners of the black plastic sensor support) on the top of the protective sensor bladder. These strings were marked to show a four-inch height from the top of the sensor as shown on the sensor in Figure 6-2 and in use in Figure 6-13. Two of these strings were placed at the two corners of the sensor located away from the right-side embedded board. These were used periodically during each round to check that the burial depth of the sensor had not shifted between runs, and therefore that the sensor remained level and buried under four inches of sand.

Figure 6-13: Beaded Chain Used to Mark Correct Pressure Sensor Burial Depth in Spring/Summer 2007 Tests

Pre-run Grooming Procedures

Three key steps were used to eliminate error due to uneven sand grooming that was experienced in December 2006 preliminary tests. The first step occurred prior to each experimental run, when any tracks or sand disturbance were dug up during sand grooming to eliminate any residual compaction. This was performed using rakes that could dig down to the level to which the sensor was buried. This process is pictured in Figure 6-14.

Figure 6-14: Sand Grooming Using Rakes to Remove Sand Compaction (Spring/Summer 2007)

The second and third grooming steps involved the smoothing of the sand into a flat surface. The two embedded boards were used as rail guides to a six-feet long 2”x4” plywood board that was dragged over the top of the sand, remaining flat against each embedded board. This ensured that the area directly before, over and after the sensor was consistently flat from run to run, and that the sensor was buried under the same exact height of sand during each round. This also ensure that, while the rear wheel of the ATV was running over the sensor, the entire vehicle was on a smooth, flat, and level earth-level surface. As a final grooming step, the areas before and after the smooth square were groomed with rakes to ensure an even entry and exit path for the vehicle. The first of these two steps is pictured in Figure 6-15.

Figure 6-15: Smoothing the Top of the Sand Pit Prior to Each Run (Spring/Summer 2007)

These three grooming steps provided a smooth, Earth-level path for the vehicle to travel over while either tire was in contact with the sensor. This was especially important for the period of time when the entire vehicle was on top of the sand pit, which included the time during which pressure measurements occurred on the rear right tire. The added sand in the beginning of the pit (that was placed over the dirt in the entry zone right before the sand pit) also allowed the vehicle to adjust to some of the traction characteristics before entering the sand pit.

Run Procedures

Prior to each run the rear rack was loaded with combinations of 5-lbs, 10-lbs, and 50-lbs weights to achieve the desired payload. The payload weights were secured to the center of the rear rack using bungee chords. The ATV was checked to see that the fuel tank remained at or above three-quarters full. One 4-ft long 2 inches x 4 inches board was placed at both the entry and exit ends of the sand pit to be used by the ATV driver as a guide at which to aim the center of the vehicle. This helped to ensure a non-maneuvering straight path so that the rear right tire ran over the center of the sensor and so that both tires remained in the sand pit.

The driver operated the vehicle using the manual transmission with electronic shift such that the vehicle remained in second gear (1.933:1 gear ratio) for the 2 mph runs, and third gear (1.333:1 gear ratio) for both the 6mph runs and the 10mph runs. The driver began operating the vehicle at the desired speed at a reasonable distance before entering the sand pit so as to ensure the most constant and consistent speed operation. Power was always applied to the wheels during measurement so that the vehicle was not coasting or braking.

Pressure pad data collection was triggered using the Tekscan I-Scan software. The first significant contact onto the pressure pad, enacted by the front right tire, triggered the recording and roughly five seconds of recording thereafter.

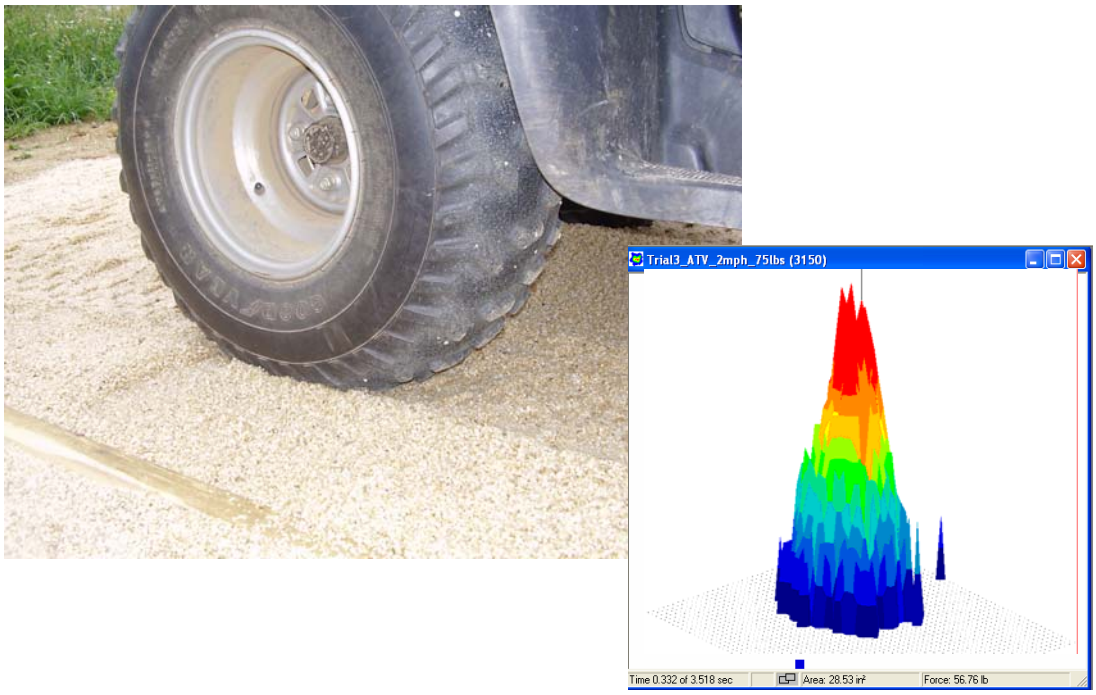

Figure 6-16: ATV Rear Tire Rolling Over Embedded Pressure Pad, and Corresponding Pressure Distribution Image

Post-run Measurement Procedures

After each run the embedded boards were used as references for sinkage measurements. An engineering scale was placed flat against the right-side board, extending through any sand crowning caused by the vehicle, and over the tracks themselves. In this manner,

"sinkage" was now, more accurately, measured as the difference between the original flat sand level and the vehicle-caused track depth, as pictured in Figure 6-17. In these new tests, six sinkage measurements were taken. Sinkage was measured at three points in the tread where the sinkage was due to carcass implantation only, and three points (directly after carcass measurements) where the sinkage was due to tread implantation. These measurements were taken close the rear edge of the sensor, the middle of the sensor, and the front (or exit) edge of the sensor. The two endpoints were marked using the aforementioned ball chains.

Figure 6-17: Sinkage Measurement Procedure for Spring/Summer 2007 Data Collection

Moisture Maintenance

A truck-mounted 500 gallon water tank with attached sprinkler was used to add moisture to the sand pits for the extensive wheeled vehicle testing on wet sand. This sprinkler imposed a rapid soaking of the pits with water sprayed over the entirety of the pit. Rakes and other tools were used to ensure an even spreading of the water.

For days when the sand pits were used for wet sand testing, the basic procedures for each run remained the same. The distinction between this testing and the dry testing was in the sand pit preparation. Three soil moisture readings (at the rear, middle, and front of the sand pit) were taken to ensure that the sand was evenly wet, both along the direction of vehicle travel and down within the sand pit, at the desired average moisture level for experimentation. Following this, every three runs over the pit a small amount of water was sprinkled evenly over the top of the water to combat evaporation and water seepage. If possible, after the 9^{th} run, another SMR reading was taken. At the end of each round (the 18^{th} run) a final SMR reading was taken to ensure that the sand moisture level had stayed consistent throughout the experimentation.

6.3.3 Multiple-Pass Experimentation of a Wheeled Vehicle

The procedures for the 100-pass tests of the lightweight wheeled ATV were similar to those outlined for the extensive wheeled vehicle tests. Each sand pit (of two) used for these experiments was initially groomed using the same procedures as outlined in Section 6.3.3. Following this initial grooming, the vehicle was run once over the pit at a speed of 10mph while carrying a 150lbs payload. After this, initial (first-run) pressure and sinkage measurements were recorded without disturbing the sand. The vehicle was then run another 99 times over the pit, with measurements (the same as outlined in Section 6.3.3) taken at increments of ten runs, totaling one hundred runs.

6.3.4 Preliminary Testing of Novel Locomotion Platforms

DARwIn conducted three trials taking continuous steps, once with a curved path and once straight across two feet of the middle medium-grade sand. Before each trial any residual compaction was raked up by hand, and the sand was groomed flat against the edges of the sand container. DARwIn was directed forward using a remote control joystick, and started from rest standing on top of the sand. DARwIn took continuous steps across the sand (no stopping or starting) until either changing direction toward the width-edge of the sand container or being stopped by the controller for robot safety. A representative from RoMeLa walked along with DARwIn as a precaution, holding his hands around DARwIn's 'head" in case of a failure (fall). Video recordings of the foot-ground interaction and of the overall walking performance were taken. Measurements of

sinkage at the center of each foot imprint were taken using the side of the container as a reference, separating left and right foot prints.

Figure 6-18: DARwIn Walking Along Sand Pit for Testing

7 EXPERIMENTAL FINDINGS AND INTERPRETATION

This chapter begins with a review of the statistical analysis tools used to process the Spring/Summer 2007 extensive lightweight wheeled vehicle tests on wet and dry sand.

The trials for the Winter 2006 tracked vehicle preliminary tests are qualitatively analyzed to make observations on contact patch properties and vehicle capabilities.

The sinkage data for the Winter 2006 wheeled vehicle preliminary tests was analyzed to test for the significance of each parameter (vehicle speed, vehicle payload, and sand grain size) on the sinkage response variable. The analysis, however, revealed a high and uneven amount of variability spread throughout the data. As such, under statistical analysis no factors were determined to be reliably significant on sinkage. This error was identified as most likely contributable to sinkage measurement methods and driver vehicle operation. Qualitative remarks are made for these experiments, including the notable contributions of these experiments to the improvements in data acquisition made in the Spring/Summer 2007 testing.

The data for the Spring/Summer extensive dry sand and wet sand testing was analyzed to test for the significance of each parameter (vehicle speed, vehicle payload, sand grain size, and moisture content of the sand) on both the (tread and carcass imprint) sinkage response variable measured at the tread indentation and the carcass indentation, as well as on the peak pressure in the contact patch, on the average pressure in the contact patch, and on the difference between the peak and average pressures in the contact patch. Testing for significance was performed using a standard statistical F-value test, based on a data model of how each parameter affects the outcome of the response variable.

The sinkage data for the Summer 2007 multiple-pass experimentation of the lightweight wheeled ATV was observationally analyzed for trends in the sinkage of the vehicle into each sand over time, and for differences between the two sands tested.

The sinkage data for the Summer 2007 preliminary trials of the walking robot DARwIn operating on sand are qualitatively analyzed to give insight into the scale of ground interaction for lightweight robots with novel locomotion platforms.

7.1 Statistical Models and Parameter Significance Tests

A data model consists of a response variable equated to the summation of effects of parameters and the interactions of parameters. The difference between the significance of a parameter and that of an interaction involving that parameter would be if, say, the speed of the vehicle alone did not dramatically affect the sinkage, but the various combinations (interactions) of speed and sand grade did affect sinkage. Models are specifically tailored to the method of data collection in order to properly account for what interactions may be present, what factors have been experimentally designed to not show an effect on the data, and which effects are fixed and which are random. An example of a data model for the effect of two parameters on a response variable might be

$$y_m = \mu + \alpha_i + \beta_j + \alpha\beta_{ij} + \varepsilon_{ijm} \tag{7.1}$$

where

$$\begin{aligned}
&\mu = \text{Mean value of the response variable} \\
&\alpha_i = \text{Effect of the } i^{th} \text{ level of the random or fixed parameter } A \\
&\beta_j = \text{Effect of the } j^{th} \text{ level of the random or fixed parameter } A \\
&\alpha\beta_{ij} = \text{Effect of the interaction of } i^{th} \text{ level of } A \text{ and the } j^{th} \text{ level of } B \\
&\varepsilon_{ijm} = \text{Random error, independent and normally distributed} \\
&\quad \text{with mean 0 and variance } \sigma_\varepsilon^2
\end{aligned} \tag{7.2}$$

where fixed effects are those resulting from factors with predetermined levels such that only inferences for those levels used in the experiment can be made, and random effects are those that result from the random selection of levels from many possible options such that those chosen can be considered to represent other levels in the selection pool. If a fixed effect interacts with another fixed effect, the interaction that results is a fixed effect. If a fixed effect interacts with a random effect, the resulting effect is a random effect.

Models can be refined and re-tested based on the results of the preliminary and subsequent F-tests on the full and refined models. For example, if the initial analysis shows that the effect of parameter B was insignificant, or the null hypothesis was not rejected, then the model could be retested eliminating β. Testing a reduced model allows for a more accurate analysis of the factors believed to be significant, by providing more

degrees of freedom for the individual test. In any given stage of refinement, if a higher-order term (two-, three, or four-factor interaction or higher) is to be tested, then its inclusive lower-order terms (main effects, main effects and two-factor interactions, main effects and two- and three- factor interactions, respectively) must be left in for data analysis regardless of their shown statistical significance. These can later be taken out on the basis of the last significance test, or at a stage of refinement that eliminates the higher-order terms containing it, assuming that the lower-order effects still show lack of statistical significance.

It should be noted that the model is not considered a data fitting, as in the tests for the response of sinkage will not give an equation to compute sinkage. The model will show which effects are or are not significant, and what level or relative importance these may have on the response variable. A separate data analysis must be done to fit the data, which requires numerical values for all parameters (exact and perfectly consistent levels of moisture, for example).

In standard F-testing a null hypothesis is formed stating that the effect of a given parameter or interaction on the response is insignificant or zero, with the alternate hypothesis being that the effect is significant or nonzero, or

$$\begin{aligned} H_0 &: \text{All } \alpha_i = 0 \\ H_a &: \text{All } \alpha_i \neq 0 \end{aligned} \qquad 7.3$$

where α_i is the effect of the i^{th} level of parameter A. When testing an interaction, the data can be sliced to identify the significance of each parameter within the interaction. The goal of an F-test is to prove, through analysis of the data for each parameter or interaction, that the null hypothesis is not true, and should therefore be rejected. Rejecting the null hypothesis indicates that the effect of a given parameter or interaction is significant. The level of significance, or the level of assurance that the parameter is significant, is shown in the *p*-value associated with each parameter. A lower *p*-value for one parameter over another indicates that the first parameter is more assuredly significant (and conclusively more significant) than the other. The *p*-value of a parameter or interaction also indicates the degree of detectible difference in the response values

(relative to the standard deviation in the data) as caused by the different levels of the parameter or interaction. If there is a large difference in the response variable values of different levels of a parameter, the lower *p*-value indicates a higher confidence that there is significance in the parameter's effect on the response.

Rejection of the null hypothesis is dependent upon the value chosen value of alpha, which represents the certainty in analysis that the null hypothesis has not been falsely rejected. If a given *p*-value is less than a chosen α, the null hypothesis is rejected. The lower the *p*-value, the higher the certainty. An α value of 0.05 represents 95% certainty, and one of 0.10 represents 90% certainty in correctly rejecting the null hypothesis. This former value represents stringent rejection criteria, and the latter value represents a more lax but acceptable rejection criteria. A *p*-value of around 0.10 then represents borderline significance of effect.

The significance of main effects can be analyzed in more detail by the adjusted *p*-values for the differences of least squares means between levels of each parameter, and by plots of the least squares means of response values related to each level of a parameter. The least squares means creates a comparison between the mean value of all data associated with one level of a given parameter and that of another level of that same parameter. The *p*-value is adjusted for more stringent testing, lowering the chance of falsely rejecting the null hypothesis that the effect is not significant.

The interaction of two parameters can be analyzed in more detail through interaction plots and data slices to see what causes the interaction to be significant. Interaction between two factors exists if the difference in the response for two levels of one factor is not constant across the levels of the second factor, indicating a response value dependence on the combination of both factors.

Interaction plots for two factors are created by analyzing the data to calculate a mean response value associated with each combination of levels of the two factors. These values are scattered on a plot of response value means versus the levels one factor (on the x-axis), with lines of constant levels of the second factor connecting sets of the scattered points. For example, if the interaction of two effects is examined, one effect having three

levels and the other having four, then twelve points would be plotted on the interaction plot (one for the average of all data taken for parameter *A* at its first level while parameter *B* is at its first level, and so forth). The profile lines (lines of constant level of the second factor) indicate the presence or lack of interaction. If the profile lines are not parallel, the interaction is significant. Nonparallel lines indicate that the expected change in the response value for a unit/level change in one factor depends on the level of the second factor (the gap shown on the plot/statistically detectible difference in response values between two or more profiles changes when changing levels of the x-axis factor). Interactions that are significant and that have profiles that appear to have similar trends (but do not cross) are orderly. Orderly refers to interactions in which the order of the means for levels of a given parameter remain the same, even if the magnitudes of differences between the levels of that parameter may change (for example, the gaps between the 2-mph and 6-mph profile lines change, but the 2-mph profile always remains above the 6-mph profile.) Orderly interactions are distinguished from parallel profile trends by the significance of the change in the gaps between the profile lines (and can be numerically distinguished using the significance of the data slices). Interactions that are significant and have dissimilar trends with crossing profiles are disorderly. A disorderly interaction might obscure main effects.

Data slices assist in providing some numerical explanation of interaction plots. The slices analyze only the response data involving both parameters in a given interaction. One parameter is held steady at one level, and the effect of each level of the second parameter on the value of the response variable is tested. This is repeated for all levels of the first parameter. If the level of detectible difference in the response variable (the *p*-value) associated with the varying factor for one level of the "steady" factor is different than that for another level of the "steady" factor, this indicates that the difference in the response variable between levels of the varying factor is not the same for all levels of the "steady" variable. Simply put, detectible difference in the response due to a change in one factor changes at different levels of the second factor.

For example, if analyzing the interaction of sand grade and vehicle speed, if the difference in the response going from 2mph to 10mph on grade 2 was different than that

of grade 5, then the 2 mph profile would be non-parallel with the 10 mph profile, and the *p*-value associated with grade 2 would be different than the *p*-value associated with grade 5. A larger the gap between profile lines for one level of the x-axis factor creates a larger *p*-value for the data slice associated with holding the x-axis factor steady and varying the profile line factor [32].

7.2 Winter 2006 Preliminary Experiments of Wheeled and Tracked Vehicles

7.2.1 MATILDA Lightweight Tracked Vehicle Test Observations

While MATILDA is specified by MESA Robotics as having a 150-lb payload capacity, preliminary experiments revealed that MATILDA would not reliably operate at lower speeds across flat sand with this heavy of payload. With several trials the 50-lb maximum payload was deemed reasonable to use in experimentation involving operation at the minimum (25%) power to the throttles.

Throughout the Winter 2006 experimentations MATILDA operated satisfactorily, only once failing to complete a data run. This failure occurred on the coarsest sand while MATILDA was set to run at the intermediate speed of 50% throttle power while carrying the intermediate payload of 25lbs. Overall, MATILDA was able to successfully operate on all sands at the minimum throttle power and maximum payload, though on occasion MATILDA, under the 50-lb payload, would not start from a full stop without increasing the throttle power above the 25% set by the experiment. After a few weeks of consistent daily use MATILDA's motors ultimately failed leading to the end of tracked wheeled experimentation.

Preliminary experiments also revealed that MATILDA was capable of climbing moderately steep (roughly 20-degree) mounds of unimproved sand of each type while not carrying payload. When 50-lb payload was added, however, during some trials MATILDA went into slip and did not have enough power to overcome the incline.

Figure 7-1: MATILDA Successfully Crossing a Large Mound of Loose Sand

Figure 7-2: MATILDA Successfully Crossing Uneven Sandy Terrain

The MATILDA robot tracks, when the vehicle operated at its highest throttle power carrying zero payload, often showed distinguishable but shallow grouser tread pattern,

while very slight sinkage of the rest of the track. For lower speeds and/or higher payloads, the entire track pattern was distinguishable for all of the test sands.

When deciding the depth to bury the pressure sensor the crew found that the image of the pressure reading caused by MATILDA running over a sensor buried under four inches of sand did not present any significant information. This lead to the different burial depths for the ATV and the MATILDA robot.

Pressure pad data taken during the Winter 2006 experimentations revealed that the 1.5-inch diameter track-supporting wheels did not create a sufficient enough normal force so as to cause any pressure readings for the length between the two main contact wheels at the front and rear of MATILDA. This is demonstrated by the force vs. time graph output from the IScan software, shown in Figure 7-3, revealing that in the time between front wheel contact and rear wheel contact, no force was measured for a 50% throttle, 50-lb payload vehicle run over finest sand Fine Sand. On some occasions, perhaps due to fluxuations in the sensor burial depth, MATILDA's impact on the pressure sensor was not distinguishable from noise in the data caused by the weight of the sand.

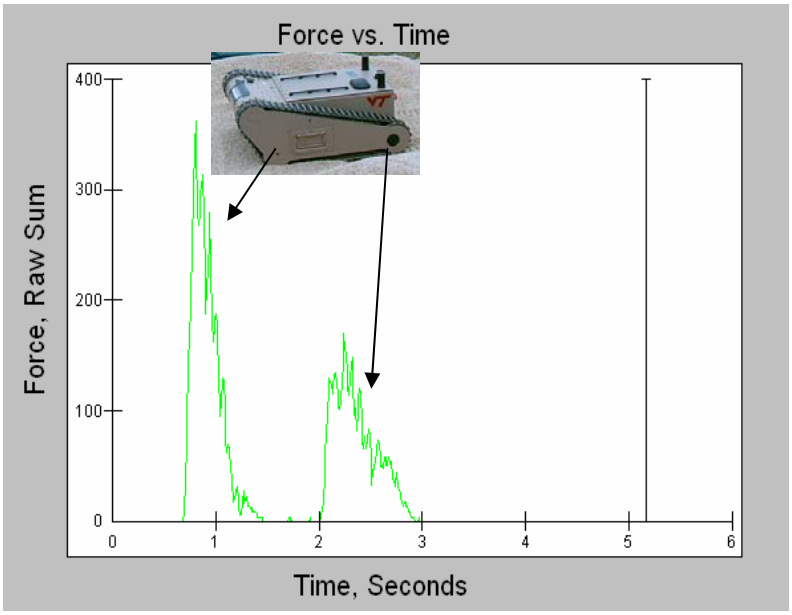

Figure 7-3: MATILDA Lightweight Tracked Vehicle Force vs. Time Graph for a Vehicle Run at 50% Throttle with 50-lb Payload

7.2.2 ATV Lightweight Wheeled Vehicle Test Data Observations

The original model for the Winter 2006 wheeled vehicle sinkage data

$$y_{ijklm} = \mu + \alpha_i + \gamma_j + \upsilon_k + \rho_m + \delta_{im} + \alpha\gamma_{ij} + \alpha\upsilon_{ik} + \gamma\upsilon_{jk} + \varepsilon_{ijkm} \quad 7.4$$

where

$$\begin{aligned}
&\mu = \text{Mean value of the sinkage} \\
&\alpha_i = \text{Fixed effect of the } i^{th} \text{ level of sand} \\
&\gamma_j = \text{Fixed effect of the } j^{th} \text{ level of vehicle speed} \\
&\upsilon_k = \text{Fixed effect of the } k^{th} \text{ level of payload} \\
&\alpha\gamma_{ij} = \text{Fixed effect of the } i^{th} \text{ sand and } j^{th} \text{ speed} \\
&\alpha\upsilon_{ik} = \text{Fixed effect of the } i^{th} \text{ sand and } k^{th} \text{ payload} \\
&\gamma\upsilon_{kl} = \text{Fixed effect of the } j^{th} \text{ speed and } k^{th} \text{ payload} \\
&\alpha\beta\gamma_{ijk} = \text{Fixed effect of the } i^{th} \text{ sand, } j^{th} \text{ moisture and } k^{th} \\
&\rho_m = \text{Random effect of the } m^{th} \text{ day} \\
&\delta_{im} = \text{Random effect for the wholeplot (sand pit) in } m^{th} \text{ round} \\
&\qquad \text{receiving the } i^{th} \text{ sand} \\
&\varepsilon_{ijkm} = \text{Random error, independent and normally distributed} \\
&\quad \text{with mean 0 and variance } \sigma_\varepsilon^2
\end{aligned} \quad 7.5$$

reduced to the results listed in Table. This table reveals that only the blocking factor day was significant to the data model. Examination of the error terms in the model data revealed a highly uneven scatter of error, which lead to the lack of distinguishable significance of any terms other than the daily blocking factor in the model.

Table 7-1: Winter 2006 Preliminary Wheeled Vehicle Sinkage Data, Type 3 Tests of Fixed Effects

Effect	Num DF	Den DF	F Value	Pr > F
day	4	11	2.87	0.0749
grade	4	11	1.30	0.3285
load	2	156	1.00	0.3709
speed	2	156	2.11	0.1251

The Winter 2006 tests of the lightweight wheeled Suzuki Eiger revealed that the vehicle was able to function reliably on all sands with all payloads.

At the 2-mph speed each of the sands showed reasonably neat tread patterns after the vehicle run. At the higher (6 mph) speed, the clearest tread patterns could be seen in the finest sands, with an observationally lower amount of sand "re-settlement" after the vehicle run. For the coarser sands the sand grains were more likely to slide around after the vehicle ran over the sand.

The driver had a short length of land in which to ramp the vehicle up to speed, and this was task could not performed with complete consistency of vehicle speed, resulting in an acceleration or deceleration of the vehicle while moving across the sand pits. During some trials not used for the experiment design, the driver applied the brakes while operating the ATV in two-wheel drive mode on sand. The vehicle was observed by members of the crew to plow a certain amount of sand in front of the front tires and a smaller amount also at the rear tires while experiencing significant slip. The tracks would be deeper than experienced in a normal run taken at the correct speeds.

During these experiments it became clear to the crew that several improvements could be made to the experiment design and collection. The vehicle speeds themselves, monitored by the driver using an analogue speed gauge, were difficult to accurately maintain. Due to the speeds being separated by only 2 mph, a driver error of 1 mph in either direction would present an opportunity for data to overlap. Beyond this, the sinkage measurements themselves were flawed, as there was no universal reference by which to measure the vehicle sinkage. If the crowing of the sand varied from run to run, as it did when observed by the crew, this variability was passed on to the data.

The pressure pad readings were also occasionally low in sensel readings (number of active sensels) during the course of the experiments. This lead to the change from a 6-inch burial depth to a 4-inch burial depth for the Spring/Summer 2007 tests.

7.3 Spring/Summer 2007 Extensive Wheeled Vehicle Tests on Dry and Wet Sand

In accordance with the split-plot experiment designed used for this testing, the full model (before data analysis and simplification) for both the tread and carcass imprint sinkage and pressure data is

$$\begin{aligned} y_{ijklm} &= \mu + \alpha_i + \beta_j + \gamma_k + \upsilon_l \\ &\quad + \alpha\beta_{ij} + \alpha\gamma_{ik} + \alpha\upsilon_{il} + \beta\gamma_{jk} + \beta\upsilon_{jl} + \gamma\upsilon_{kl} \\ &\quad + \alpha\beta\gamma_{ijk} + \alpha\beta\upsilon_{ijl} + \alpha\gamma\upsilon_{ikl} + \beta\gamma\upsilon_{jkl} \\ &\quad + \alpha\beta\gamma\upsilon_{ijk}l + \rho_m + \delta_{ijm} + \varepsilon_{ijklm} \end{aligned} \tag{7.6}$$

where

μ = Mean value of the response variable
α_i = Fixed effect of the i^{th} level of sand
β_j = Fixed effect of the j^{th} level of moisture
γ_k = Fixed effect of the k^{th} level of vehicle speed
υ_l = Fixed effect of the l^{th} level of payload
$\alpha\beta_{ij}$ = Fixed effect of the i^{th} sand and j^{th} moisture
$\alpha\gamma_{ik}$ = Fixed effect of the i^{th} sand and k^{th} speed
$\alpha\upsilon_{il}$ = Fixed effect of the i^{th} sand and l^{th} payload
$\beta\gamma_{jk}$ = Fixed effect of the j^{th} moisture and k^{th} speed
$\beta\upsilon_{jl}$ = Fixed effect of the j^{th} moisture and l^{th} payload
$\gamma\upsilon_{kl}$ = Fixed effect of the k^{th} speed and l^{th} payload
$\alpha\beta\gamma_{ijk}$ = Fixed effect of the i^{th} sand, j^{th} moisture and k^{th} speed
$\alpha\beta\upsilon_{ijl}$ = Fixed effect of the i^{th} sand, j^{th} moisture and l^{th} payload
$\alpha\gamma\upsilon_{ikl}$ = Fixed effect of the i^{th} sand, k^{th} speed and l^{th} payload
$\beta\gamma\upsilon_{jkl}$ = Fixed effect of the j^{th} moisture, k^{th} speed and l^{th} payload
$\alpha\beta\gamma\upsilon_{ijkl}$ = Fixed effect of the i^{th} sand, j^{th} moisture, k^{th} speed and l^{th} payload
ρ_m = Random effect of the m^{th} round
δ_{ijm} = Random effect for the wholeplot (sand pit) in m^{th} round receiving the i^{th} sand and j^{th} moisture
ε_{ijklm} = Random error, independent and normally distributed with mean 0 and variance σ_ε^2

7.7

where ρ_m and δ_{ijm} are mutually independent. When used, this model was analyzed using Statistical Analysis Software (SAS) v. 9.1 to process the data.

The three measurements of carcass imprint sinkage taken in each run were averaged to create one "carcass sinkage" data point per trial. The same was done for the tread imprint sinkage.

The pressure distribution data was processed to create three descriptive values: Peak pressure (average of top 20 values) in the contact patch, average pressure in the contact patch, and the difference between the two. Each data run produced a time series of frames

of pressure distribution pictures. To create the peak pressure (average of top 20 values), the Tekscan Iscan software was used to record the peak pressure felt by each sensel throughout the recording. From this picture, like the one shown in Figure 7-4, the top 20 values (including duplicate occurrences, if any) were extracted and averaged to compute the "peak" pressure. As can be observed in Figure 7-4, these correspond with the center of the tread pattern, where the sinkage was measured. To create the average pressure in the contact patch, the Tekscan Iscan software was used to record the average pressure felt by each sensel, only including non-zero values indicating that the tire was in contact with the area over the sensor. From this picture, like the one shown in Figure 7-5, the average of all of those values was taken to create a single "average" pressure in the contact patch. The third value for sinkage analysis is the difference between these two previous values, which can be used to indicate the spread of pressure within the contact patch.

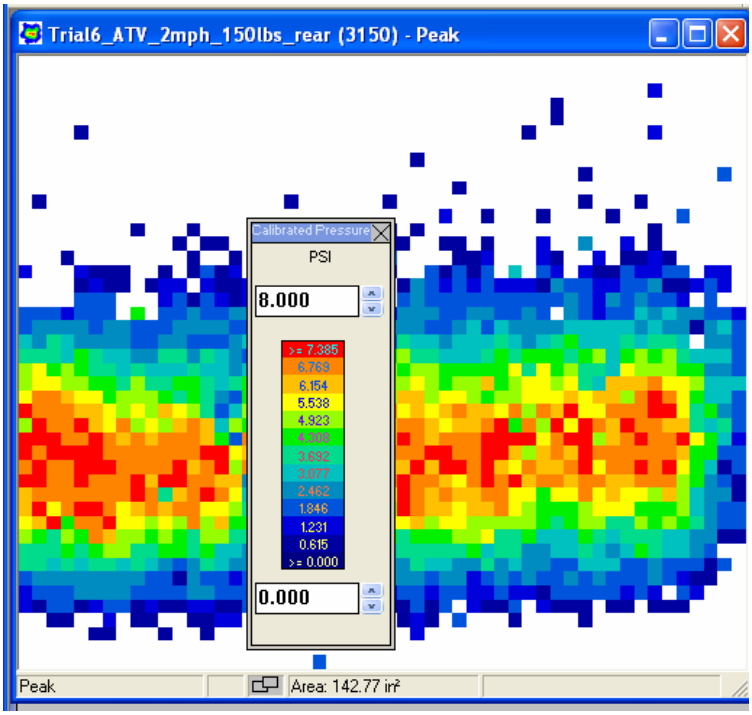

Figure 7-4: Peak Pressure Measured by the Sensels of the Tekscan Iscan 3150 Pressure Pad in throughout the Data Run Time History (Spring/Summer 2007 Tests)

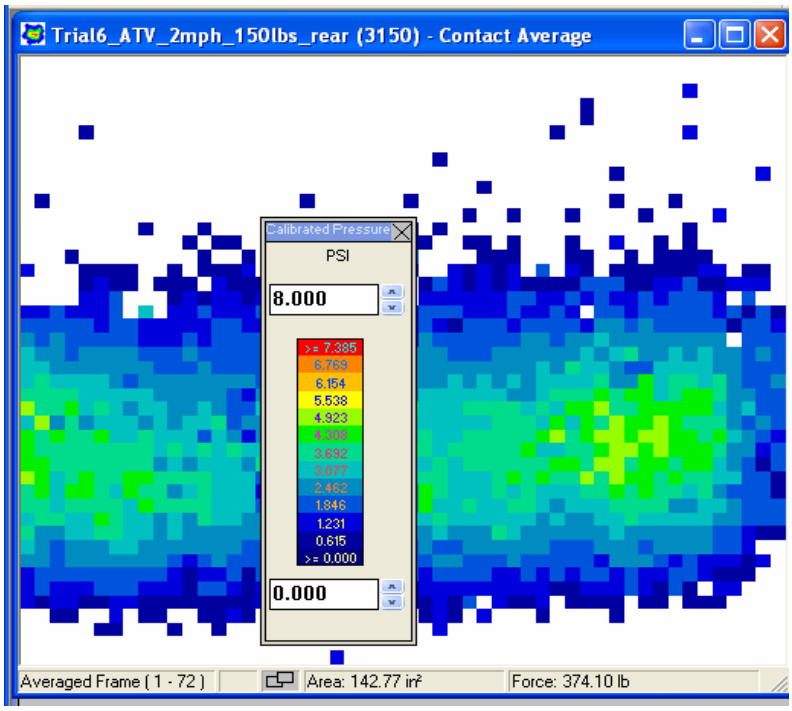

Figure 7-5: Average Pressure Measured by the Sensels of the Tekscan Iscan 3150 Pressure Pad in throughout the Data Run Time History (Spring/Summer 2007 Tests)

In this section, the full step-by-step analysis of the two sinkage models is shown to demonstrate the process of data refinement and the identification of significant main effects and interactions. The pressure data is presented with the final model and significance values (*p*-values) of only terms existing in the final model, followed by a review of significant two-level interaction terms.

The results of the analysis of the carcass and tread sinkage data, and the peak, average, and difference pressures are shown in

Table 7-2. This table shows which effects and interactions are significant for each of the response variables. Highly significant effects and interactions, with $p \leq 0.05$ are marked with H, while borderline significant effects and interactions, with $0.05 < p \leq 0.10$, are marked with B.

Table 7-2: Significance of Parameters in Spring/Summer 2007 Carcass Imprint and Tread Imprint Sinkage, Peak Pressure, Average Pressure, and Difference Pressure Models

	Sand	Speed	Payload	Sand *Moist	Sand *Speed	Sand *Payload	Moist *Speed	Speed *Payload	Sand *Moisture *Speed	Sand *Moisture *Payload
Carcass Sinkage		H	B	B	B					
Tread Sinkage				B			H			
Peak Pressure	H	H	H		H	H	H	B		H
Average Pressure	H	H	H		H		B		H	
Difference Pressure	H	H	H		H	H	H			H

7.3.1 Sinkage Data

Carcass Imprint Sinkage Data

The results of the F-tests performed on the full data model shown in Equation 7.5, applied to the carcass imprint sinkage, are shown in Table 7-3 all have values around or above 0.50, and can be eliminated from the model. The two-level and lower interactions are left in the model for further analysis and refinement. Had a three-level interaction not been eliminated, the two encompassed two-level interactions would have been left in for the next round of analysis testing.

Table 7-3: Spring/Summer 2007 Carcass Sinkage Data Full (Unrefined) Model Type 3 Tests of Fixed Effects

Effect	Num DF	Den DF	F Value	Pr > F
Grade	3	18	0.96	0.4323
Moisture	1	6	0.00	0.9520
Speed	2	480	6.24	0.0021
Payload	2	480	2.43	0.0888
Grade*Moisture	3	18	3.00	0.0580
Grade*Speed	6	480	1.92	0.0755

Grade*Payload	6	480	0.22	0.9694
Moisture*Speed	2	480	0.04	0.9636
Moisture*Payload	2	480	0.68	0.5065
Speed*Payload	4	480	0.66	0.6211
~~*Grade*Moisture*Pload*~~	~~*6*~~	~~*480*~~	~~*0.57*~~	~~*0.7573*~~
~~*Grade*Moisture*Speed*~~	~~*6*~~	~~*480*~~	~~*0.90*~~	~~*0.4954*~~
~~*Moistu*Speed*Payload*~~	~~*4*~~	~~*480*~~	~~*0.19*~~	~~*0.9434*~~
~~*Grade*Speed*Payload*~~	~~*12*~~	~~*480*~~	~~*0.32*~~	~~*0.9859*~~
~~*Grad*Mois*Speed*Payl*~~	~~*12*~~	~~*480*~~	~~*0.75*~~	~~*0.6988*~~

The first refined model, resulting from the analysis of the full model,

$$\begin{aligned} y_{ijklm} &= \mu + \alpha_i + \beta_j + \gamma_k + \upsilon_l \\ &\quad + \alpha\beta_{ij} + \alpha\gamma_{ik} + \alpha\upsilon_{il} + \beta\gamma_{jk} + \beta\upsilon_{jl} + \gamma\upsilon_{kl} \\ &\quad + \rho_m + \delta_{ijm} + \varepsilon_{ijklm} \end{aligned} \tag{7.8}$$

where

μ = Mean value of the response variable
α_i = Fixed effect of the i^{th} level of sand
β_j = Fixed effect of the j^{th} level of moisture
γ_k = Fixed effect of the k^{th} level of vehicle speed
υ_l = Fixed effect of the l^{th} level of payload
$\alpha\beta_{ij}$ = Fixed effect of the i^{th} sand and j^{th} moisture
$\alpha\gamma_{ik}$ = Fixed effect of the i^{th} sand and k^{th} speed
$\alpha\upsilon_{il}$ = Fixed effect of the i^{th} sand and l^{th} payload
$\beta\gamma_{jk}$ = Fixed effect of the j^{th} moisture and k^{th} speed
$\beta\upsilon_{jl}$ = Fixed effect of the j^{th} moisture and l^{th} payload
$\gamma\upsilon_{kl}$ = Fixed effect of the k^{th} speed and l^{th} payload
ρ_m = Random effect of the m^{th} round
δ_{ijm} = Random effect for the wholeplot (sand pit) in m^{th} round receiving the i^{th} sand and j^{th} moisture
ε_{ijklm} = Random error, independent and normally distributed with mean 0 and variance σ_ε^2 7.9

was tested for significance of each factor, the results of which are shown in Table 7-4 where the highest order effects that are not at all statistically significant are italicized and

crossed out. Payload on its own is borderline significant (with $\alpha = 0.10$ as the test significance threshold). Speed is highly significant. Moisture, on its own, and sand grade/grain size on its own are each not significant, but not eliminated in testing because of their presence in higher-order interactions. The significance of moisture and grade can be shown in their interaction with each other (significant), and the interaction of grade and speed (borderline significant). As the latter of these interactions (sand grain size and speed) is slightly above the borderline threshold these values set up for a second refined model for significance testing.

Table 7-4: Spring/Summer 2007 Carcass Sinkage Data, First Refined Model Type 3 Tests of Fixed Effects

Effect	Num DF	Den DF	F Value	Pr > F
Grade	*3*	*18*	*0.96*	*0.4323*
Moisture	*1*	*6*	*0.00*	*0.9520*
Speed	2	520	6.47	0.0017
Payload	2	520	2.52	0.0813
Grade*Moisture	3	18	3.00	0.0580
Grade*Speed	6	520	1.77	0.1037
~~*Grade*Payload*~~	~~*6*~~	~~*520*~~	~~*0.21*~~	~~*0.9743*~~
~~*Moisture*Speed*~~	~~*2*~~	~~*520*~~	~~*0.04*~~	~~*0.9623*~~
~~*Moisture*Payload*~~	~~*2*~~	~~*520*~~	~~*0.71*~~	~~*0.4941*~~
~~*Payload*Speed*~~	~~*4*~~	~~*520*~~	~~*0.70*~~	~~*0.5896*~~

The second refined model, serving as the final Spring/Summer 2007 carcass imprint sinkage data model

$$y_{ijklm} = \mu + \underbrace{\alpha_i + \beta_j}_{\text{Terms not significant Present in test because of appearance in higher-order terms}} + \gamma_k + \upsilon_l + \alpha\beta_{ij} + \alpha\gamma_{ik} + \rho_m + \delta_{ijm} + \varepsilon_{ijklm} \qquad 7.10$$

where

$$
\begin{aligned}
&\mu = \text{Mean value of the response variable} \\
&\alpha_i = \text{Fixed effect of the } i^{th} \text{ level of sand} \\
&\beta_j = \text{Fixed effect of the } j^{th} \text{ level of moisture} \\
&\gamma_k = \text{Fixed effect of the } k^{th} \text{ level of vehicle speed} \\
&\upsilon_l = \text{Fixed effect of the } l^{th} \text{ level of payload} \\
&\alpha\beta_{ij} = \text{Fixed effect of the } i^{th} \text{ sand and } j^{th} \text{ moisture} \\
&\alpha\gamma_{ik} = \text{Fixed effect of the } i^{th} \text{ sand and } k^{th} \text{ speed} \\
&\rho_m = \text{Random effect of the } m^{th} \text{ round} \\
&\delta_{ijm} = \text{Random effect for the wholeplot (sand pit) in } m^{th} \text{ round} \\
&\qquad \text{receiving the } i^{th} \text{ sand and } j^{th} \text{ moisture} \\
&\varepsilon_{ijklm} = \text{Random error, independent and normally distributed} \\
&\quad \text{with mean 0 and variance } \sigma_\varepsilon^2
\end{aligned}
\qquad 7.11
$$

where ρ_m and δ_{ijm} are mutually independent, was tested for significance of each factor, the results of which are shown Table 7-5. As both highest-order terms are significant, this test can serve as the basis for the final model. Lower-order terms contained within the significant higher-order terms can be eliminated based upon their *p*-values. The data requires no further refinement testing.

Table 7-5: Spring/Summer 2007 Carcass Sinkage Data, Second Model Final Type 3 Tests of Fixed Effects

Effect	Num DF	Den DF	F Value	Pr > F
~~*Grade*~~	~~*3*~~	~~*18*~~	~~*0.96*~~	~~*0.4323*~~
~~*Moisture*~~	~~*1*~~	~~*6*~~	~~*0.00*~~	~~*0.9520*~~
Speed	2	534	6.96	0.0010
Payload	2	534	2.28	0.1032
Grade*Moisture	4	11.1	2.28	0.0580
Grade*Speed	6	534	1.80	0.0978

The final model for the carcass sinkage data is thus

$$
y_{ijklm} = \mu + \gamma_k + \upsilon_l + \alpha\beta_{ij} + \alpha\gamma_{ik} + \rho_m + \delta_{ijm} + \varepsilon_{ijklm} \qquad 7.12
$$

where

μ = Mean value of the response variable

γ_k = Fixed effect of the k^{th} level of vehicle speed

υ_l = Fixed effect of the l^{th} level of payload

$\alpha\beta_{ij}$ = Fixed effect of the i^{th} sand and j^{th} moisture

$\alpha\gamma_{ik}$ = Fixed effect of the i^{th} sand and k^{th} speed

ρ_m = Random effect of the m^{th} round

δ_{ijm} = Random effect for the wholeplot (sand pit) in m^{th} round receiving the i^{th} sand and j^{th} moisture

ε_{ijklm} = Random error, independent and normally distributed with mean 0 and variance σ_ε^2

7.13

The contributions of particular levels of parameters to the *p*-values of the main effects can be studied through the differences of the least means squares of carcass sinkage for each parameter level, and graphically represented by the least squares means plots for each parameter. The cause of significance of an interaction of two parameters can be seen studied through data slices and graphically represented with interaction plots.

The main effects examined in the full model of the Spring/Summer 2007 carcass imprint sinkage data can be further scrutinized using Table 7-6. The first three lines in the table show that the difference in effect on the carcass imprint sinkage is most significant between the 0-lb payload and the 150-lb payload, and not detectible between the other two compared levels. The next part of the table shows that the difference in effect on the carcass imprint sinkage is most significant between operation speeds of 2 mph and 10 mph, and borderline significant between speeds of 2 mph and 6 mph. The rest of the table validates the lack of appearance of moisture content and sand grain size/grade as individual parameters (main effects) in the final model.

Table 7-6: Spring/Summer 2007 Carcass Sinkage Data, Differences of Least Means Squares to Compare Main Effects/Parameters

Effect	Moisture	grade	Payload	Speed	Moisture	grade	Payload	Speed	AdjP
grade		2				3			0.6571
grade		2				4			0.9844
grade		2				5			0.4618
grade		3				4			0.8493
grade		3				5			0.9871
grade		4				5			0.6707

Moisture	Dry		Wet		0.9520
Speed		2		6	0.0557
Speed		2		10	0.0013
Speed		6		10	0.4326
Payload	0		75		0.2723
Payload	0		150		0.0747
Payload	75		150		0.7962

The significance of the main effects tested in the full model of the Spring/Summer 2007 carcass imprint data can be seen in plots of the least squares means of the carcass imprint sinkage for each of the levels of the main effects parameters shown in Figure 7-6. These plots graphically represent the data used for comparisons made in Table 7-6. The *p*-value on each plot is associated with the last model refinement in which the parameter was tested. The main effect of speed shows a statistically significant increase in carcass sinkage with increasing speed, though only half as much for an increase from 6 mph to 10 mph as there is for an increase from 2 mph to 6 mph. The overall increase is 16mm, which is not a great amount when compared with the size of the vehicle itself. The same pattern is true for increased payload, although this effect is less significant because the change in sinkage between 75 lb payload and 150 lb payload is only half that of what it is when increasing speed from 6 mph and 10 mph. Again, these changes are only slight.

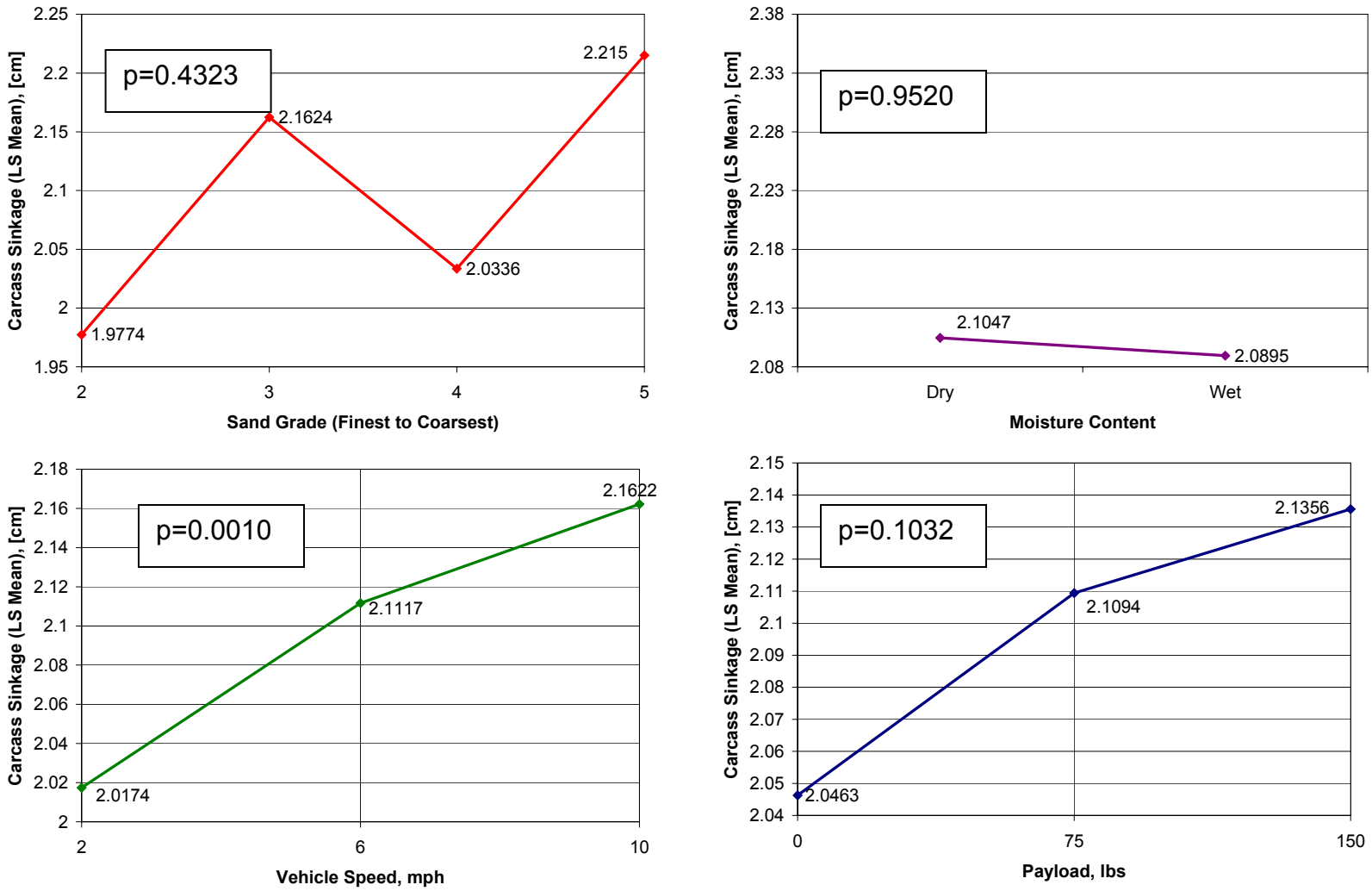

Figure 7-6: Least Squares Means of Spring/Summer 2007 Carcass Imprint Sinkage for Tested Main Effects

The data slices in Table 7-7 present information behind the two interactions in the final model of the Spring/Summer 2007 carcass imprint sinkage data. The first row of data in the chart can be read as the analysis of the sand grade-vehicle speed interaction isolating data from grade 2 and testing the significance (on the carcass sinkage) of varying the speed. As will be shown, the effect of interactions on the change of values of carcass and tread are greater in magnitude than those in the main effects.

Table 7-7: Spring/Summer 2007 Carcass Sinkage Data, Data Slices for Interactions in Final Refined Model

Effect	Moisture	grade	Speed	F Value	Pr>F
Grade*Moisture		2		3.27	0.0918
Grade*Moisture		3		0.00	0.9935
Grade*Moisture		4		0.30	0.5910
Grade*Moisture		5		1.15	0.3022
Grade*Moisture	Dry			0.96	0.4321
Grade*Moisture	Wet			2.59	0.0848
Grade*Speed		2		3.85	0.0220
Grade*Speed		3		4.60	0.0105
Grade*Speed		4		3.11	0.0456
Grade*Speed		5		0.45	0.6366
Grade*Speed			2	1.99	0.1424
Grade*Speed			6	0.72	0.5485
Grade*Speed			10	0.52	0.6739

The first four lines of Table 7-7, examining the sand grade-moisture content interaction, show that the difference between dry and wet moisture content is borderline significant on sand 2 (the finest sand in this test), but not on the other three sand grades. This shows in the interaction plot shown in Figure 7-7 where the biggest difference in carcass sinkage between the dry and wet profile line occurs at grade 2. The disorderly behavior of the profile lines contributes to the significance of this interaction. The behavior of dry sand seems to include an overall slight (statistically insignificant) decrease in carcass sinkage with an increase of grain size, while wet sand shows the opposite behavior with an overall increase (borderline significant) of sinkage with increasing grain size.

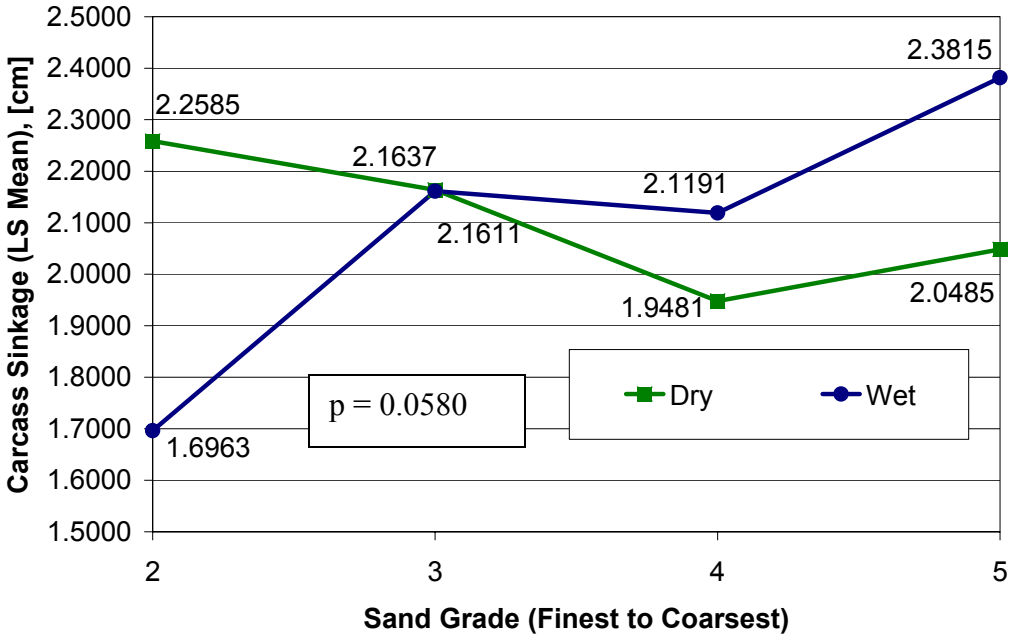

Figure 7-7: Spring/Summer 2007 Carcass Imprint Sinkage Data, Grade-Moisture Interaction (Moisture Profiles)

The next two lines in Table 7-7 examine the sand grade-moisture interaction holding the moisture level constant, and indicate that the differences in the carcass sinkage values between various levels of sand grain size are borderline significantly detectible for wet sand, but not at all (relative to the standard deviation) for dry sand. This shows in the interaction plot shown in Figure 7-8 where the most significant gaps between sand grade profile lines are at the wet level. This also shows that the most significant difference between dry and wet occurs with the slope along sand grade 2, while the other profile lines are horizontal or nearly horizontal, indicating no detectible difference in carcass sinkage going from dry to wet sand moisture. Again, this interaction exhibits disorderly behavior, with the grade 2 line (downward sloping) showing dramatically different behavior than the grade 3, 4, and 5 profiles (nearly horizontal, or slightly increasing). This indicates that the finest sand grade (grade 2) will affect a borderline significant decrease in carcass sinkage when wet, while sand 3 (a medium grade) stays roughly the same when wet, and grades 4 and 5 (medium sand that is coarser than grade 3, and a

coarse sand) have slight (not statistically significant) increases in carcass sinkage when wet.

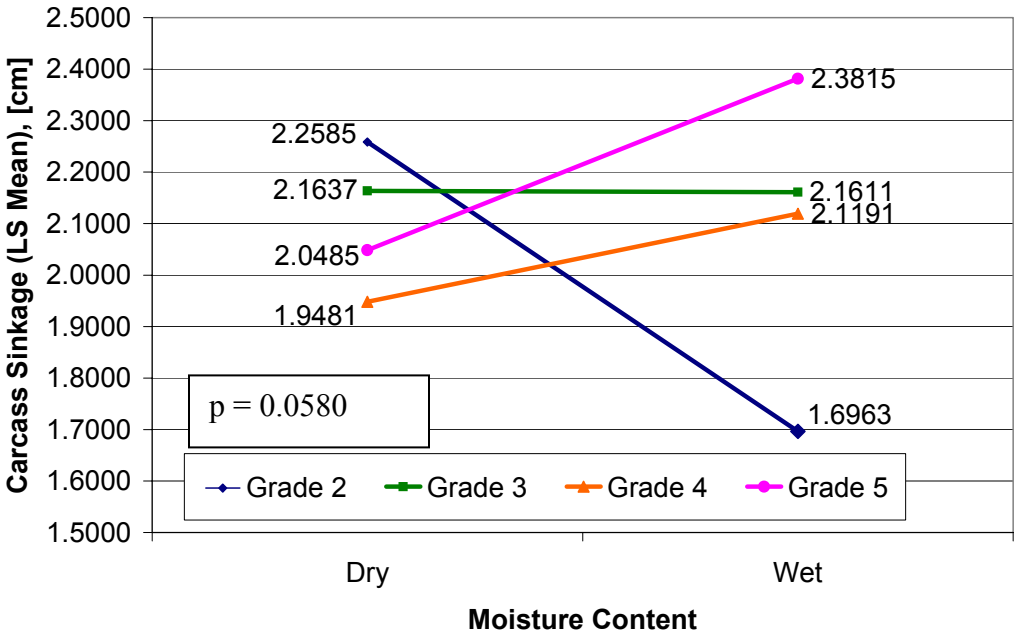

Figure 7-8: Spring/Summer 2007 Carcass Imprint Sinkage Data, Grade-Moisture Interaction (Grade Profiles)

The next four lines of Table 7-7, examining the grade-speed interaction, show that for the sand grades 2, 3 and 4, (numbered in order of increasing grain size) there is a significantly detectible difference in the carcass sinkage associated with different levels of speed (p-values below 0.05). For sand grade 5, the coarsest sand, there is not a detectible difference between the carcass sinkage associated with the different levels of speed (p-value not in the "significant" range). Simply put, differences amongst speeds show clearly on the fine and two medium sands (sands 2, 3, and 4) and not on the coarsest sand (sand 5). This difference in *p*-values (between highly significant and not at all significant) is what makes this interaction term borderline significant. These *p*-values are represented in the interaction plot shown in Figure 7-9, which shows parallel (and roughly equidistant) lines of constant speed over sand grades 2, 3, and 4. This indicates that for these three grades the differences between speeds are distinct (and of almost equal value) regardless of which sand grade the vehicle operates on (the carcass imprint

sinkage for the vehicle operating at 2 mph is roughly 0.20cm lower than that for 10 mph on grades 2, 3 and 4.) For grade 5, however, the carcass imprint sinkage for the vehicle operating at 2 mph is 0.04cm higher than that for 10mph on grade 5). In fact, the carcass sinkages at this grade are all quite close, which validates the high *p*-value for the grade 5 slice of the speed-grade interaction (indicating no significant differences of the carcass sinkage variable between the speeds.) If the grade 5 data did not appear in this data set, no interaction would be present. This interaction is disorderly due to the effects of sand grade 5 on the response of the carcass sinkage to speed. With the exception of grade 5, the carcass sinkage for the 2-mph speed is significantly lesser than that for the 6-mph speed is significantly lesser than that for the 10-mph speed.

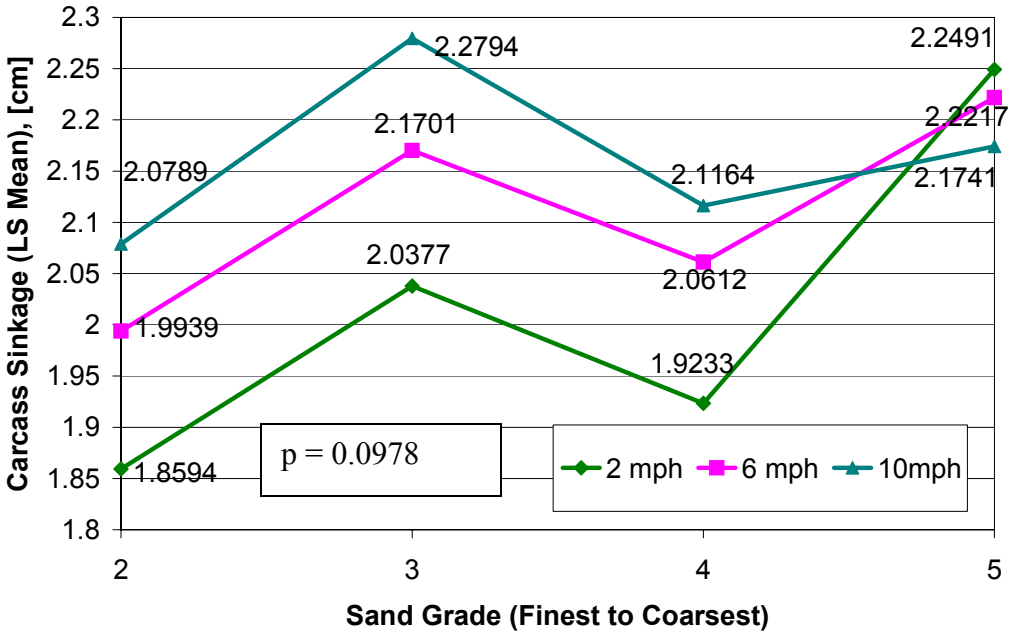

Figure 7-9: Spring/Summer 2007 Carcass Imprint Sinkage Data, Grade-Speed Interaction (Speed Profiles)

The last three lines of Table 7-7, examining the sand grade-vehicle speed interaction, show that the difference in carcass sinkage values between the various sand grades is greater at the 2 mph vehicle speed than the others. This is represented in the interaction plot shown in Figure 7-10, where the biggest gap between profile lines of constant sand grade occurs at the 2mph speed. The gap is smaller for the other grades that are

associated with large *p*-values in the non-significant range, verifying that the difference between grades for the 5 mph and 10 mph speeds is not detectible, relative to the standard deviation in the data. With the exception of grade 5, the sinkage for the finest grade (grade 2) is slightly lower than that for grade 3, is lower than that for grade 4, showing an increase in carcass sinkage with an increase in grain size for each tested speed, however these difference are not statistically significant.

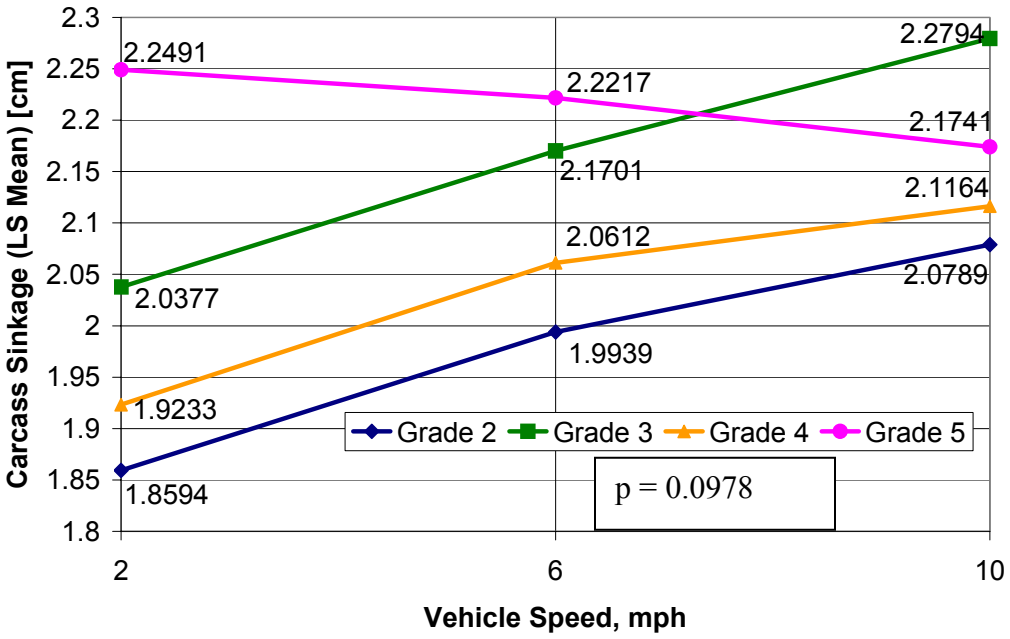

Figure 7-10: Spring/Summer 2007 Carcass Imprint Sinkage Data, Grade-Speed Interaction (Grade Profiles)

Table 7-8 shows the standard deviations spread amongst the data. Observing data by isolating each level of each parameter, the number of times a data point including that particular level is counted, and the standard deviation of the data at this isolated level was calculated. This table shows that, for each parameter the various levels have similar standard deviations, indicating that no one level had a significantly different amount of error than another. This table also shows that, amongst the various parameters the values for standard deviation are similar, around 0.37 cm.

Table 7-8: Spring/Summer 2007 Carcass Sinkage Data, Standard Deviations of Test Parameters

Standard deviations by GRADE

grade	FREQ	std
2	144	0.38567
3	144	0.36818
4	144	0.37502
5	144	0.35148

Standard deviations by MOISTURE

Moisture	FREQ	std
Dry	360	0.36315
Wet	216	0.38025

Standard deviations by SPEED

Speed	FREQ	std
2	192	0.37226
6	192	0.34923
10	192	0.38743

Standard deviations by LOAD

Payload	FREQ	std
0	192	0.39521
75	192	0.36752
150	192	0.34551

Tread Imprint Sinkage Data

The results of the F-tests performed on the full data model shown in Equation 7.5, applied to the tread imprint sinkage, are shown in Table 7-9 showing the SAS v9.1 output. The last column shows the *p*-values from each significance test. It can be seen that the three- and four-level interactions, italicized and crossed out, all have values around or above 0.50, and can be eliminated from the model. The two-level and lower interactions are left in the model for further analysis and refinement.

Table 7-9: Spring/Summer 2007 Tread Sinkage Data, Full (Unrefined) Model Type 3 Tests of Fixed Effects

Effect	Num DF	Den DF	F Value	Pr > F
Grade	3	18	0.38	0.7664
Moisture	1	6	0.87	0.3863
Speed	2	480	0.35	0.7060
Payload	2	480	0.81	0.4441

Grade*Moisture	3	18	3.00	0.0578
Grade*Speed	6	480	1.26	0.2760
Grade*Payload	6	480	0.45	0.8450
Moisture*Payload	2	480	0.55	0.5754
Moisture*Speed	2	480	3.83	0.0223
Payload*Speed	4	480	0.27	0.8985
~~*Moist*Grade*Payload*~~	~~*6*~~	~~*480*~~	~~*0.51*~~	~~*0.7989*~~
~~*Grade*Moisture*Speed*~~	~~*6*~~	~~*480*~~	~~*0.96*~~	~~*0.4517*~~
~~*Moist*Payload*Speed*~~	~~*4*~~	~~*480*~~	~~*0.22*~~	~~*0.9252*~~
~~*Grade*Payload*Speed*~~	~~*12*~~	~~*480*~~	~~*0.40*~~	~~*0.9646*~~
~~*Mois*grad*Payl*Speed*~~	~~*12*~~	~~*480*~~	~~*0.96*~~	~~*0.4836*~~

The first refined model resulting from the analysis of the full model

$$\begin{aligned} y_{ijklm} &= \mu + \alpha_i + \beta_j + \gamma_k + \upsilon_l \\ &\quad + \alpha\beta_{ij} + \alpha\gamma_{ik} + \alpha\upsilon_{il} + \beta\gamma_{jk} + \beta\upsilon_{jl} + \gamma\upsilon_{kl} \\ &\quad + \rho_m + \delta_{ijm} + \varepsilon_{ijklm} \end{aligned} \qquad 7.14$$

where

μ = Mean value of the response variable

α_i = Fixed effect of the i^{th} level of sand

β_j = Fixed effect of the j^{th} level of moisture

γ_k = Fixed effect of the k^{th} level of vehicle speed

υ_l = Fixed effect of the l^{th} level of payload

$\alpha\beta_{ij}$ = Fixed effect of the i^{th} sand and j^{th} moisture

$\alpha\gamma_{ik}$ = Fixed effect of the i^{th} sand and k^{th} speed

$\alpha\upsilon_{il}$ = Fixed effect of the i^{th} sand and l^{th} payload

$\beta\gamma_{jk}$ = Fixed effect of the j^{th} moisture and k^{th} speed

$\beta\upsilon_{jl}$ = Fixed effect of the j^{th} moisture and l^{th} payload

$\gamma\upsilon_{kl}$ = Fixed effect of the k^{th} speed and l^{th} payload

ρ_m = Random effect of the m^{th} round

δ_{ijm} = Random effect for the wholeplot (sand pit) in m^{th} round receiving the i^{th} sand and j^{th} moisture

ε_{ijklm} = Random error, independent and normally distributed with mean 0 and variance σ_ε^2 7.15

was tested for significance of each factor, the results of which are shown in Table 7-10 where the highest-order effects that are not at all statistically significant and are not contained in any higher-order effects are italicized and crossed out. Payload shows no significance in any form in the final model (as a main effect or as a part of an interaction) and can be eliminated. The significance of moisture and speed can be seen in their interaction with each other (highly significant), and the significance of moisture and sand grade can be shown in their interaction with each other (closely highly significant). Their inclusive lower-order terms (contained main effects of grade, moisture and speed) are left in the model for statistical refinement.

Table 7-10: Spring/Summer 2007 Tread Sinkage Data, First Refined Model Type 3 Tests of Fixed Effects

Effect	Num DF	Den DF	F Value	Pr > F
Grade	*3*	*18*	*0.38*	*0.7664*
Moisture	*1*	*6*	*0.87*	*0.3863*
Speed	*2*	*520*	*0.36*	*0.6987*
~~*Payload*~~	~~*2*~~	~~*520*~~	~~*0.84*~~	~~*0.4333*~~
Grade*Moisture	3	18	3.00	0.0578
~~*Grade*Speed*~~	~~*6*~~	~~*520*~~	~~*1.20*~~	~~*0.3038*~~
~~*Grade*Payload*~~	~~*6*~~	~~*520*~~	~~*0.55*~~	~~*0.7684*~~
Moisture*Speed	2	520	3.95	0.0199
~~*Moisture*Payload*~~	~~*2*~~	~~*520*~~	~~*0.57*~~	~~*0.5659*~~
~~*Payload*Speed*~~	~~*4*~~	~~*520*~~	~~*0.28*~~	~~*0.8914*~~

The second refined model for the Spring/Summer 2007 tread imprint sinkage data

$$y_{ijklm} = \mu + \alpha_i + \beta_j + \gamma_k + \alpha\beta_{ij} + \beta\gamma_{jk} + \rho_m + \delta_{ijm} + \varepsilon_{ijklm} \qquad 7.16$$

Terms not significant Present in test because of appearance in higher-order terms

where

μ = Mean value of the tread sinkage

α_i = Fixed effect of the i^{th} level of sand

β_j = Fixed effect of the j^{th} level of moisture

γ_k = Fixed effect of the k^{th} level of vehicle speed

$\alpha\beta_{ij}$ = Fixed effect of the i^{th} sand and j^{th} moisture

$\beta\gamma_{jk}$ = Fixed effect of the j^{th} moisture and k^{th} speed 7.17

ρ_m = Random effect of the m^{th} round

δ_{ijm} = Random effect for the wholeplot (sand pit) in m^{th} round receiving the i^{th} sand and j^{th} moisture

ε_{ijklm} = Random error, independent and normally distributed with mean 0 and variance σ_ε^2

was tested for significance of each factor, the results of which are shown in Table 7-11, where terms without statistical significance are italicized and crossed out. As both high-order interactions are significant and all terms not present in higher-order terms have been eliminated, this serves as the basis for the final model for the tread data. Unlike the carcass imprint sinkage data, for the tread imprint sinkage data no single fixed effect (moisture, payload, speed, or grade on its own) shows significance. As the interaction of moisture and sand grain size (grade) hovers slightly above a highly significant *p*-value (0.05), one more data analysis was run on the second reduced model.

Table 7-11: Spring/Summer 2007 Tread Sinkage Data, Final Model Type 3 Tests of Fixed Effects

Effect	Num DF	Den DF	F Value	Pr > F
~~*Grade*~~	~~*3*~~	~~*18*~~	~~*0.38*~~	~~*0.7664*~~
~~*Moisture*~~	~~*1*~~	~~*6*~~	~~*0.87*~~	~~*0.3863*~~
~~*Speed*~~	~~*2*~~	~~*480*~~	~~*0.35*~~	~~*0.6959*~~
Grade*Moisture	3	18	3.00	0.0578
Moisture*Speed	2	480	3.83	0.0190

The main effects in the final model of the Spring/Summer 2007 tread imprint sinkage data can be further scrutinized using Table 7-12. The lack of significance of any between-level comparisons for any parameters validates the lack of appearance of a main effect in the final model.

Table 7-12: Spring/Summer 2007 Tread Imprint Sinkage Data, Differences of Least Squares Means to Compare Main Effects/Parameters

Effect	Moisture	grade	Payload	Speed	Moisture	grade	Payload	Speed	AdjP
grade		2				3			0.8395
grade		2				4			0.9999
grade		2				5			0.8811
grade		3				4			0.8661
grade		3				5			0.9997
grade		4				5			0.8557
Moisture	Dry				Wet				0.3863
Speed				2				6	0.8544
Speed				2				10	0.6806
Speed				6				10	0.9510
Payload			0				75		0.5845
Payload			0				150		0.4431
Payload			75				150		0.9714

The lack of significance to the main effects shown in Table 7-12 can also be seen in plots of the least squares means of the tread imprint sinkage for each of the levels of the significant main effects parameters shown in Figure 7-11. These plots are to the same scale as the counterpart carcass sinkage plots. As can be seen, effects that were significant in carcass sinkage do not show the same spread of values in the tread sinkage data, so as to overcome standard deviation in the data and create significant differences. Grade, moisture, and speed, however, do show impact through interactions between the parameters. The *p*-value on the each plot is associated with the last model refinement in which the parameter was tested.

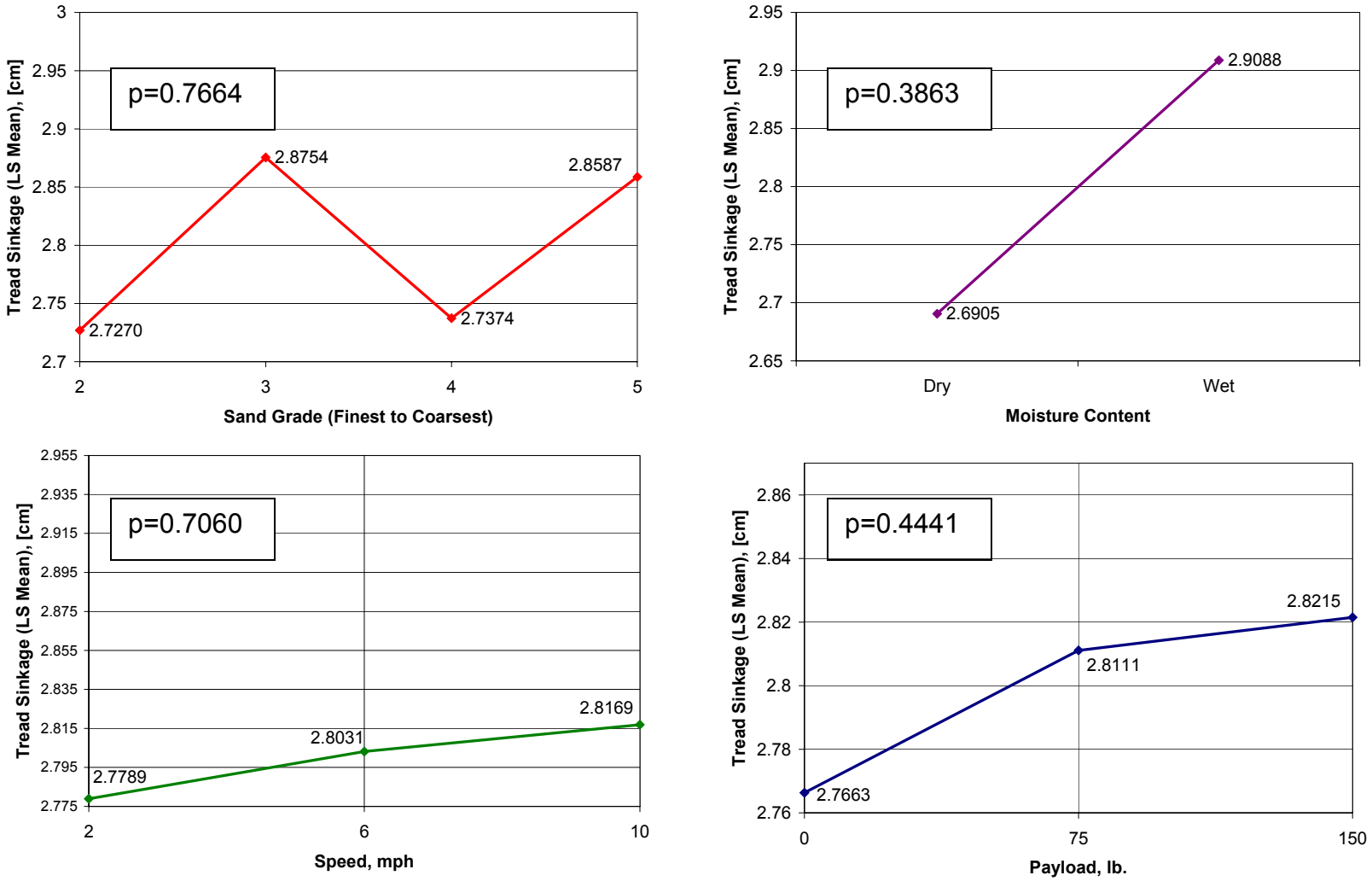

Figure 7-11: Least Squares Means of Spring/Summer 2007 Tread Imprint Sinkage for Tested Main Effects

The data slices in Table 7-13 present information behind the two interactions in the final model of the Spring/Summer 2007 tread imprint sinkage data. The first row of data in the chart can be read as the analysis of the sand grade-vehicle speed interaction isolating data from grade 2 and testing the significance (on the tread sinkage) of varying the speed.

Table 7-13: Spring/Summer 2007 Tread Sinkage Data, Data Slices For Interactions in Final Refined Model

Effect	Moisture	grade	Speed	F Value	Pr>F
Grade*Moisture		2		1.68	0.2119
Grade*Moisture		3		0.79	0.3863
Grade*Moisture		4		1.86	0.1911
Grade*Moisture		5		3.14	0.0944
Grade*Moisture	Dry			1.45	0.2621
Grade*Moisture	Wet			1.84	0.1763
*Grade*Speed*		*2*		*1.62*	*0.1999*
*Grade*Speed*		*3*		*0.61*	*0.5441*
*Grade*Speed*		*4*		*0.17*	*0.8466*
*Grade*Speed*		*5*		*1.53*	*0.2172*
*Grade*Speed*			*2*	*0.90*	*0.4570*
*Grade*Speed*			*6*	*0.31*	*0.8163*
*Grade*Speed*			*10*	*0.28*	*0.8387*
Moisture*Speed			2	0.12	0.7371
Moisture*Speed			6	0.95	0.3639
Moisture*Speed			10	1.99	0.2039
Moisture*Speed	Dry			1.29	0.2771
Moisture*Speed	Wet			2.67	0.0700

The first four lines (highlighted in grey) of Table 7-13, referring to the sand grade-moisture content interaction, indicate a borderline significance for the difference of the tread sinkage varying moisture content on sand grade 5. The other sand grades do not show significant *p*-values for varying moisture content. This shows in the interaction plot shown in Figure 7-12a, where the biggest difference in carcass sinkage between the dry and wet profile line occurs at grade 5. These non-parallel lines indicate significance of the interaction term. The next two lines in Table 7-13 examine the sand grade-moisture interaction holding the moisture level constant, and indicate that the differences in the carcass sinkage values between various levels of sand grain size are not significantly detectible for wet or dry moisture content. However these trends in the interaction plot shown in Figure 7-12b, resembling the corresponding plot for the carcass sinkage data,

exhibit nonparallel trends with changing gap sizes and order with respect to greatness of response magnitude, which makes the interaction term significant. In this interaction grade 2, the finest sand, seems to affect a small (though statistically insignificant) decrease in tread imprint sinkage when wet (versus dry), while the other coarser (than grade 2) grades show an increase in tread imprint sinkage when wet. Only the increase on grade 5 is statistically significant, and it is borderline. The magnitude of the difference in sinkage for sand 2 when wet and dry, though, is almost the same as that for sand 5. These trends are similar to those shown in the tread sinkage data.

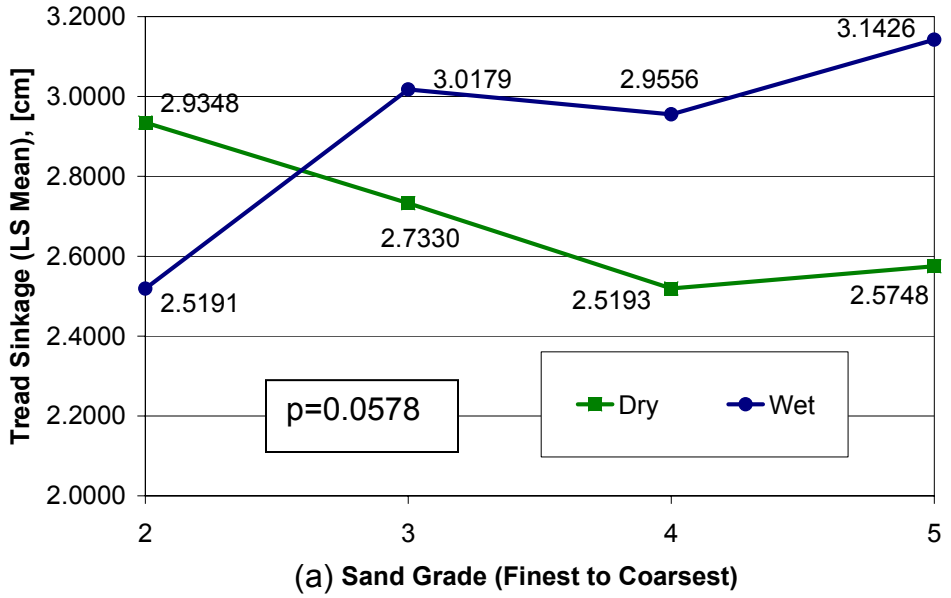

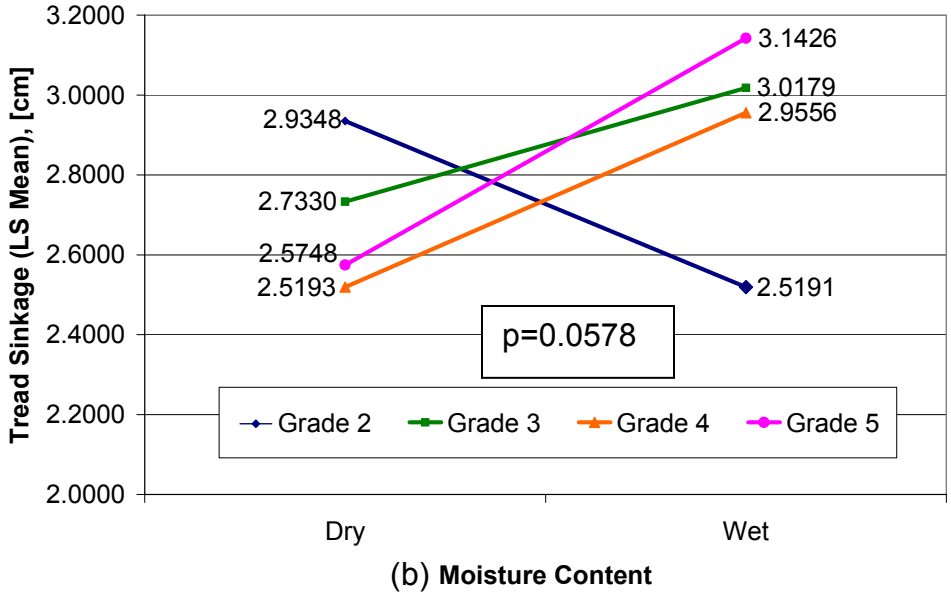

Figure 7-12: Spring/Summer 2007 Tread Imprint Sinkage Data, Grade-Moisture Interaction (a) Moisture Profiles and (b) Grade Profiles

The next seven lines of Table 7-13 do not show any interaction between sand grade and vehicle speed for tread sinkage. Examining the interaction plots shown in Figure 7-13, similarities can be seen in trends appearing in the corresponding plots for the carcass sinkage. This interaction is not significant because the differences in the response variables are not large enough to overcome the standard deviation in the data (the values

are too close, relative to the standard deviation). While the standard deviations between tread imprint sinkage data and carcass imprint sinkage data are almost equal, the gaps shown here are not as large as those seen in the carcass sinkage data, as can bee seen using the same scales between the similar plots.

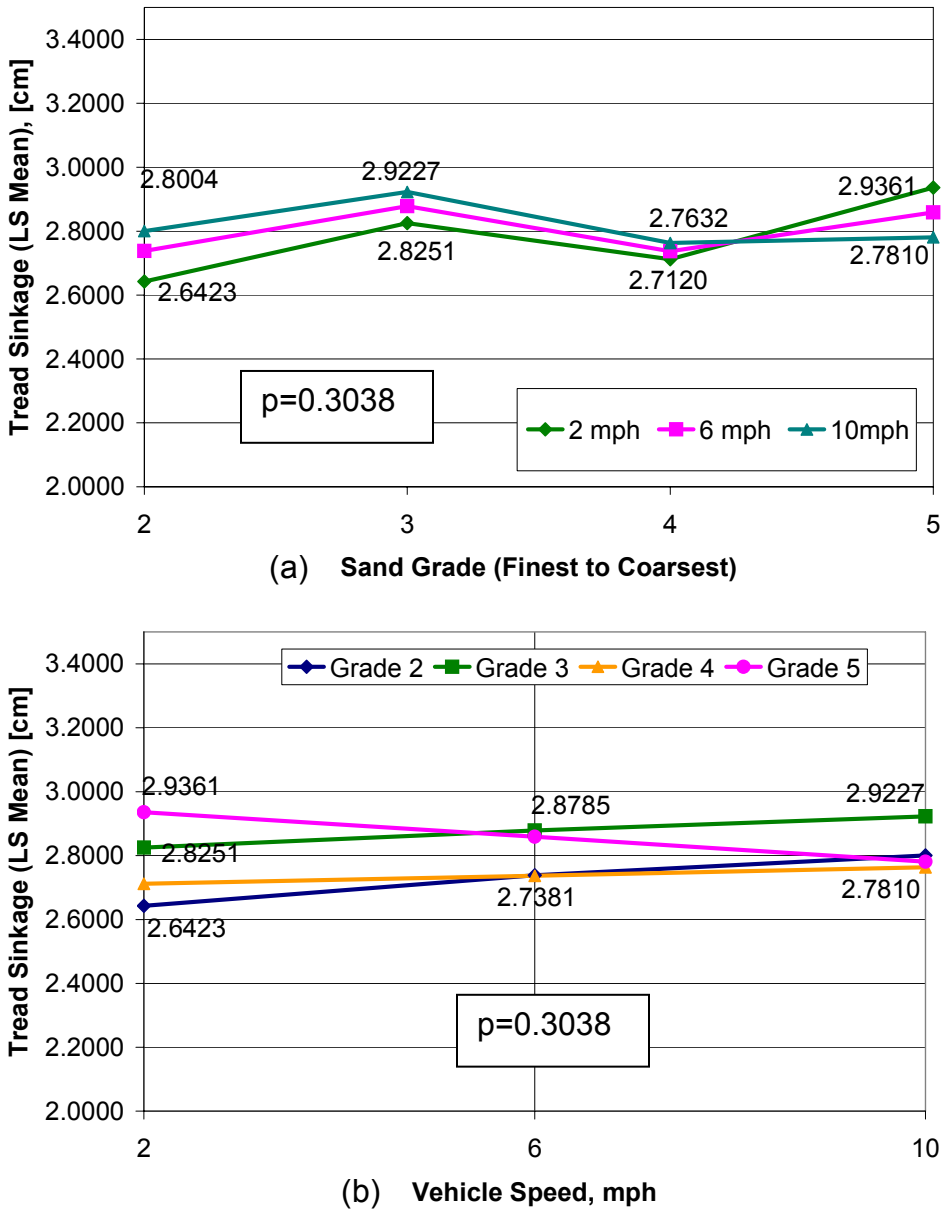

Figure 7-13: Spring/Summer 2007 Tread Imprint Sinkage Data, Grade-Speed Interaction (a) Speed Profiles and (b) Grade Profiles

The last set of five lines of Table 7-13, referring to the moisture content-vehicle speed interaction indicate a borderline significance in varying speed along the wet moisture content level, and no significance to the same for the dry moisture content level. This difference shows in the interaction plots with non-parallel profile lines, exhibited in Figure 7-14, where more significant gaps exist between speeds at the wet moisture content level than at the dry. The interaction appears disorderly with speed slices, and orderly with moisture content slices. The increase in carcass sinkage with increasing speed on wet sand is borderline significant.

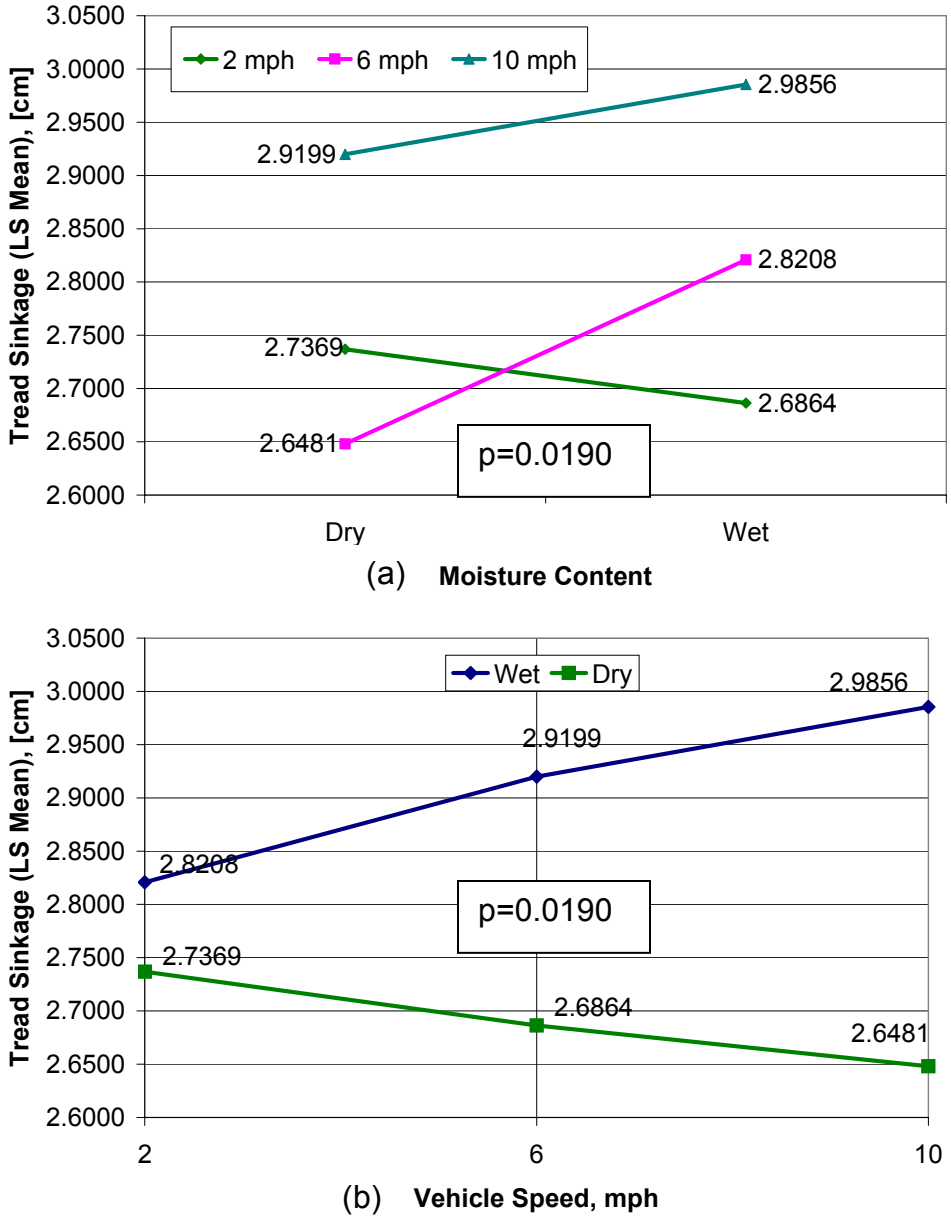

Figure 7-14: Spring/Summer 2007 Tread Imprint Sinkage Data, Grade-Moisture Interaction (a) Speed Profiles and (b) Moisture Profiles

Table 7-14 shows the standard deviations spread amongst the data. Observing data by isolating each level of each parameter, the number of times a data point including that particular level is counted, and the standard deviation of the data at this isolated level was calculated. This table shows that, for each parameter the various levels have similar standard deviations, indicating that no one level had a significantly different amount of

error than another. This table also shows that, amongst the various parameters the values for standard deviation are similar, around 0.40 cm.

Table 7-14: Spring/Summer 2007 Tread Sinkage Data, Standard Deviations of Test Parameters

Standard deviations by GRADE

grade	FREQ	std
2	144	0.43893
3	144	0.42206
4	144	0.40387
5	144	0.37752

Standard deviations by MOISTURE

Moisture	FREQ	std
Dry	360	0.40092
Wet	216	0.42603

Standard deviations by SPEED

Speed	FREQ	std
2	192	0.41177
6	192	0.39729
10	192	0.42313

Standard deviations by LOAD

Payload	FREQ	std
0	192	0.44453
75	192	0.41175
150	192	0.37322

The direct significance of speed on carcass sinkage, where an increase in vehicle speed affects an increase in carcass sinkage, is counter-intuitive. The overall direct affect of increasing from 2 mph results to 10 mph results is around 14.46 mm, which is just 6.9% of the overall mean of all the carcass imprint data. The direct contribution of increasing payload affecting an increase in carcass sinkage, while intuitive, only represents an 8.93mm corresponding to an increase from 0 to 150lb, or 4.25% of the overall mean of all the carcass imprint data. This could be an indication of why these two effects do not appear in the tread imprint data.

The effect of the sand grade-speed interaction on carcass can be attributed to the results discussed in observations during the Winter 2006 trials. When the ATV runs over the

finer grades, especially at higher speeds, less settling and movement was seen in these finer grades than was seen in the coarser sand grade. This phenomenon is directly shown in the interaction plots, where the coarsest sand grade is considerably different than the others, with the sinkage results so close together that they are statistically indistinguishable from one another, and where the sinkage of the 10 mph profile drops below that of the other, lower speeds.

The tread imprint data and the carcass imprint data each share a common borderline significant term of sand grade-moisture content interaction. The interaction between sand grade and moisture content can be attributed to the difference in void spaces in each of the sands allowing for water to create a surface tension bond between smaller sand particles while draining through larger ones.

7.3.2 Pressure Data

Peak Pressure in the Contact Patch

Using methodologies as outlined in Section 7.3.1, the full model for the peak pressure in the contact patch was reduced to a final model of

$$y_{ijklm} = \mu + \alpha_i + \gamma_k + \upsilon_l + \alpha\gamma_{ik} + \alpha\upsilon_{il} + \beta\gamma_{jk} + \gamma\upsilon_{kl} + \alpha\beta\upsilon_{ijl} + \rho_m + \delta_{ijm} + \varepsilon_{ijklm} \quad 7.18$$

where

μ = Mean value of the response variable

α_i = Fixed effect of the i^{th} level of sand

γ_k = Fixed effect of the k^{th} level of vehicle speed

υ_l = Fixed effect of the l^{th} level of payload

$\alpha\gamma_{ik}$ = Fixed effect of the i^{th} sand and k^{th} speed

$\alpha\upsilon_{il}$ = Fixed effect of the i^{th} sand and l^{th} payload

$\beta\gamma_{jk}$ = Fixed effect of the j^{th} moisture and k^{th} speed

$\gamma\upsilon_{kl}$ = Fixed effect of the k^{th} speed and l^{th} payload

$\alpha\beta\upsilon_{ijl}$ = Fixed effect of the i^{th} sand, j^{th} moisture and l^{th} payload

ρ_m = Random effect of the m^{th} round

δ_{ijm} = Random effect for the wholeplot (sand pit) in m^{th} round receiving the i^{th} sand and j^{th} moisture

ε_{ijklm} = Random error, independent and normally distributed with mean 0 and variance σ_ε^2 7.19

where ρ_m and δ_{ijm} are mutually independent, was tested for significance of each factor, the results of which are shown in Table 7-15. This table shows that all effects, with the exception of the borderline-significant payload-speed interaction, are highly significant.

Table 7-15: Spring/Summer 2007 Peak Pressure Data, Final Model Type 3 Tests of Fixed Effects

Effect	Num DF	Den DF	F Value	Pr > F
Grade	3	18	85.94	<.0001
Speed	2	512	337.49	<.0001
Payload	2	512	267.72	<.0001
Grade*Speed	6	512	11.68	<.0001
Grade*Payload	6	512	4.95	<.0001
Moisture*Speed	2	512	8.54	0.0002
Speed*Payload	4	512	1.97	0.0971
Grade*Moist*Payload	6	512	2.64	0.0155

As shown in Table 7-15, the differences of least squares means of the peak pressure for the payload and speed main effects all have adjusted *p*-values of <0.001. Concerning the sand grade main effect Only differences between sand grades 2 and 5, grades 3 and 5, and grades 4 and 5 are significant, indicating a dramatic difference between sand grade 5 and the other three grades. The high *p*-values for the differences of least squares means

between the sand grades 2, 3, and 4 indicate that these sands behave similarly, and that no statistical differences between their effects can be seen, relative to the standard deviation in the data.

Table 7-16: Spring/Summer 2007 Peak Pressure Data, Differences of Least Squares, Means to Compare Main Effects/Parameters

Effect	Moisture	grade	Payload	Speed	Moisture	grade	Payload	Speed	AdjP
grade		2				3			0.7125
grade		2				4			0.4410
grade		2				5			<0.0001
grade		3				4			0.9664
grade		3				5			<0.0001
grade		4				5			<0.0001
Moisture	Dry				Wet				0.3285
Speed				2				6	<0.0001
Speed				2				10	<0.0001
Speed				6				10	<0.0001
Payload			0				75		<0.0001
Payload			0				150		<0.0001
Payload			75				150		<0.0001

The significance of the main effects tested in the full model of the Spring/Summer 2007 peak pressure data can be seen in plots of the least squares means of the peak pressure for each of the levels of the main effects parameters shown in Figure 7-15. These plots graphically represent the data used for comparisons made in Table 7-15. The *p*-value on each plot is associated with the last model refinement in which the parameter was tested.

AS with the sinkage data, the speed and payload are significant main effects, these time with more substantial magnitudes in compared to the rough averages of the data for each of these effects. Peak pressure seems to increase with increasing grain diameter size, taking a large leap up at the coarsest sand used in this study. Speed takes on the expected form where a lower speed imparts a higher peak pressure onto the soil. Again vehicle speed is shown to be a significant main contribution, where decreasing speed affects an increase in payload.

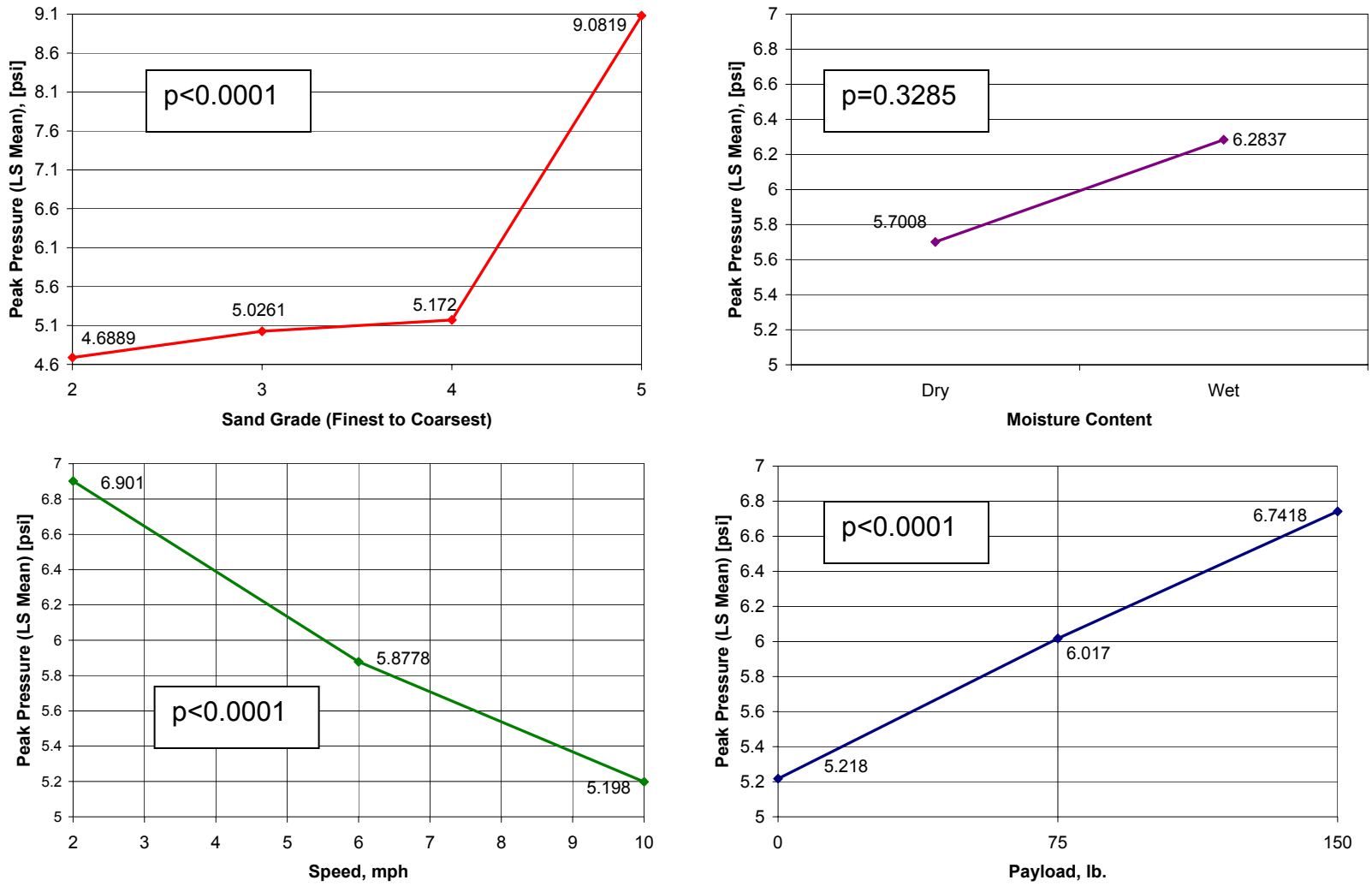

Figure 7-15: Least Squares Means of Spring/Summer 2007 Peak Pressure Data for Tested Main Effects

The data slices in Table 7-17 present information behind the interactions appearing in the final model of the Spring/Summer 2007 peak pressure data. The first row of data in the chart can be read as the analysis of the sand grade-vehicle speed interaction isolating data from grade 2 and testing the significance (on the carcass sinkage) of varying the speed. The sand grade-vehicle speed interaction, payload-speed interaction, and sand grade-payload interaction each have slices with highly significant *p*-values, meaning that for each slice of data the effect of varying the second parameter is large (relative to the standard deviation) and clear. To see what, then, makes the interaction terms significant, interaction plots of least squares means are needed.

Table 7-17: Spring/Summer 2007 Peak Pressure Data, Data Slices for Interactions in Final Refined Model

Effect	Moisture	Grade	Payload	Speed	F-Value	Pr>F
Grade*Speed		2			64.41	<.0001
Grade*Speed		3			74.06	<.0001
Grade*Speed		4			59.19	<.0001
Grade*Speed		5			189.42	<.0001
Grade*Speed				2	91.65	<.0001
Grade*Speed				6	90.74	<.0001
Grade*Speed				10	53.52	<.0001
Grade*Payload		2			35.32	<.0001
Grade*Payload		3			59.59	<.0001
Grade*Payload		4			64.68	<.0001
Grade*Payload		5			122.97	<.0001
Grade*Payload			0		65.50	<.0001
Grade*Payload			75		73.18	<.0001
Grade*Payload			150		93.79	<.0001
Moisture*Speed	Dry				158.58	<.0001
Moisture*Speed	Wet				181.76	<.0001
Moisture*Speed				2	2.55	0.1597
Moisture*Speed				6	0.86	0.3873
Moisture*Speed				10	0.40	0.5485
Speed*Payload			0		94.46	<.0001
Speed*Payload			75		120.19	<.0001
Speed*Payload			150		140.82	<.0001
Speed*Payload				2	108.16	<.0001
Speed*Payload				6	110.08	<.0001
Speed*Payload				10	64.99	<.0001
Gde*Moist*Pyload	Dry				43.75	<.0001
Gde*Moist*Pyload	Wet				35.37	<.0001
Gde*Moist*Pyload		2			15.92	<.0001

Gde*Moist*Pyload	3		26.77	<.0001
Gde*Moist*Pyload	4		27.33	<.0001
Gde*Moist*Pyload	5		49.34	<.0001
Grd*Moist*Pyload		0	31.66	<.0001
Grd*Moist*Pyload		75	34.09	<.0001
Grd*Moist*Pyload		150	42.63	<.0001

Figure 7-16, examining the grade-speed interaction, shows that the difference/gap between the peak pressure for 2 mph and that for 6 mph in the grade-speed interaction changes between grades, decreasing slightly when changing from grade 2 to grade 3, then decreasing more when changing from grade 3 to grade 4, then dramatically increasing when changing from grade 4 to grade 5, as shown by the orange circles highlighting the gaps. This corresponds to the examination of the first two speed-payload data slices in Table 7-17. These gaps well overcome the standard error for the grade-speed interaction, and thus are part of what makes this interaction significant. Similar behavior can be seen in the comparison of 2 mph and 10 mph profiles. The examination of the last three data slices of this interaction reveals that the slopes of lines of constant speeds between going between grades also represent significant changes in the peak pressure data. The grade-speed interaction is orderly, where for any given sand the peak pressure increases with decreasing speed. This trend is the opposite to that shown for carcass imprint sinkage.

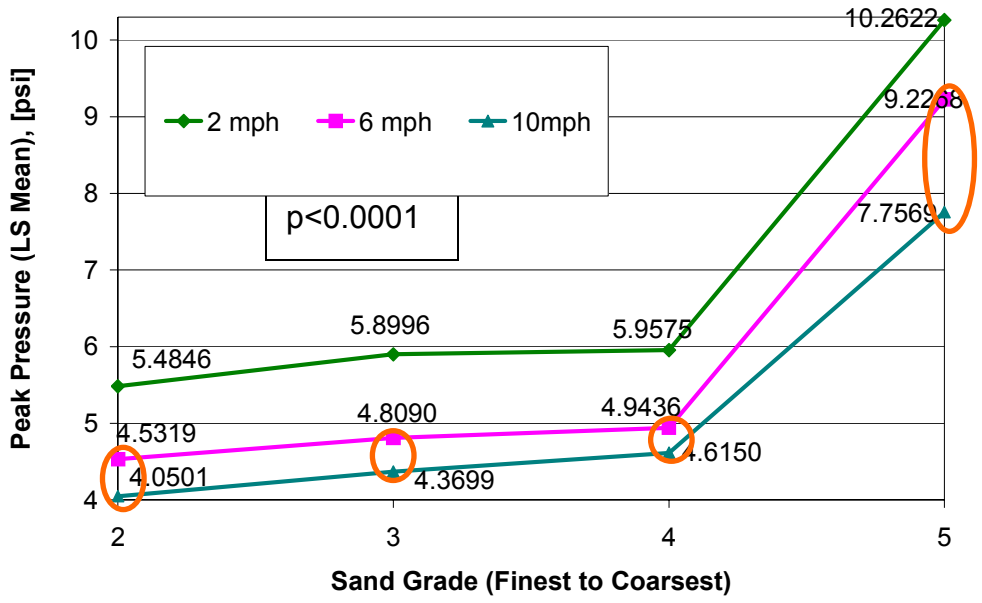

Figure 7-16: Spring/Summer 2007 Peak Pressure Data, Grade-Speed Interaction (Speed Profiles)

Figure 7-17, examining the grade-payload interaction, shows that the slopes of the constant speed profiles going between sand grades are significant, corresponding to what is shown in the first four lines of the grade-payload slices shown in Table 7-17. This figure also shows fluctuating gaps between the three pairs of payloads while going from grade to grade. For example, the gap between the 75-lbs payload profile and the 150-lbs payload profile increases going from grade 2 to grade 3, decreases when going from grade 3 to grade 4, and increases again more dramatically when going from grade 4 to grade 5. These fluctuations in gaps between constant speed profiles correspond to examining the last three lines of the grade-payload data slice. The grade-payload interaction is orderly, where for any given sand the peak pressure increases with increasing payload.

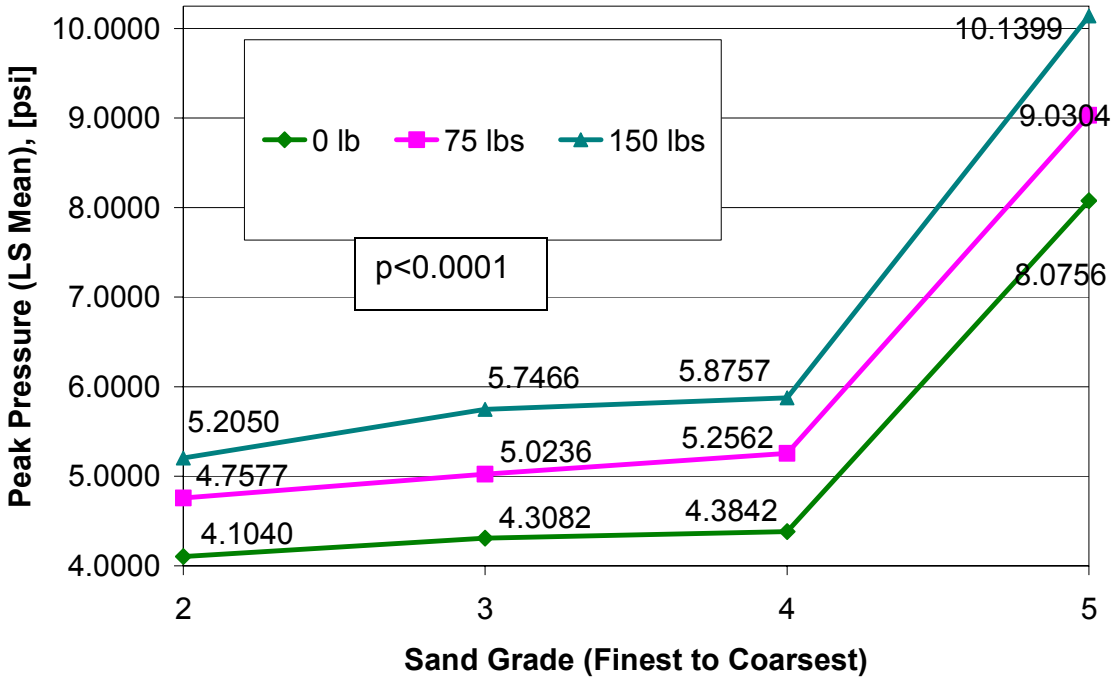

Figure 7-17: Spring/Summer 2007 Peak Pressure Data, Grade-Payload Interaction (Payload Profiles)

Figure 7-18, examining the moisture-speed interaction, shows the gap between profiles decreasing with increasing speed, although not significantly with respect to the standard deviation in the data, corresponding to higher *p*-values in the last three slices of the moisture-speed interaction examined in Table 7-17. The first two lines of the moisture-speed interaction slices shown in Table 7-17 show that the decreases in the peak pressure along constant moisture lines moving up in speed are highly significant. This orderly interaction shows that, for both the dry moisture level and the wet, there is a significant decrease in peak pressure with an increase in vehicle speed. This trend is opposite to the borderline increase in carcass imprint sinkage with increasing speed on wet sand

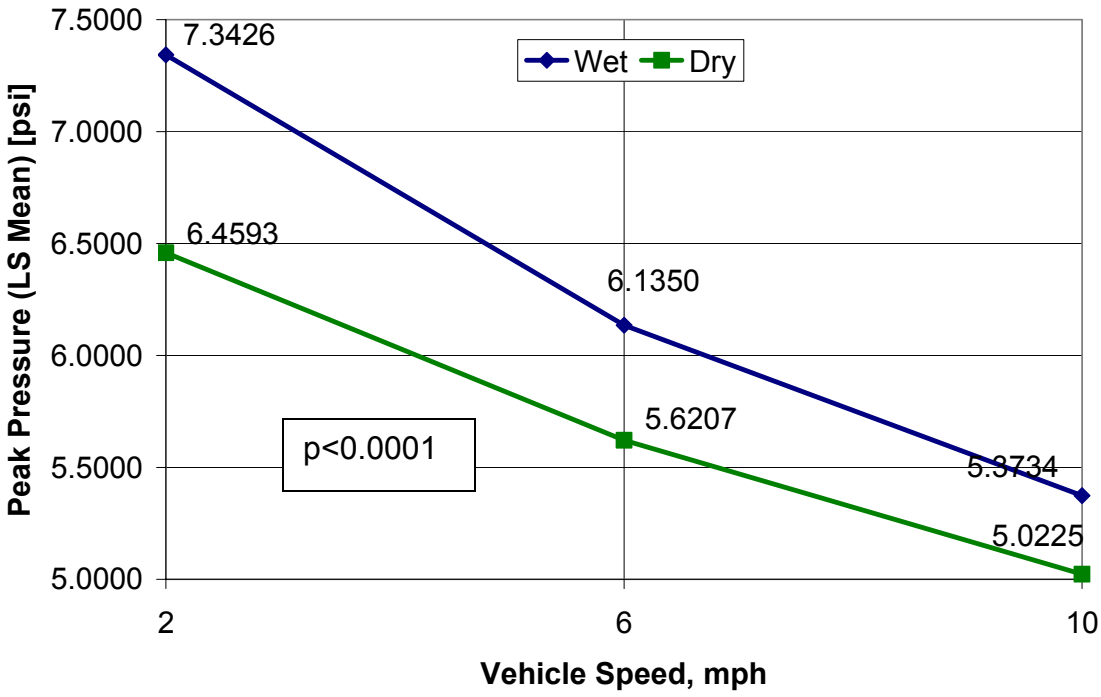

Figure 7-18: Spring/Summer 2007 Peak Pressure Data Moisture-Speed Interaction (Moisture Profiles)

Figure 7-19, examining the speed-payload interaction for the peak pressure data, shows that the gaps between the constant payload profiles of least squares means fluctuate between vehicle speeds. For instance, for the difference in peak pressure for 0-lb payload and 75-lb payload the gap decreases slightly when changing from 2 mph to 6 mph, and decreases more dramatically when changing from 6 mph to 10 mph. This corresponds to the examining the first two lines of the speed-payload data slices shown in Table 7-17. The slopes of the constant payload profiles are significant, and correspond to the low *p*-values shown in the last three lines of data slices for the speed-payload interaction. This orderly interaction is only borderline significant, which explains why the differences in profile plots are only slight. This interaction shows that, for any given vehicle speed, an increase in payload affects an increase in peak pressure, and for any given payload a decrease in vehicle speed affects an increase in peak pressure.

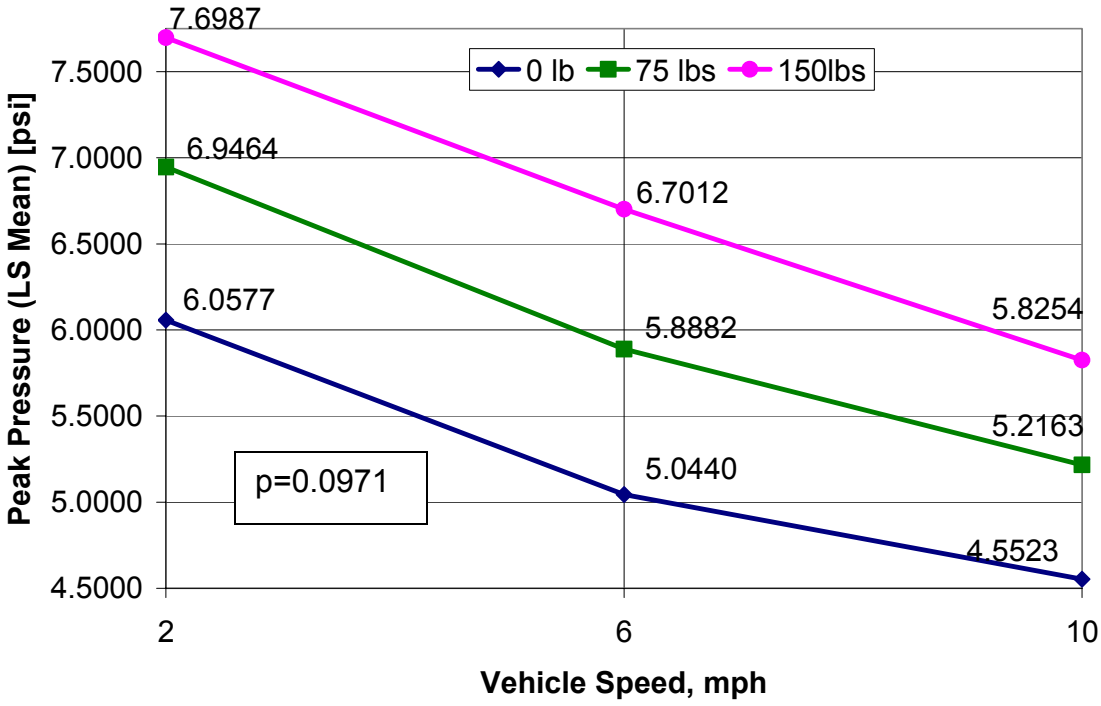

Figure 7-19: Spring/Summer 2007 Peak Pressure Data, Speed-Payload Interaction (Payload Profiles)

Table 7-18 shows the standard deviations spread amongst the data. Observing data by isolating each level of each parameter, the number of times a data point including that particular level is counted, and the standard deviation of the data at this isolated level was calculated. This table shows that, for each parameter the various levels have similar standard deviations (relative to the means of the measured pressure data), indicating that no one level had a significantly different amount of error than another. This table also shows that, amongst the various parameters the values for standard deviation are similar, around 0.60 psi.

Table 7-18: Spring/Summer 2007 Peak Pressure Data, Standard Deviations of Test Parameters

Standard deviations by GRADE

grade	FREQ	std
2	144	0.42225
3	144	0.38313
4	144	0.71798
5	144	0.75226

Standard deviations by MOISTURE

Moisture	FREQ	std
Dry	360	0.63649
Wet	216	0.50938

Standard deviations by SPEED

Speed	FREQ	std
2	192	0.55023
6	192	0.46263
10	192	0.73274

Standard deviations by LOAD

Payload	FREQ	std
0	192	0.48956
75	192	0.67248
150	192	0.60176

Average Pressure in the Contact Patch

Using methodologies as outlined in Section 7.3.1, the full model for the peak pressure in the contact patch was reduced to a final model of

$$y_{ijklm} = \mu + \alpha_i + \gamma_k + \upsilon_l + \alpha\gamma_{ik} + \beta\gamma_{jk} + \alpha\beta\gamma_{ijk} + \rho_m + \delta_{ijm} + \varepsilon_{ijklm} \qquad 7.20$$

where

$$\begin{aligned}
&\mu = \text{Mean value of the response variable} \\
&\alpha_i = \text{Fixed effect of the } i^{th} \text{ level of sand} \\
&\gamma_k = \text{Fixed effect of the } k^{th} \text{ level of vehicle speed} \\
&\upsilon_l = \text{Fixed effect of the } l^{th} \text{ level of payload} \\
&\alpha\gamma_{ik} = \text{Fixed effect of the } i^{th} \text{ sand and } k^{th} \text{ speed} \\
&\beta\gamma_{jk} = \text{Fixed effect of the } j^{th} \text{ moisture and } k^{th} \text{ speed} \\
&\alpha\beta\gamma_{ijk} = \text{Fixed effect of the } i^{th} \text{ sand, } j^{th} \text{ moisture and } k^{th} \text{ speed} \\
&\rho_m = \text{Random effect of the } m^{th} \text{ round} \\
&\delta_{ijm} = \text{Random effect for the wholeplot (sand pit) in } m^{th} \text{ round} \\
&\qquad \text{receiving the } i^{th} \text{ sand and } j^{th} \text{ moisture} \\
&\varepsilon_{ijklm} = \text{Random error, independent and normally distributed} \\
&\quad \text{with mean 0 and variance } \sigma_\varepsilon^2
\end{aligned} \qquad 7.21$$

where δ_{im} and δ_{jm} are mutually independent, was tested for significance of each factor, the results of which are shown in Table 7-19. This table shows that all effects, with the exception of the borderline-significant moisture content-vehicle speed interaction, are highly significant.

Table 7-19: Spring/Summer 2007 Peak Pressure Data, Final Model Type 3 Tests of Fixed Effects

Effect	Num DF	Den DF	F Value	Pr > F
Grade	3	18	85.94	0.0001
Speed	2	512	337.49	<.0001
Payload	2	512	267.72	<.0001
Grade*Speed	6	512	11.68	<.0001
Moisture*Speed	2	512	8.54	0.0798
Grade*Moist*Speed	6	512	2.64	0.0054

As shown in Table 7-20 the differences of least squares means of average pressure data for the payload and speed main effects all have adjusted *p*-values of <0.001. Concerning grade, only differences between sand grade 2 and sand grade 5, sand grade 3 and sand grade 5, and sand grade 4 and sand grade 5 are significant, indicating a dramatic difference between sand grade 5 and the other three grades. The high *p*-values for the differences of least squares means between the sand grades 2, 3, and 4 indicate that these sands behave similarly, and that no statistical differences between their effects can be seen, relative to the standard deviation in the data.

Table 7-20: Spring/Summer 2007 Average Pressure Data Differences of Least Squares Means to Compare Main Effects/Parameters

Effect	Moisture	grade	Payload	Speed	Moisture	grade	Payload	Speed	AdjP
grade		2				3			0.8927
grade		2				4			0.9234
grade		2				5			<0.0002
grade		3				4			0.9998
grade		3				5			0.0011
grade		4				5			0.0009
Moisture	Dry				Wet				0.1415
Speed				2				6	<0.0001
Speed				2				10	<0.0001
Speed				6				10	<0.0001
Payload			0				75		<0.0001
Payload			0				150		<0.0001
Payload			75				150		<0.0001

The significance of the main effects tested in the full model of the Spring/Summer 2007 peak pressure data can be seen in plots of the least squares means of the peak pressure for each of the levels of the main effects parameters shown in Figure 7-20. These plots graphically represent the data used for comparisons made in Table 7-20. The *p*-value on each plot is associated with the last model refinement in which the parameter was tested. The same three significant effects show for the average pressure data as the peak pressure data, but there are some notable differences. The grade effect has a similar pattern to that for the peak pressure, where the average pressure is highest at the coarsest sand with a series of some closer values representing the other three sands.

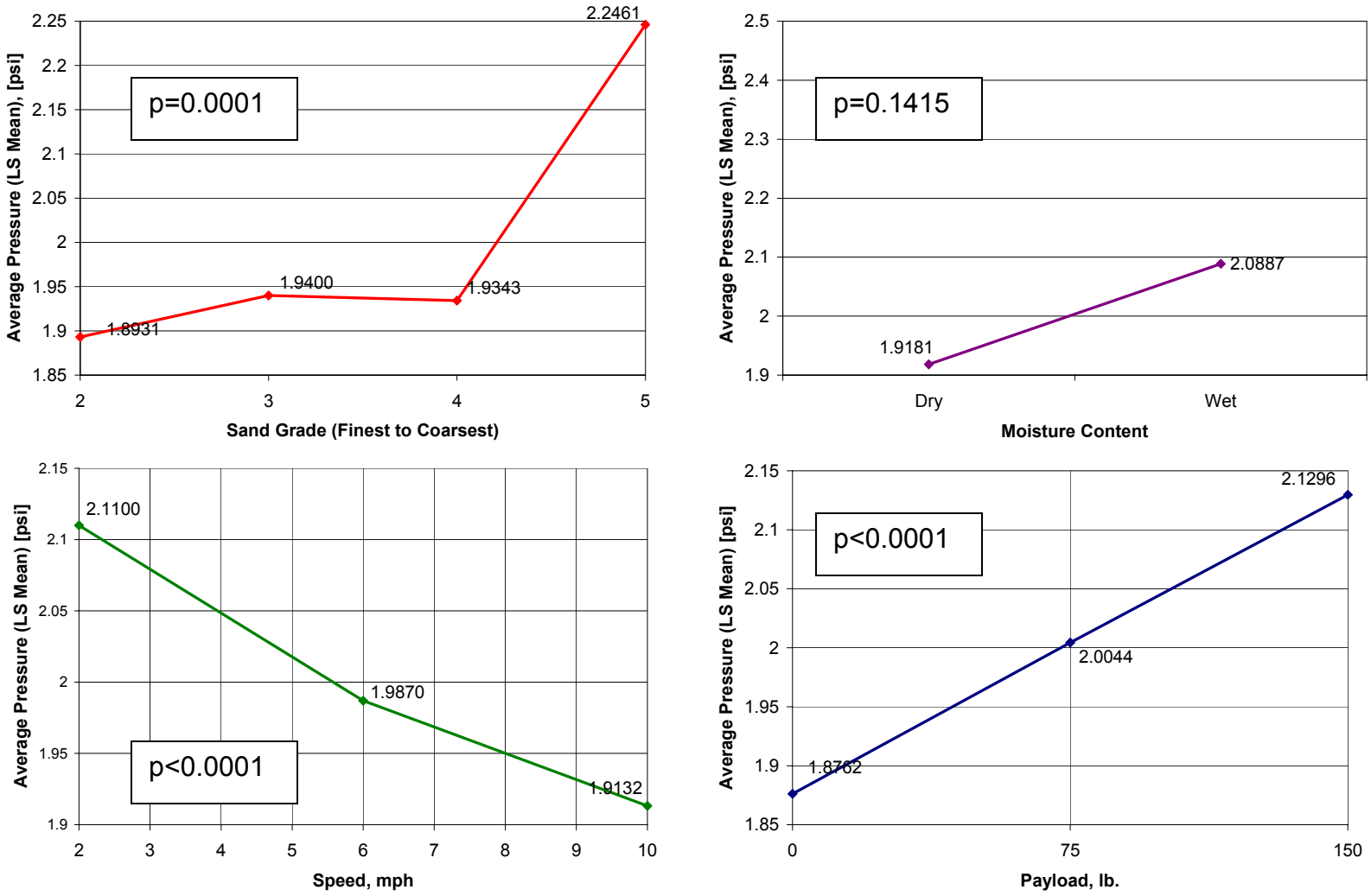

Figure 7-20: Least Squares Means of Spring/Summer 2007 Average Pressure Data for Tested Main Effects

The data slices in Table 7-21 present information behind the interactions in the final model of the Spring/Summer 2007 peak pressure data. The first row of data in the chart can be read as the analysis of the sand grade-vehicle speed interaction isolating data from grade 2 and testing the significance (on the carcass sinkage) of varying the speed. The sand grade-vehicle speed interaction, payload-speed interaction, and sand grade-payload interaction each have slices with highly significant *p*-values, meaning that for each slice of data the effect of varying the second parameter is large (relative to the standard deviation) and clear. To see what, then, makes the interaction terms significant, interaction plots of least squares means are needed.

Table 7-21: Spring/Summer 2007 Average Pressure Data, Data Slices For Interactions in Final Refined Model

Effect	Moisture	Grade	Payload	Speed	F-Value	Pr>F
Grade*Speed		2			64.41	<.0001
Grade*Speed		3			74.06	<.0001
Grade*Speed		4			59.19	<.0001
Grade*Speed		5			189.42	<.0001
Grade*Speed				2	91.65	0.0056
Grade*Speed				6	90.74	<.0001
Grade*Speed				10	53.52	0.0002
Moisture*Speed				2	2.55	0.0906
Moisture*Speed				6	0.86	0.1452
Moisture*Speed				10	0.40	0.2223
Moisture*Speed	Dry				158.58	<.0001
Moisture*Speed	Wet				181.76	<.0001

Figure 7-21, examining the grade-speed interaction, shows that the differences (gaps) between the peak pressures for the constant speed profiles fluctuate, as supported by first three grade-speed data slices in Table 7-21. The crossing of the 2 mph and 6-mph profiles also shows the significance of the interaction (non-parallel trends). These gaps well overcome the standard error for the grade-speed interaction, and thus are part of what makes this interaction significant. The slopes to the segments of the profiles are also significant, as supported by the last three lines of the grade-speed data slices. This interaction is disorderly, due to the crossing lines. With the exception of the coarsest sand grade, grade 5, on any given sand there is an increase in average pressure with decreasing

speed, which is similar to the trends for peak pressure, and opposite to that for the carcass imprint sinkage.

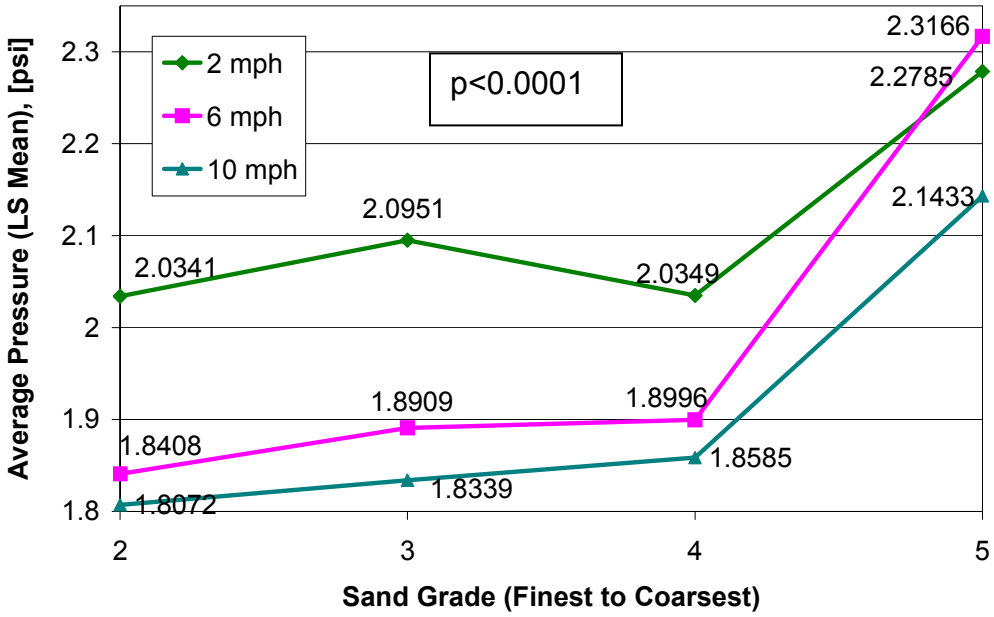

Figure 7-21: Spring/Summer 2007 Average Pressure Data, Grade-Speed Interaction (Speed Profiles)

Figure 7-22, examining the moisture-speed interaction, shows the gap between profiles decreasing with increasing speed, however the gap is only significant (borderline) at the 2 mph speed, as supported by the first three lines of the moisture-speed data slices in Table 7-21. The slopes of the constant moisture profile lines, however, are significant and significantly different, as supported by the last two data slices. This orderly interaction shows that, for both the dry moisture level and the wet, there is a significant decrease in average pressure with an increase in vehicle speed, which are the same trends shown for the peak pressure data.

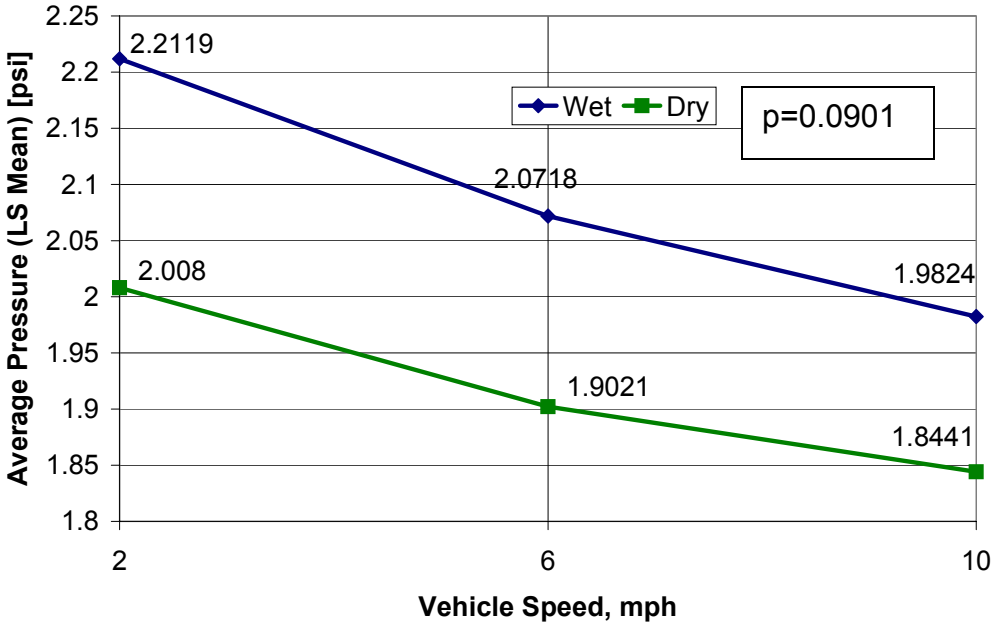

Figure 7-22: Spring/Summer 2007 Average Pressure Data, Moisture-Speed Interaction (Moisture Content Profiles)

Table 7-18 shows the standard deviations spread amongst the data. Observing data by isolating each level of each parameter, the number of times a data point including that particular level is counted, and the standard deviation of the data at this isolated level was calculated. This table shows that, for each parameter the various levels have similar standard deviations (relative to the means of the measured pressure data), indicating that no one level had a significantly different amount of error than another. This table also shows that, amongst the various parameters the values for standard deviation are similar, around 0.13 psi.

Table 7-22: Spring/Summer 2007 Average Pressure Data, Standard Deviations of Test Parameters

Standard deviations by GRADE

grade	FREQ	std
2	144	0.10786
3	144	0.11759
4	144	0.13788
5	144	0.15940

Standard deviations by MOISTURE

Moisture	FREQ	std
Dry	360	0.12864
Wet	216	0.13733

Standard deviations by SPEED

Speed	FREQ	std
2	192	0.11410
6	192	0.16084
10	192	0.12843

Standard deviations by LOAD

Payload	FREQ	std
0	192	0.12288
75	192	0.09652
150	192	0.16672

Differential between Peak and Average Pressures (Difference of Pressures)

Using methodologies as outlined in Section 7.3.1, the full model for the peak pressure in the contact patch was reduced to a final model of

$$y_{ijklm} = \mu + \alpha_i + \gamma_k + \upsilon_l + \alpha\gamma_{ik} + \alpha\upsilon_{il} + \beta\gamma_{jk} + \alpha\beta\upsilon_{ijl} + \rho_m + \delta_{ijm} + \varepsilon_{ijklm} \qquad 7.22$$

where

7.23

where δ_{im} and δ_{jm} are mutually independent, was tested for significance of each factor, the results of which are shown in Table 7-15. This table shows that all effects are highly significant.

Table 7-23: Spring/Summer 2007 Difference of Pressures Data, Final Model Type 3 Tests of Fixed Effects

Effect	Num DF	Den DF	F Value	Pr > F
Grade	3	18	85.94	<.0001
Speed	2	512	337.49	<.0001
Payload	2	512	267.72	<.0001
Grade*Speed	6	512	11.68	<.0001
Grade*Payload	6	512	4.95	<.0001
Moisture*Speed	6	512	4.95	0.0003
Grade*Moist*Payload	6	512	2.64	0.0098

As shown in Table 7-15, the differences of least squares means of the peak pressure for the payload and speed main effects all have adjusted *p*-values of <0.001. Concerning the sand grade main effect Only differences between sand grades 2 and 5, grades 3 and 5, and grades 4 and 5 are significant, indicating a dramatic difference between sand grade 5 and the other three grades. The high *p*-values for the differences of least squares means between the sand grades 2, 3, and 4 indicate that these sands behave similarly, and that no statistical differences between their effects can be seen, relative to the standard deviation in the data.

Table 7-24: Spring/Summer 2007 Difference of Pressures Data, Differences of Least Squares Means to Compare Main Effects/Parameters

Effect	Moisture	grade	Payload	Speed	Moisture	grade	Payload	Speed	AdjP
grade		2				3			0.6735
grade		2				4			0.3405
grade		2				5			<0.0001
grade		3				4			0.9340
grade		3				5			<0.0001
grade		4				5			<0.0001
Moisture	Dry				Wet				0.3953
Speed				2				6	<0.0001
Speed				2				10	<0.0001
Speed				6				10	<0.0001
Payload			0				75		<0.0001
Payload			0				150		<0.0001
Payload			75				150		<0.0001

The significance of the main effects tested in the full model of the Spring/Summer 2007 difference of pressures can be seen in plots of the least squares means of the peak pressure for each of the levels of the main effects parameters shown in Figure 7-15. These plots graphically represent the data used for comparisons made in Table 7-15. The *p*-value on each plot is associated with the last model refinement in which the parameter was tested. Again, the same factors showing significance and patterns for peak and average data (sensibly) exist for the differences of pressures.. Moisture content presents its affect on the data through interaction terms.

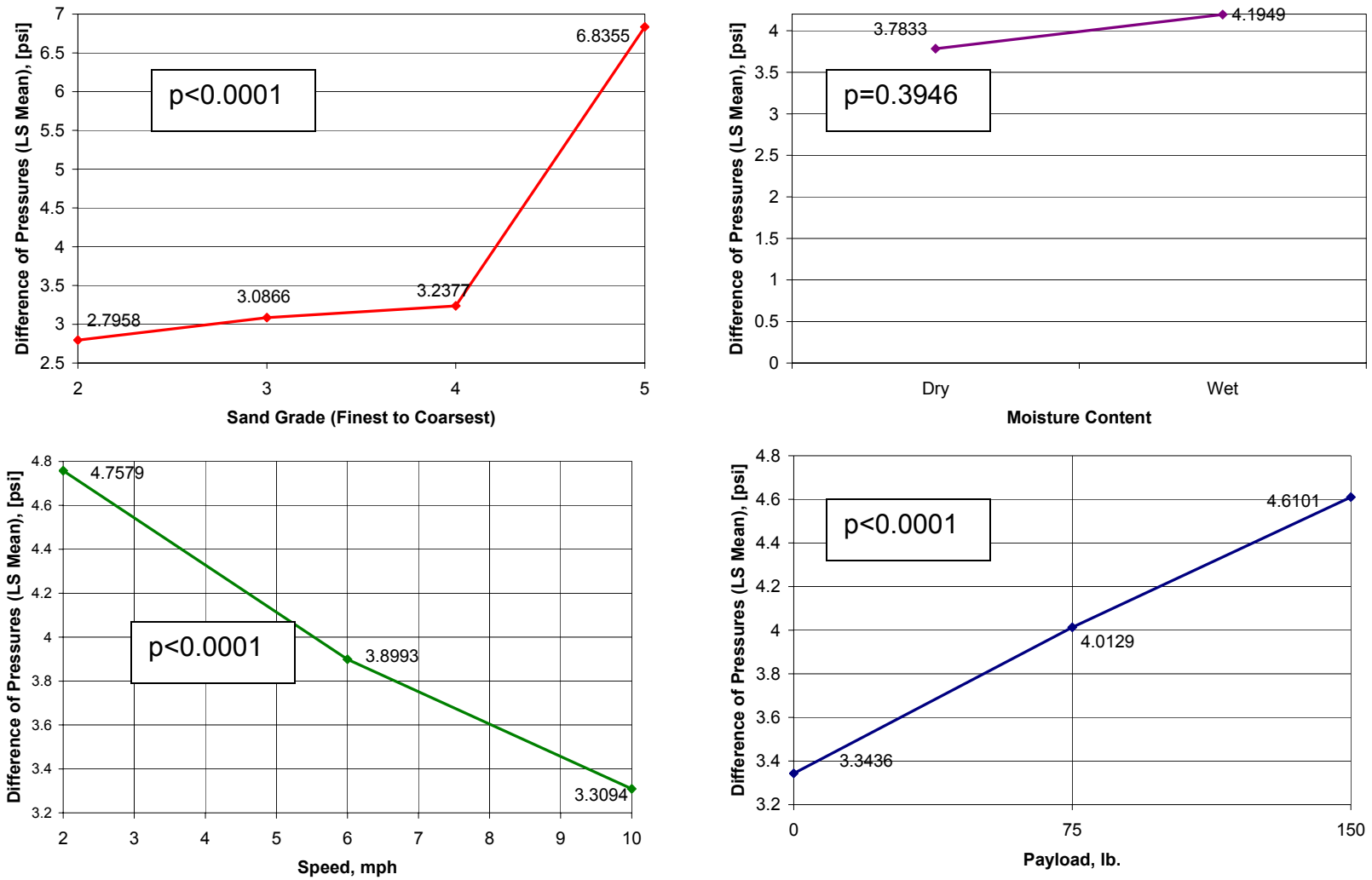

Figure 7-23: Least Squares Means of Spring/Summer 2007 Difference of Pressures Data for Tested Main Effects

The data slices in Table 7-25 present information behind the interactions appearing in the final model of the Spring/Summer 2007 peak pressure data. The first row of data in the chart can be read as the analysis of the sand grade-vehicle speed interaction isolating data from grade 2 and testing the significance (on the carcass sinkage) of varying the speed. The sand grade-vehicle speed interaction and the sand grade-payload interaction each have slices with highly significant *p*-values, meaning that for each slice of data the effect of varying the second parameter is large (relative to the standard deviation) and clear. To see what, then, makes the interaction terms significant, interaction plots of least squares means are needed.

Table 7-25: Spring/Summer 2007 Differences of Pressures Data, Data Slices for Interactions in Final Refined Model

Effect	Moisture	Grade	Payload	Speed	F-Value	Pr>F
Grade*Speed		2			64.41	<.0001
Grade*Speed		3			74.06	<.0001
Grade*Speed		4			59.19	<.0001
Grade*Speed		5			189.42	<.0001
Grade*Speed				2	91.65	<.0001
Grade*Speed				6	90.74	<.0001
Grade*Speed				10	53.52	<.0001
Grade*Payload		2			35.32	<.0001
Grade*Payload		3			59.59	<.0001
Grade*Payload		4			64.68	<.0001
Grade*Payload		5			122.97	<.0001
Grade*Payload			0		65.50	<.0001
Grade*Payload			75		73.18	<.0001
Grade*Payload			150		93.79	<.0001
Moisture*Speed				2	2.55	<.0001
Moisture*Speed				6	0.86	<.0001
Moisture*Speed				10	0.40	<.0001
Moisture*Speed	Dry				158.58	<.0001
Moisture*Speed	Wet				181.76	<.0001
Gde*Moist*Pyload	Dry				43.75	<.0001
Gde*Moist*Pyload	Wet				35.37	<.0001
Gde*Moist*Pyload		2			15.92	<.0001
Gde*Moist*Pyload		3			26.77	<.0001
Gde*Moist*Pyload		4			27.33	<.0001
Gde*Moist*Pyload		5			49.34	<.0001
Grd*Moist*Pyload			0		31.66	<.0001
Grd*Moist*Pyload			75		34.09	<.0001
Grd*Moist*Pyload			150		42.63	<.0001

Figure 7-24, examining the grade-speed interaction, shows that the differences (gaps) between the peak pressures for the constant speed profiles fluctuate, as supported by first three grade-speed data slices in Table 7-25. These gaps overcome the standard error for the grade-speed interaction, and thus are part of what makes this interaction significant. The slopes to the segments of the profiles are also significant, as supported by the last three lines of the grade-speed data slices. This orderly interaction shows that on any given grade the difference of pressures is increases with decreasing speed. This is similar to the trends seen in the carcass imprint sinkage, and in the peak and average pressure.

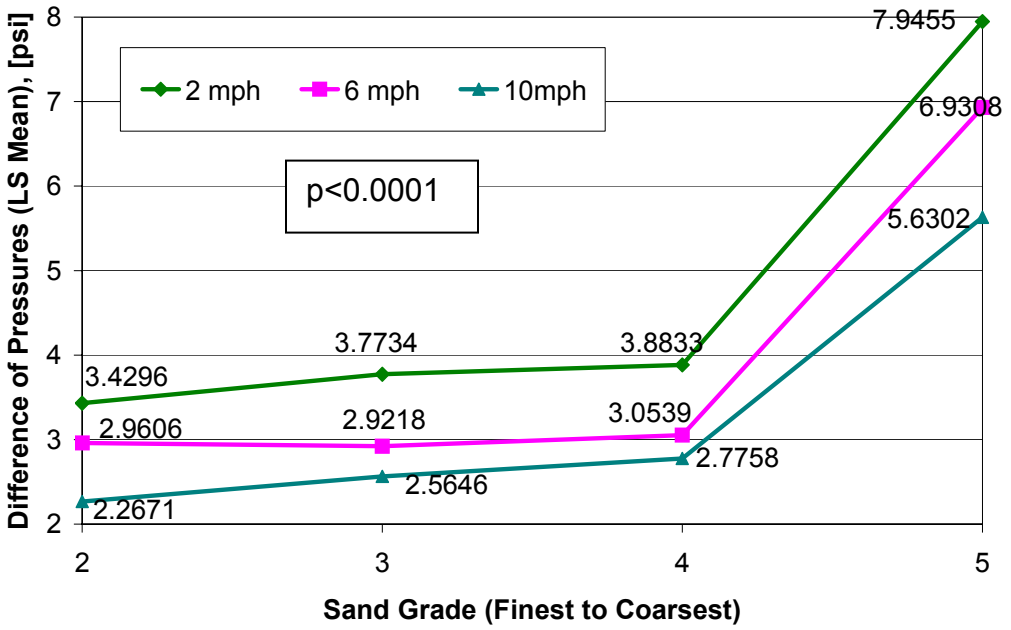

Figure 7-24: Spring/Summer 2007 Difference of Pressures Data, Grade-Speed Interaction (Speed Profiles)

Figure 7-25, examining the grade-payload interaction, shows that the slopes of the constant speed profiles going between sand grades are significant, corresponding to what is shown in the first four lines of the grade-payload slices shown in Table 7-25. This figure also shows fluctuating gaps between the three pairs of payloads while going from grade to grade. For example, the gap between the 75-lbs payload profile and the 150-lbs payload profile increases going from grade 2 to grade 3, decreases when going from grade 3 to grade 4, and increases again more dramatically when going from grade 4 to

grade 5. These fluctuations in gaps between constant speed profiles correspond to examining the last three lines of the grade-payload data slice. The grade-payload interaction is orderly, where for any given sand the peak pressure increases with increasing payload. This trend is exhibited in the peak pressure data as well.

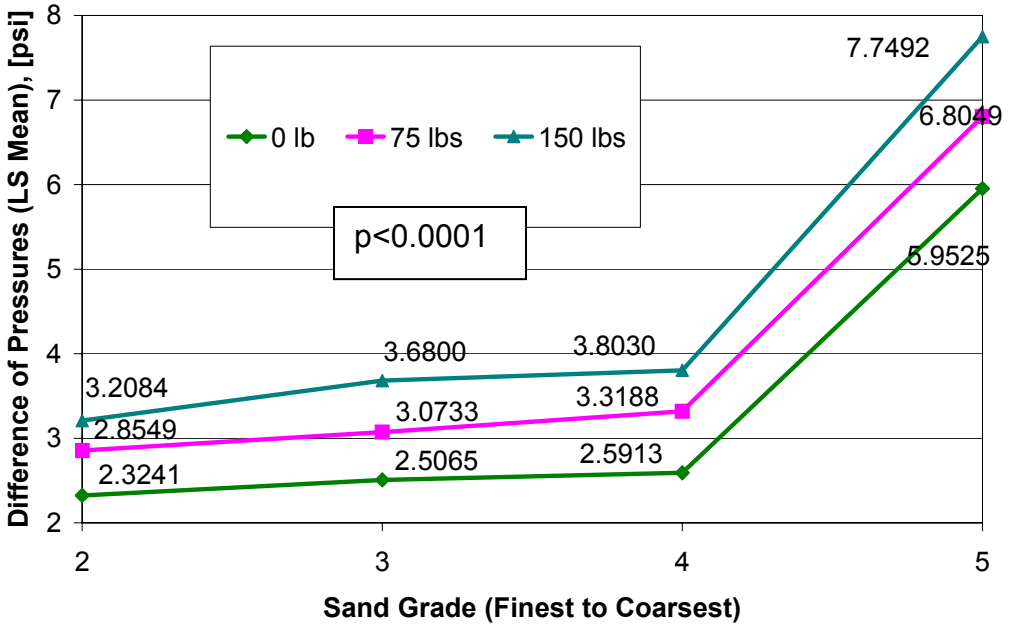

Figure 7-25: Spring/Summer 2007 Difference of Pressures Data, Grade-Payload Interaction (Payload Profiles)

Figure 7-26 examining the moisture-speed interaction, shows the gap between profiles decreasing with increasing speed, with significance to all differences between the profiles, as supported by the first three lines of the moisture-speed data slices in Table 7-25. The slopes of the constant moisture profile lines, are also significant and significantly different, as supported by the last two data slices. This orderly interaction shows that, for both the dry moisture level and the wet, there is a significant decrease in the difference of pressures with an increase in vehicle speed, which are the same trends shown for the peak pressure data and the average pressure data.

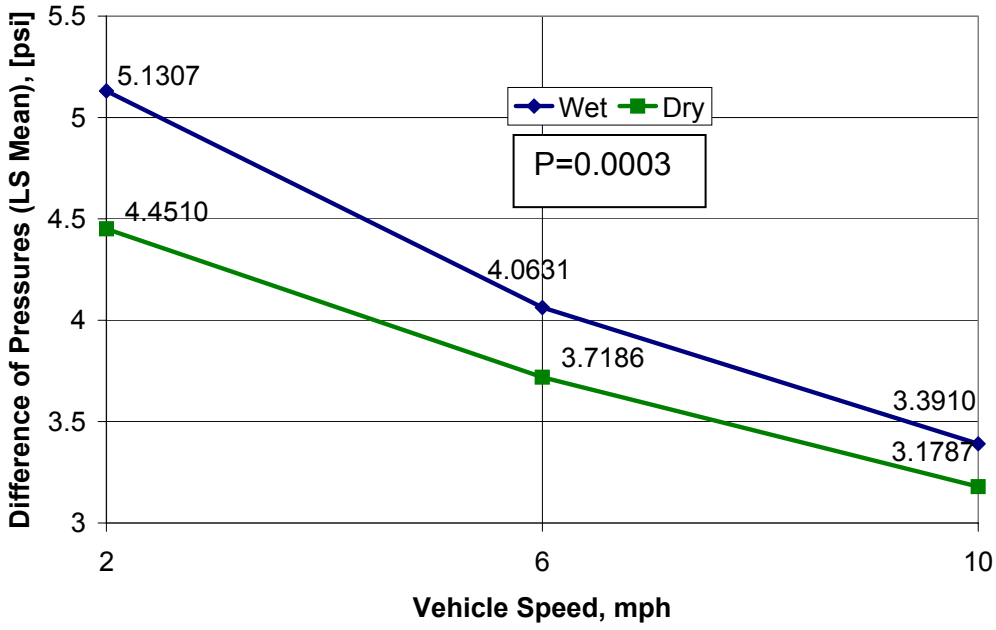

Figure 7-26: Spring/Summer 2007 Difference of Pressures Data, Moisture-Speed Interaction (Moisture Profiles)

For the three pressures, a higher number of factors of significance appear in the final models than for the sinkage data sets. The sand-speed interaction, discussed with the sinkage data, may have a similar effect on pressure data. Certain sands, when undergoing a slower-moving force, shift more and perhaps cause a greater transfer of force to the pressure pad. As the different gradations have been observed by the crew to scatter (for coarser sands) or compact neatly depending on the vehicle speed. The moisture-speed interaction certainly has an effect on the pressure data, as the strength measurable strength characteristics of sand change depending on water content and associated surface tension of the water particles caught between sand grains. The speed-payload interactions may represent a tradeoff in traction. Increasing speed while increasing payload provides an interesting challenge to developing tractive effort.

7.4 Multiple-Pass Experimentation

The least squares mean values of the peak, average and difference pressure of the Honda ATV operating at 10 mph carrying 150 lbs payload across the coarse-grain Best Sand 550

and across the fine-grain sand Best Sand 430 are presented in Table 7-26. As the 100-pass experiments were performed on the sand after the extensive wet tests, there was some residual moisture in the sand, therefore the LS means take into account both wet and dry sand data.

Table 7-26: Summary of Least Squares Means Pressure Data from Spring/Summer 2007 Extensive ATV Tests

Response Data	Estimate	Standard Error
Grade 5		
Peak Pressure (psi)	8.5722	0.3693
Average Contact Pressure (psi)	2.2656	0.3071
Difference of Pressures (psi)	6.3066	0.3071
Grade 2		
Peak Pressure (psi)	4.4738	0.3690
Average Contact Pressure (psi)	1.8792	0.07300
Difference of Pressures (psi)	2.5947	0.3071

As can be found by inspecting Figure 7-27, the pressures experienced within the coarsest sand are notably and consistently higher than those measured within the fine sand, which aligns with the data presented in Table 7-26. Both the trials on coarse sand and those on fine sand maintain pressures higher peak pressure and difference of pressures values than those listed in Table 7-26, which can be expected with some moisture in the sand, as demonstrated in the Spring/Summer 2007 data analysis trends.

The peak pressure trendlines for both sands show an initial peak pressure value that drops after a certain number of data runs (10-20 for the coarse sand, and 30 for the fine sand), followed by a series of rises and falls in the values showing a certain amount of oscillation around a center value, all of which begins at around 50 passes. The series of rises and falls can be corresponds to a loss of a neatly observable tread pattern after about 50 runs, as noted by the crew. This is possibly partially contributable to operator error via drift in repeated path across the sand, although the sinkage data indicates a certain level of consistency. The behavior after 50 runs may also in part reflect a phenomenon that, in general, dense sand has a tendency to become looser and loose sand has a tendency to become denser when affected by a disturbance force [10, 11]. It is important to note that in the top twelve inches of sand, unless purposely compacted by a large amount of force (for the purpose of construction, for instance), it is acceptable to consider sand as loose.

It is also noteworthy that, as the vehicle sinks farther into the sand while compacting some part of it and displacing the rest, the effective burial depth of the sensor changes.

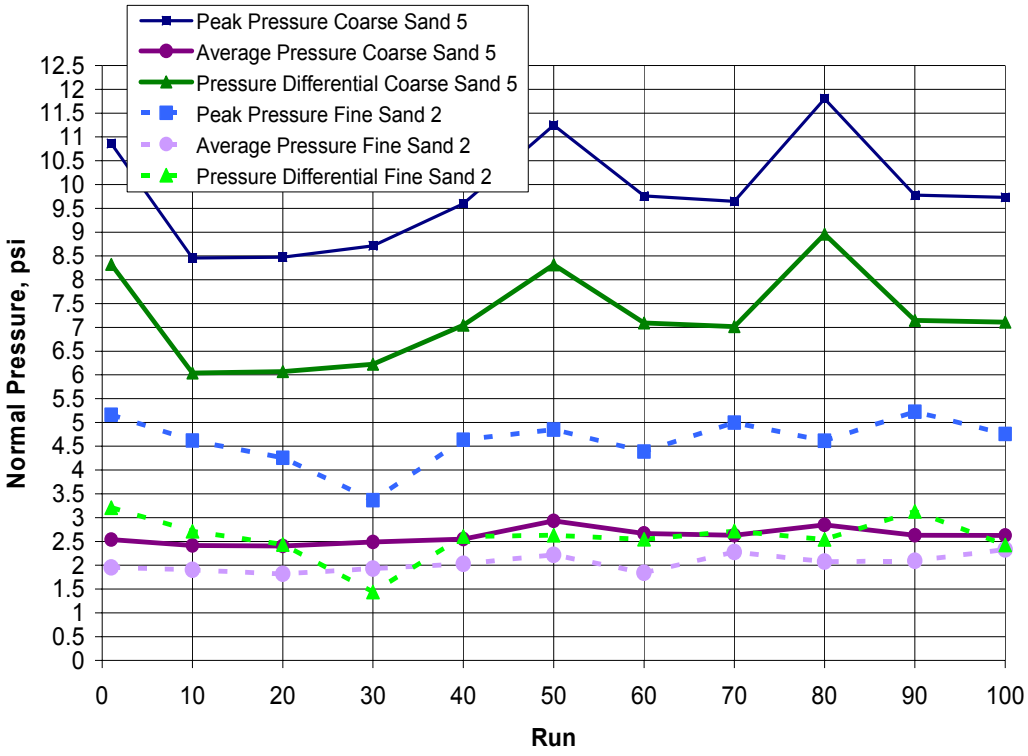

Figure 7-27: 100-Pass ATV Pressure Data

The least squares mean values of the carcass sinkage and tread sinkage of the Honda ATV operating at 10 mph carrying 150 lbs payload across the coarse-grain Best Sand 550 and across the fine-grain sand Best Sand 430 are presented in Table 7-27, again utilizing both wet and dry sand data.

Table 7-27: Summary of Least Squares Means Sinkage Data from Spring/Summer 2007 Extensive ATV Tests

Response Data	Estimate	Standard Error
Grade 5		
Carcass Sinkage (cm)	2.2339	0.1828
Tread Sinkage (cm)	2.8572	0.1923
Grade 2		
Carcass Sinkage (cm)	2.1067	0.1828
Tread Sinkage (cm)	2.8294	0.1923

The time history of the sinkage data, as shown in Figure 7-28, shows that, with the exception of the tread sinkage on the coarse sand, all initial values are within the expected range (as defined by the least squares mean and standard deviation) afforded in the Spring/Summer 2007 extensive testing. These trends show a clear rise in the sinkage values over the time history of the data collection, with a decreasing rate of rise. The tread sinkage over the last twenty runs fully plateaus, The clearest (smoothest) trend with what seems to be the least amount of noise in the data is the carcass sinkage on the coarse sand. Notably, the difference between the tread readings and carcass measurements for the fine sand are more spaced together than their coarse sand counterparts. As observed beginning in Winter 2006, it is common that the finer sands have more distinguishably neat tread patters, so that this phenomenon is expected.

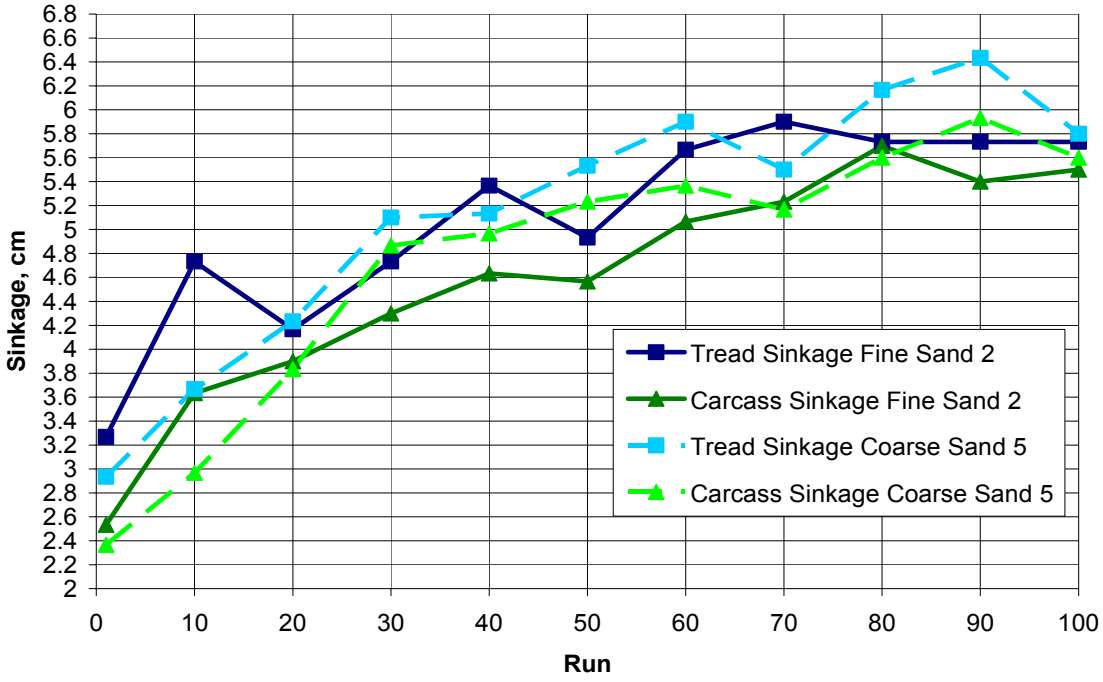

Figure 7-28: 100-Pass ATV Sinkage Data

7.5 Preliminary Testing of Novel Locomotion Platforms

DARwIn, with an unloaded weight of approximately 4 lbs and a total foot contact area of 24.4 in^2 has a nominal standing foot pressure of 0.164psi. This lightweight walking robot was observed for the synthesis of stepping pattern and the foot sinkage into a medium-

grade sand. At full forward sped DARwIn took roughly one step per second, and traversed a 27.1-inch path (center to center distance between first and last foot imprints) in 22 seconds at an average speed of roughly 1.25 in/sec (0.08 mph).

Synthesis of Steps

DARwIn executed his steps in three parts, mimicking the human heel-toe pattern of foot placement. From the stance of two feet flat against the sand, the first foot was picked up and the heel was flexed. The foot was moved forward, occasionally not clear of the sand surface and instead shuffling along the sand, and then replaced as the stance foot. During this replacement, the foot slides back plowing some of the sand behind it to form an angled foot imprint, as can be seen in Figure 7-29. Figure 7-30 shows the shuffling of the foot.

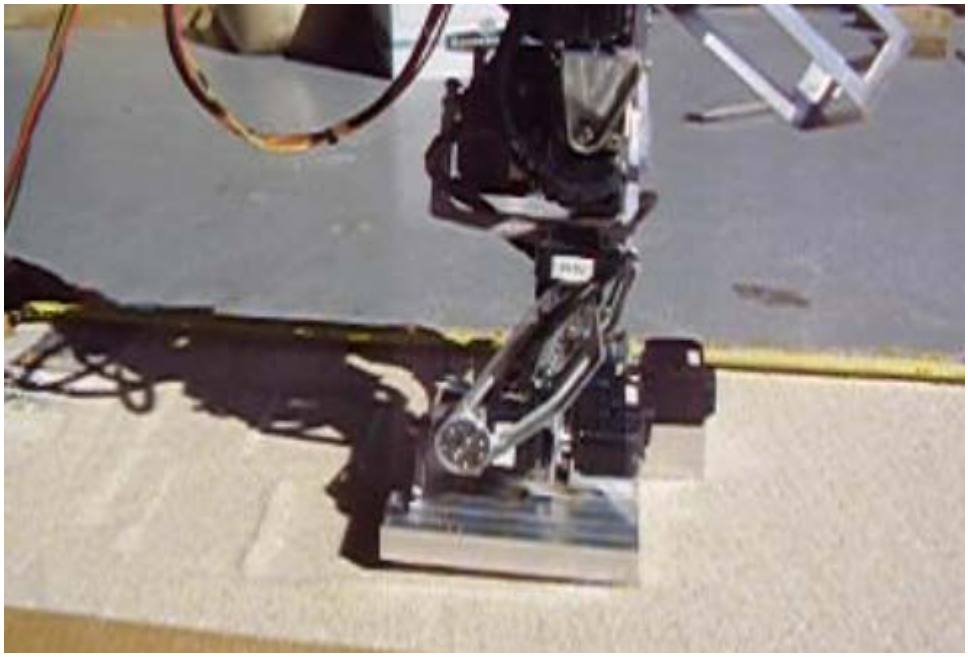

Figure 7-29: DARwIn Right Foot Being Picked Up from Stance

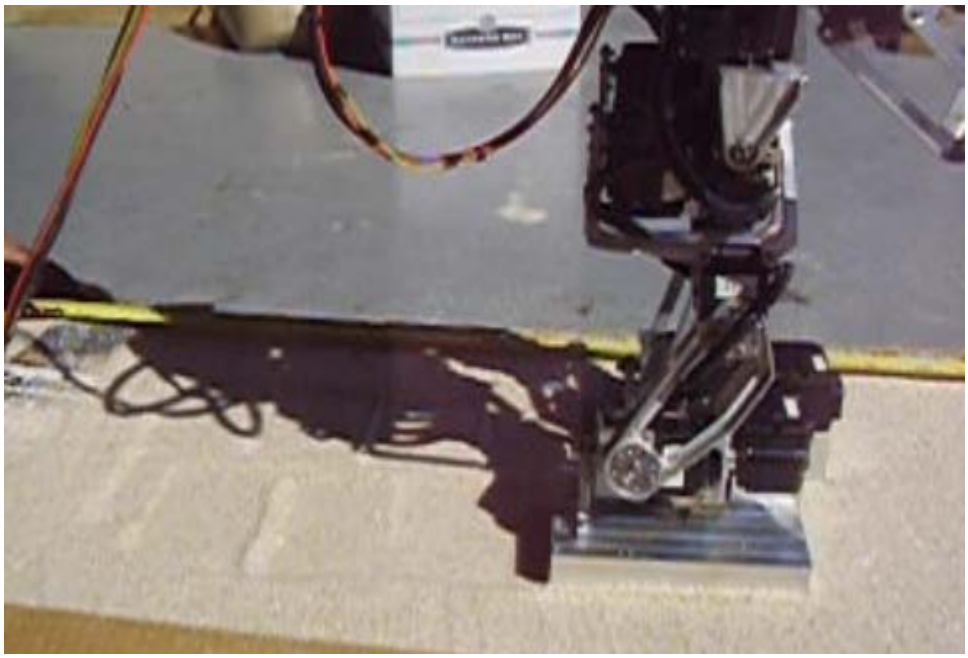

Figure 7-30: DARwIn Right Foot Shuffling in Sand

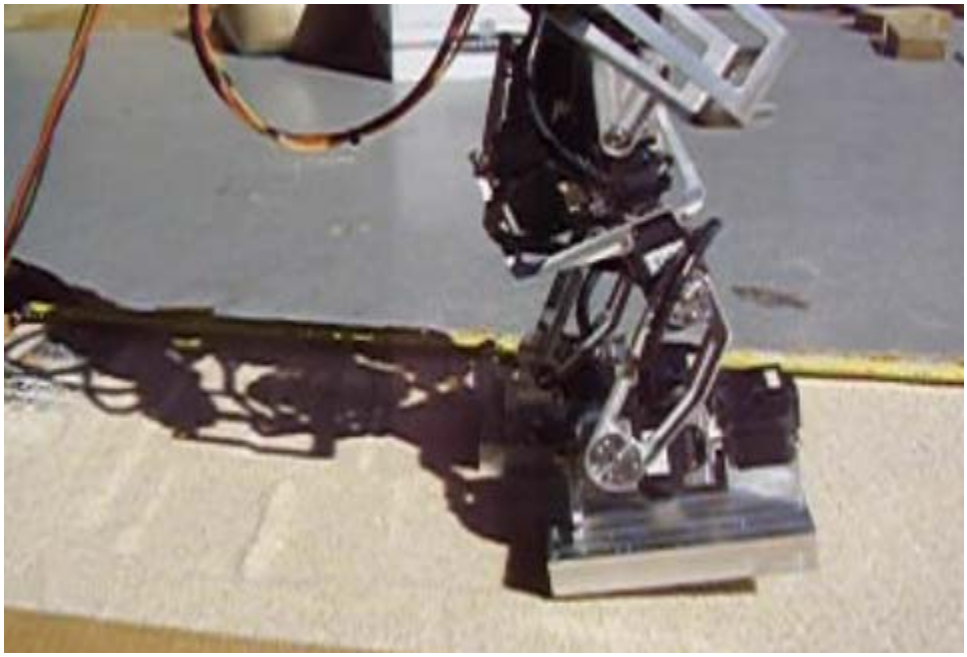

Figure 7-31: DARwIn Right Foot with Flexed Heel Ready for Placement

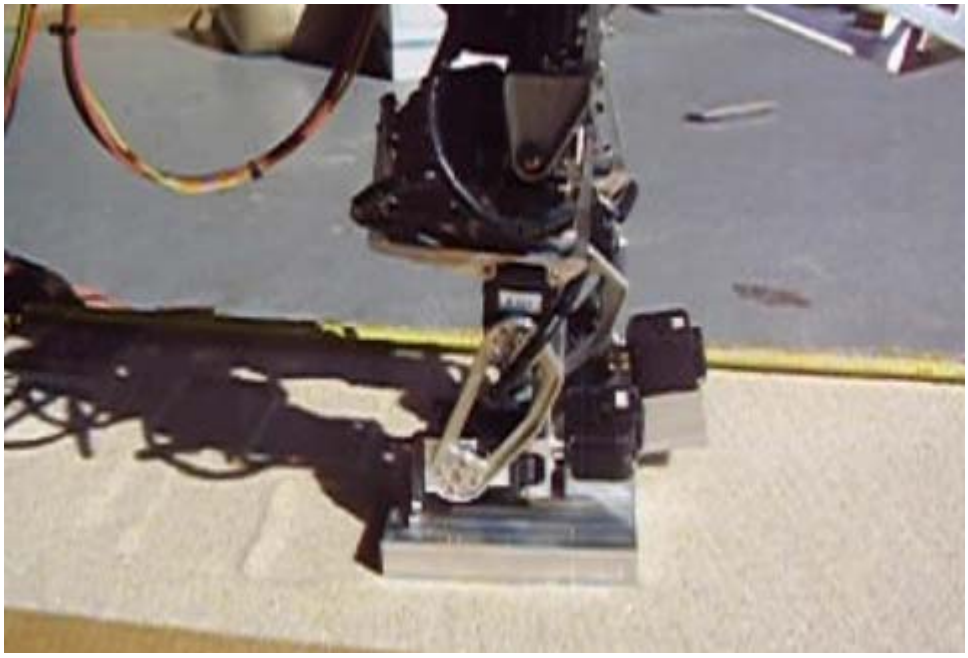

Figure 7-32: DARwIn Right Foot Replaced as Stance Leg, Showing Dragging Marks Behind as Angled Imprints:

Sinkage Measurements

DARwIn's first data trial consisted two parts, where in the first part of the trial run DARwIn moved relatively straight forward, afterwards maneuvering to the left, as pictured in Figure 7-33. The sinkage measurements from that sequence are shown in Table 7-28. This table clearly shows a heavy shift in the to higher values left foot sinkage more than double that of right foot sinkage toward the end of the trial when the robot was moving left.

Table 7-28: DARwIn Walking Robot Test 1 Sinkage Measurements

Right Foot (cm)	Left Foot (cm)
0.5	0.4
0.5	0.6
0.5	0.3
0.4	0.3
0.3	0.2
0.2	0.4
0.3	0.3
0.1	0.4
0.2	0.5
0.2	0.6

Average Right	Average Left
0.32	0.40

Average: 0.36cm

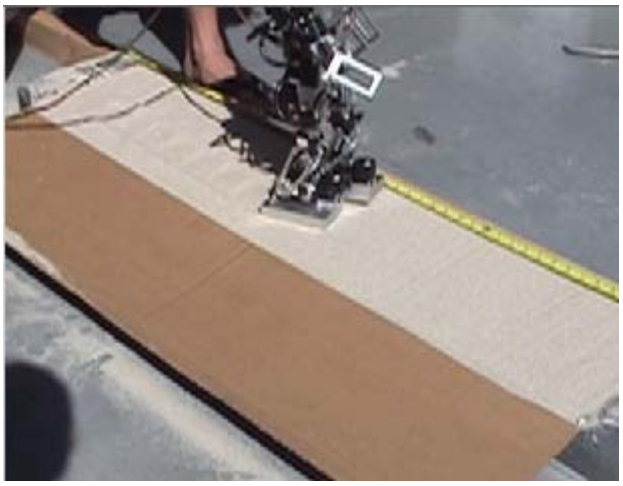

Figure 7-33: DARwIn in First Trial Run, Veering to the Left from Straight-forward Path

These low values for ground sinkage shown in Table 7-29 indicate potential benefits during performance of tasks on sand. The low sinkage indicates a lower potential for failure due to sand buildup in front of the foot (what can be thought of as an effective equivalent to wheeled vehicle compactive resistance). Beyond this, DARwIn's gait is adaptable and can be trained to avoid dragging of the feet (whereas conventional wheeled and tracked vehicles cannot adapt their locomotion platforms.) If, however, the shuffling

and digging into sand cannot be avoided, it could lead to potential failure especially if any weight is added to DARwIn, or if an uphill climb is attempted.

Table 7-29: DARwIn Foot Sinkage Measurements for Straight-Line Walking on Sand

	Darwin Test 2		Darwin Test 3	
R foot (cm)	L foot (cm)		R foot (cm)	L foot (cm)
	0.3	0.2	0.4	0.3
	0.3	0.3	0.3	0.3
	0.3	0.3	0.4	0.4
	0.2	0.2	0.3	0.3
	0.2	0.3	0.3	0.5
	0.4	0.4	0.3	0.4
	0.3	0.3	0.3	0.4
	0.3	0.4	0.3	0.4
	0.3	0.3	0.4	0.3
	0.2	0.4	0.2	0.2
	0.3	0.4	0.3	0.3
			0.3	0.4
			0.4	0.3
			0.4	
Avg:0.281818		0.318182	0.318182	0.345455

8 CONCLUSIONS AND FUTURE WORK

The Mobility Metrics Matrix (MMM) serves as a tool to assess the mobility of lightweight vehicles for their mission-specific suitability and performance in order to choose the best candidate for a given mission. User-defined mission needs are linked to vehicle-ground interaction, performance, geometry and sensitivity measures by high, low or adverse relationships. These markers of relation set up for the weighting of vehicle parameters, along with the weighting of importance of mission needs, to culminate into a mission-specific rank for each vehicle based on it's performance of a given parameter. These weighting factors are left for the user to define, based on experience and theory in the specific application. The MMM is adaptable for expansion into other categories of mission needs and vehicle parameters.

The next step in MMM development would be to experimentally validate the system using available lightweight vehicles and mission scenarios. Wheeled and tracked vehicles, being the most widely available and the most understood, would be the logical choices. After refinement of the system, the next case study should involve the comparison of a traditional wheeled and/or tracked vehicle with robot(s) utilizing novel locomotion platforms.

As the development of robots with novel forms of locomotion—such as bipedal robots like DARwIn, tripedal robots like STriDER, and spoke-wheel robots like IMPASS under development at RoMeLa—continues, increasingly more opportunities to replace humans in dull, dirty, and dangerous jobs arise. The adaptable gait of the robots presents both a systematic advantage over traditional wheeled and tracked vehicles, and a complex problem in understanding their locomotion on soft terrain. Proposed models based on the interaction of existing tools such as blades in soil cutting machines and the cone penetrometer with the ground, and on theoretical preliminary examination of robots with similar walking patterns, present the basis for future development of robot foot-ground interaction. As the prototypes go through stages of improvement, they should be tested as done in this study, perhaps with a larger amount of data collection, to get preliminary understandings of the foot interaction with soft ground. As the prototypes become more

solid in their locomotion across soft terrain, they should be under extensive scenarios, much like those presented in this study for lightweight wheeled vehicles, to decipher the most important factors on their interaction with the ground. The models proposed in this study may be validated with some of the experimental data.

Preliminary testing of a lightweight autonomous tracked vehicle, MATILDA, revealed a reasonably consistent performance of the vehicle across sand with grains almost the size of clay, through medium grades of sand, and over sand so coarse it is almost gravel. MATILDA, throughout the experiments, was only shown to fail on one occasion at an intermediate speed (50% throttle power) and payload (25 lbs) over the finest grain sand used in this study. MATILDA did show promise in some preliminary performance tests, driving over tall mounds of sands while carrying 25-lb and 50-lb payloads. While the exact MATILDA used in the preliminary experiments is no longer function, future work should include the continuation of extensive testing of MATILDA or another similar lightweight tracked vehicle, much like what was done in this study for lightweight wheeled vehicles.

Extensive testing of a lightweight wheeled ATV was done on four sands ranging from fine to medium to coarse (as coarse as available without being classified as a gravel) at either dry or damp moisture contents, traveling at speeds of 2 mph, 6 mph, and 10 mph while carrying payloads of 0 lb, 75 lbs and 150 lbs (in addition to driver weight). These tests were performed to find which of those factors and/or interactions had significant impact on the sinkage of the wheels into the ground (divided amongst carcass imprint sinkage and tread imprint sinkage) and on the pressure distribution in the contact patch as measured by the average of the top twenty pressures felt sensed during time history of the contact patch, the average of the time history of pressures in the contact patch, and the difference between those two values.

The carcass imprint sinkage was most significantly affected by the vehicle speed, and borderline affected by the carried payload, the sand grade-moisture interaction, and the sand grade-speed interaction. The tread imprint sinkage was most affected by the sand

moisture-speed interaction and borderline affected by the sand grade-moisture interaction.

All pressure measurements were highly affected by sand grade, vehicle speed, carried payload, sand grade-speed interaction,.

The peak pressure in the contact patch was highly affected by the sand grade-payload interaction, sand grade-moisture interaction, and sand grade-moisture-carried payload interaction. The peak pressure was borderline affected by the sand grade-vehicle payload interaction.

The average pressure in the contact patch was significantly affected by the three-way sand grade-moisture content-vehicle speed interaction, and borderline affected by the moisture-speed interaction.

The difference of pressures in the contact patch was significantly affected by the sand moisture-speed interaction (which also appears highly significant in the peak pressure) and by the three-way sand grade-moisture content-vehicle speed interaction.

The pressure data in this study can be updated in the future to include the impact of the pressure sensor burial depth of four inches on the data collected in order to predict the pressure at the exact site of vehicle-ground interaction. This data can be used to check for the application of the traditional heavyweight vehicle models developed by M. G. Bekker for their use in lightweight vehicle models.

In the future these experiments can be continued with more extensive measurement of the soil moisture during experimental trials in order to develop more precise relationships between the soil moisture content and the pressure distribution in the contact patch and the vehicle sinkage into the ground.

REFERENCES

1. Staff, J.C.o., *Dictionary of Military and Associated Terms*, D.o. Defense, Editor. 1974, JCS Pub 1.
2. Bekker, M.G., *Theory of Land Locomotion: The Mechanics of Vehicle Mobility*. 1956, Ann Arbor, MI: University of Michigan Press.
3. Bekker, M.G., *Off-the-Road Locomotion: Research and Development in Terramechanics*. 1960, Ann Arbor, MI: University of Michigan Press.
4. Bekker, M.G., *Introduction to Terrain-Vehicle Systems*. 1969, Ann Arbor, MI: University of Michigan Press.
5. Wong, J.Y., *Theory of Ground Vehicles*. 2001, New York, NY: John Wiley & Sons.
6. United States Marine Corps: Ground Combat Element Branch, E.R.D., Marine Corps Development Command, *Memorandum on the Desired Operational Performance Characteristics for a Tactical Unmanned Ground Vehicle*. 2000.
7. Gerhart, G., S. Laughery, and R. Goetz. *Off-Road Vehicle Locomotion Using Bekker's Model*. in *SPIE Defense & Security Conference*. 2006. Orlando.
8. Haueisen, B., et al. *Case Study of the Evaluation and Verification of a PackBot Model in NRMM*. in *SAE 2005 World Congress & Exhibition Session: Military Vehicle Autonomous Systems*. 2005. Detroit, MI, USA.
9. Rohani, B. and G.Y. Baladi, *Correlation of Cone Index With Soil Properties*, in *Cone Penetration Testing and Experience. Proceedings of the ASCE National Convention*. 1981, American Society of Civil Engineers: New York, NY.
10. Seed, H. and K. Lee, *Drained Strength Characteristics of Sands.* Journal of the Soil Mechanics and Foundations Division, Proceedings of the American Society of Civil Engineers, 1967. **93**(SM6): p. 29.
11. Seed, H. and K. Lee, *Undrained Strength Characteristics of Cohesionless Soils.* Journal of the Soil Mechanics and Foundations Division, Proceedings of the American Society of Civil Engineers, 1967. **93**(SM6): p. 29.
12. Whitlow, R., *Basic Soil Mechanics*. 4th Edition ed. 2000: Prentice Hall.

13. *Annual Book of ASTM Standards: ASTM D2488 Standard Practice for Description and Identification of Soils (Visual-Manual Procedure)*. Vol. 4.08. 2007: ASTM International.
14. *Annual Book of ASTM Standards: ASTM D2487 Classification of Soils for Engineering Purposes (Unified Soil Classification System)*. Vol. 4.08. 2007: ASTM International.
15. *Annual Book of ASTM Standards: ASTM D653 Standard Terminology Relating to Soil, Rock, and Contained Fluids*. Vol. 4.08. 2007: ASTM International.
16. Schroeder, W.L., *Soils in Construction*. 1980, New York: NY: John Wiley & Sons, Inc.
17. Friedman, G.M., *Distinction between dune, beach, and river sands from their textural characteristics.* Journal of Sedimentary Petrology, 1961. **31**(4): p. 414-429.
18. Komar, P.D., *Beach Processes and Sedimentation*. 1997: Prentice Hall.
19. Worley, M., *Interviews with Dr. Thomas L. Brandon*. 2007.
20. Cho, G.-C., J. Dodds, and J.C. Santamarina, *Particle Shape Effects on Packing Density, Stiffness, and Strength: Natural and Crushed Sands.* Journal of Geotechnical and Geoenvironmental Engineering, 2006. **132**(5): p. 12.
21. *Fairmount Minerals Website: Silica Sands – high purity grain, foundry, silica*. [Internet Website] [cited 2006 1 April 2006]; Available from: http://www.fairmountminerals.com/interior.asp?page=BestSandCorp&category=Locations&level1=BestSandCorp.
22. *Annual Book of ASTM Standards: ASTM D653 Standard Terminology Relating to Soil, Rock, and Contained Fluids*. Vol. 4.08. 2004: ASTM International.
23. Worley, M.E., et al., *The Development of an Assessment Tool for the Mobility of Lightweight Autonomous Vehicles on Coastal Terrain*, in *SPIE Defense & Security*. 2007: Orlando, FL.
24. Prasad, B., *Trends and Perspectives: Review of QFD and Related Deployment Techniques.* Journal of Manufacturing System, 1998. **17**(3).
25. Todd, D.J., *Walking Machines: an Introduction to Legged Robots*. 1985, London: Chapman and Hall.

26. Crumbley, L., *Virginia Tech students gearing up for $1million Grand Challenge*, in *VTNews* 10 March 2004.
27. Hong, D.W., *Biologically Inspired Locomotion Strategies: Novel Ground Mobile Robots at RoMeLa*, in *The 3rd International Conference on Ubiquitous Robots and Ambient Intelligence (URAI 2006)*. 2006: Seoul, S. Korea.
28. Ingvast, J., *Derivation of ground interaction models for plastic soils specially suited for walking robots*. 2002, Dept. of Machine Design, Brinellv: Stockholm, Sweden.
29. Heaston, J. and D.W. Hong, *Design Optimization of a Novel Tripedal Locomotion Robot Through Simulation and Experiments for a Single Step Dynamic Gait*, in *31st ASME Mechanisms and Robotics Conference*. 2007: Las Vegas, Nevada.
30. Karmakar, S. and R.L. Kushwaha, *CFD Simulations of Dynamic Soil-tool Interaction*, in *The 15th International Conference of the International Society of Terrain-Vehicle Systems (ISTVS 2005)*. 2005: Hayama, Japan.
31. *Honda 2004 FourTrax Rancher ES TRX350TE Manual*, Honda Publications.
32. Ott, R.L. and M.T. Longnecker, *An Introduction to Statistical Methods and Data Analysis*. 3rd ed. 2001, Pacific Grove, CA: Duxbury/Thomson Learning.
33. Peterson, R.G., *Agricultural Field Experiments: Design and Analysis*. 1994, New York, NY: Marcel Dekker, Inc.

APPENDIX: SPRING/SUMMER 2007 RAW DATA EXCERPTS

Table A-1 presents an excerpt of the raw data for the sinkage measurements for the Spring/Summer 2007 extensive wheeled vehicle tests on wet and dry sand.

Table A - 1: Excerpt of Raw Sinkage Data from Spring/Summer 2007 Extensive Lightweight Wheeled Vehicle Tests on Dry and Wet Sand

Round	Moisture	Grade	Speed [mph]	Payload [lbs]	Sinkage_Carcass [cm]	Sinkage_Tread [cm]	Sinkage_Diff. (Tread – Carc) [cm]
1	Dry	4	2	75	2.067	2.700	0.633
1	Dry	4	6	0	2.633	3.433	0.800
1	Dry	4	6	150	1.967	2.567	0.600
1	Dry	4	10	0	2.100	2.767	0.667
1	Dry	4	6	75	1.133	1.700	0.567
1	Dry	4	2	150	0.467	1.333	0.867
1	Dry	4	2	0	1.433	2.100	0.667
1	Dry	4	10	150	0.700	1.233	0.533
1	Dry	4	10	75	1.467	1.833	0.367
1	Dry	4	2	75	1.467	2.200	0.733
1	Dry	4	10	150	1.700	2.033	0.333
1	Dry	4	10	75	1.533	1.800	0.267
1	Dry	4	6	0	1.567	2.333	0.767
1	Dry	4	2	150	1.700	2.200	0.500
1	Dry	4	2	0	1.333	2.133	0.800
1	Dry	4	10	0	1.833	2.300	0.467
1	Dry	4	6	75	1.667	2.000	0.333
1	Dry	4	6	150	1.767	2.233	0.467
1	Dry	3	6	75	2.600	2.900	0.300
1	Dry	3	6	0	2.633	3.267	0.633
1	Dry	3	2	150	2.400	3.267	0.867
1	Dry	3	10	0	3.200	3.467	0.267
1	Dry	3	6	150	2.300	2.733	0.433
1	Dry	3	10	75	2.533	2.967	0.433
1	Dry	3	10	150	3.033	3.267	0.233
1	Dry	3	2	0	1.633	2.267	0.633
1	Dry	3	2	75	2.233	2.833	0.600
1	Dry	3	6	0	2.033	2.067	0.033
1	Dry	3	6	150	2.600	3.333	0.733
1	Dry	3	2	0	2.367	3.233	0.867
1	Dry	3	6	75	2.333	3.067	0.733
1	Dry	3	10	150	2.667	3.233	0.567
1	Dry	3	10	0	2.300	2.600	0.300
1	Dry	3	10	75	2.067	2.467	0.400
1	Dry	3	2	75	1.867	2.467	0.600
1	Dry	3	2	150	1.833	2.633	0.800
1	Dry	5	2	75	1.733	2.300	0.567
1	Dry	5	10	0	1.867	2.067	0.200

1	Dry	5	10	75	1.367	1.200	-0.167
1	Dry	5	6	150	1.767	2.267	0.500
1	Dry	5	10	150	1.600	2.100	0.500
1	Dry	5	6	75	1.867	2.200	0.333
1	Dry	5	6	0	2.400	2.800	0.400
1	Dry	5	2	150	2.267	3.067	0.800
1	Dry	5	2	0	1.833	2.267	0.433
1	Dry	5	10	0	2.133	2.600	0.467
1	Dry	5	2	0	2.333	2.867	0.533
1	Dry	5	6	150	2.633	3.200	0.567
1	Dry	5	10	75	3.133	3.367	0.233
1	Dry	5	2	150	2.800	3.333	0.533
1	Dry	5	10	150	2.900	3.133	0.233
1	Dry	5	6	0	2.433	2.667	0.233
1	Dry	5	2	75	2.533	2.767	0.233
1	Dry	5	6	75	2.600	2.967	0.367
1	Dry	2	2	150	1.900	2.767	0.867
1	Dry	2	2	75	3.100	4.133	1.033
1	Dry	2	10	150	3.167	3.800	0.633
1	Dry	2	2	0	3.067	4.033	0.967
1	Dry	2	6	0	3.100	3.800	0.700
1	Dry	2	6	75	3.100	3.833	0.733
1	Dry	2	6	150	3.733	4.433	0.700
1	Dry	2	10	75	3.833	4.500	0.667
1	Dry	2	10	0	4.233	4.233	0.000
1	Dry	2	6	0	3.167	4.100	0.933
1	Dry	2	6	150	2.800	3.333	0.533
1	Dry	2	2	75	3.067	3.467	0.400
1	Dry	2	10	0	3.200	4.200	1.000
1	Dry	2	10	150	2.767	3.533	0.767
1	Dry	2	6	75	2.567	3.133	0.567
1	Dry	2	10	75	3.100	3.833	0.733
1	Dry	2	2	0	2.267	2.833	0.567
1	Dry	2	2	150	2.233	2.767	0.533
6	Wet	3	6	75	3.100	4.033	0.933
6	Wet	3	6	0	2.367	3.433	1.067
6	Wet	3	2	0	2.767	3.667	0.900
6	Wet	3	6	150	3.033	3.933	0.900
6	Wet	3	2	150	2.633	3.767	1.133
6	Wet	3	2	75	2.567	3.467	0.900
6	Wet	3	10	0	2.633	3.367	0.733
6	Wet	3	10	75	2.700	3.633	0.933
6	Wet	3	10	150	2.667	3.533	0.867
6	Wet	3	10	0	3.100	4.300	1.200
6	Wet	3	6	150	3.033	3.867	0.833
6	Wet	3	2	0	2.367	3.333	0.967
6	Wet	3	10	150	2.067	2.967	0.900
6	Wet	3	6	75	2.467	3.433	0.967
6	Wet	3	2	75	2.033	3.000	0.967

6	Wet	3	2	150	2.033	2.900	0.867
6	Wet	3	10	75	2.867	3.800	0.933
6	Wet	3	6	0	2.567	3.467	0.900
6	Wet	4	2	75	2.933	3.900	0.967
6	Wet	4	2	150	2.367	3.233	0.867
6	Wet	4	6	75	2.233	2.800	0.567
6	Wet	4	2	0	1.567	2.400	0.833
6	Wet	4	6	150	2.467	3.167	0.700
6	Wet	4	6	0	1.800	2.667	0.867
6	Wet	4	10	0	2.900	3.633	0.733
6	Wet	4	10	75	2.133	2.967	0.833
6	Wet	4	10	150	2.233	3.067	0.833
6	Wet	4	6	75	1.700	2.700	1.000
6	Wet	4	2	150	2.200	3.133	0.933
6	Wet	4	6	0	1.900	2.733	0.833
6	Wet	4	10	150	2.200	2.867	0.667
6	Wet	4	2	0	1.833	2.500	0.667
6	Wet	4	6	150	2.067	2.667	0.600
6	Wet	4	2	75	1.833	2.700	0.867
6	Wet	4	10	75	2.967	3.667	0.700
6	Wet	4	10	0	1.667	2.433	0.767
6	Wet	5	6	0	3.500	4.367	0.867
6	Wet	5	2	150	2.700	3.400	0.700
6	Wet	5	10	0	2.500	3.133	0.633
6	Wet	5	6	75	2.467	3.067	0.600
6	Wet	5	6	150	2.533	3.467	0.933
6	Wet	5	2	75	2.100	3.000	0.900
6	Wet	5	10	150	2.400	3.133	0.733
6	Wet	5	2	0	1.567	2.433	0.867
6	Wet	5	10	75	1.933	2.700	0.767
6	Wet	5	6	150	2.033	2.633	0.600
6	Wet	5	10	0	1.833	2.433	0.600
6	Wet	5	6	0	1.633	2.433	0.800
6	Wet	5	6	75	2.533	3.000	0.467
6	Wet	5	2	150	1.933	2.533	0.600
6	Wet	5	10	75	2.400	3.133	0.733
6	Wet	5	2	75	2.267	3.033	0.767
6	Wet	5	2	0	2.767	3.433	0.667
6	Wet	5	10	150	2.133	2.633	0.500
6	Wet	2	2	0	2.533	3.600	1.067
6	Wet	2	6	75	2.333	3.100	0.767
6	Wet	2	2	75	2.233	3.367	1.133
6	Wet	2	2	150	1.567	2.800	1.233
6	Wet	2	6	150	2.033	3.033	1.000
6	Wet	2	10	150	2.233	3.367	1.133
6	Wet	2	6	0	1.667	2.533	0.867
6	Wet	2	10	75	2.167	2.933	0.767
6	Wet	2	10	0	1.833	2.867	1.033
6	Wet	2	6	150	2.033	2.433	0.400

6	Wet	2	2	75	1.500	2.167	0.667
6	Wet	2	10	150	2.033	2.800	0.767
6	Wet	2	6	75	1.733	2.533	0.800
6	Wet	2	2	150	2.000	2.667	0.667
6	Wet	2	10	0	2.000	2.600	0.600
6	Wet	2	10	75	1.433	2.267	0.833
6	Wet	2	6	0	1.067	1.933	0.867
6	Wet	2	2	0	1.000	1.700	0.700

Table A-2 presents an excerpt of the raw data for the contact patch pressure measurements for the Spring/Summer 2007 extensive wheeled vehicle tests on wet and dry sand.

Table A - 2: Excerpt of Raw Pressure Data from Spring/Summer 2007 Extensive Lightweight Wheeled Vehicle Tests on Dry and Wet Sand

Round	Moisture	Grade	Speed [mph]	Payload [lbs]	Pressure_Peak [psi]	Pressure_Avg [psi]	Pressure_Difference (Peak - Average) [psi]
1	Dry	4	2	75	5.71525	1.922309013	3.792940987
1	Dry	4	6	0	3.67605	1.622720901	2.053329099
1	Dry	4	6	150	4.48685	1.770588732	2.716261268
1	Dry	4	10	0	3.31845	1.625483721	1.692966279
1	Dry	4	6	75	3.9514	1.700721932	2.250678068
1	Dry	4	2	150	5.98065	1.966858524	4.013791476
1	Dry	4	2	0	4.82705	1.76322619	3.06382381
1	Dry	4	10	150	3.9995	1.757558931	2.241941069
1	Dry	4	10	75	4.0316	1.784204449	2.247395551
1	Dry	4	2	75	5.05585	1.890836399	3.165013601
1	Dry	4	10	150	4.7282	1.871161117	2.857038883
1	Dry	4	10	75	3.0342	1.626042918	1.408157082
1	Dry	4	6	0	3.04885	1.490124248	1.558725752
1	Dry	4	2	150	5.9076	1.951051661	3.956548339
1	Dry	4	2	0	3.985	1.655501176	2.329498824
1	Dry	4	10	0	3.3328	1.616601732	1.716198268
1	Dry	4	6	75	4.5612	1.80996701	2.75123299
1	Dry	4	6	150	4.83325	1.90939303	2.92385697
1	Dry	3	6	75	3.2529	1.583027642	1.669872358
1	Dry	3	6	0	2.18395	1.281463343	0.902486657
1	Dry	3	2	150	4.8476	1.837413662	3.010186338
1	Dry	3	10	0	1.97125	1.287017391	0.684232609
1	Dry	3	6	150	3.5213	1.693828267	1.827471733
1	Dry	3	10	75	2.8564	1.508217452	1.348182548
1	Dry	3	10	150	3.23845	1.598869258	1.639580742
1	Dry	3	2	0	4.04665	1.830705669	2.215944331

1	Dry	3	2	75	3.8615	1.653783156	2.207716844
1	Dry	3	6	0	2.8074	1.492735426	1.314664574
1	Dry	3	6	150	3.95255	1.690119948	2.262430052
1	Dry	3	2	0	3.17605	1.549652466	1.626397534
1	Dry	3	6	75	3.0655	1.518665899	1.546834101
1	Dry	3	10	150	3.19155	1.612365314	1.579184686
1	Dry	3	10	0	2.46845	1.437324385	1.031125615
1	Dry	3	10	75	3.0651	1.638161252	1.426938748
1	Dry	3	2	75	3.99945	1.702005203	2.297444797
1	Dry	3	2	150	4.75825	1.879827458	2.878422542
1	Dry	5	2	75	7.1517	1.91525712	5.23644288
1	Dry	5	10	0	5.77135	1.835433566	3.935916434
1	Dry	5	10	75	6.75565	1.944181818	4.811468182
1	Dry	5	6	150	7.37585	1.984434715	5.391415285
1	Dry	5	10	150	6.5512	1.887119666	4.664080334
1	Dry	5	6	75	7.71715	1.987936893	5.729213107
1	Dry	5	6	0	7.27815	1.952980907	5.325169093
1	Dry	5	2	150	8.4951	2.060531183	6.434568817
1	Dry	5	2	0	7.1902	1.897598651	5.292601349
1	Dry	5	10	0	6.14865	1.86971705	4.27893295
1	Dry	5	2	0	7.40625	1.873074882	5.533175118
1	Dry	5	6	150	8.6326	2.766716837	5.865883163
1	Dry	5	10	75	5.8347	1.953939175	3.880760825
1	Dry	5	2	150	8.382	1.949027778	6.432972222
1	Dry	5	10	150	6.90825	1.921632323	4.986617677
1	Dry	5	6	0	6.81935	1.861868256	4.957481744
1	Dry	5	2	75	7.53905	1.952557658	5.586492342
1	Dry	5	6	75	6.79345	1.881171617	4.912278383
1	Dry	2	2	150	2.95445	1.459318621	1.495131379
1	Dry	2	2	75	3.8923	1.670104567	2.222195433
1	Dry	2	10	150	3.0496	1.588349456	1.461250544
1	Dry	2	2	0	2.7773	1.402724758	1.374575242
1	Dry	2	6	0	2.8732	1.478407051	1.394792949
1	Dry	2	6	75	3.45915	1.629406869	1.829743131
1	Dry	2	6	150	3.49075	1.667277834	1.823472166
1	Dry	2	10	75	3.0178	1.54826817	1.46953183
1	Dry	2	10	0	2.6486	1.483171617	1.165428383
1	Dry	2	6	0	2.63245	1.374950161	1.257499839
1	Dry	2	6	150	3.33455	1.590059032	1.744490968
1	Dry	2	2	75	3.11295	1.48125182	1.63169818
1	Dry	2	10	0	1.73235	1.297167742	0.435182258
1	Dry	2	10	150	3.42785	1.600557057	1.827292943
1	Dry	2	6	75	3.50625	1.625788177	1.880461823
1	Dry	2	10	75	3.23925	1.599278902	1.639971098
1	Dry	2	2	0	3.5523	1.592643525	1.959656475
1	Dry	2	2	150	4.42695	1.763333678	2.663616322
6	Wet	3	6	75	5.68785	2.084168776	3.603681224
6	Wet	3	6	0	5.2777	1.995086379	3.282613621
6	Wet	3	2	0	6.6439	2.234095324	4.409804676

6	Wet	3	6	150	6.097	2.167481025	3.929518975
6	Wet	3	2	150	8.2057	2.420695197	5.785004803
6	Wet	3	2	75	6.5287	2.241798068	4.286901932
6	Wet	3	10	0	4.13285	1.770660099	2.362189901
6	Wet	3	10	75	5.27475	2.019441572	3.255308428
6	Wet	3	10	150	4.6024	1.898076223	2.704323777
6	Wet	3	10	0	4.22675	1.72894844	2.49780156
6	Wet	3	6	150	5.7319	2.072672367	3.659227633
6	Wet	3	2	0	5.15965	1.973337945	3.186312055
6	Wet	3	10	150	5.5562	2.096017598	3.460182402
6	Wet	3	6	75	5.3812	2.018971545	3.362228455
6	Wet	3	2	75	6.57175	2.204329362	4.367420638
6	Wet	3	2	150	6.9433	2.333661524	4.609638476
6	Wet	3	10	75	4.8772	2.027423581	2.849776419
6	Wet	3	6	0	4.28815	1.743749701	2.544400299
6	Wet	4	2	75	7.09865	2.205802124	4.892847876
6	Wet	4	2	150	7.83185	2.415389268	5.416460732
6	Wet	4	6	75	7.04195	2.248958242	4.792991758
6	Wet	4	2	0	6.88605	2.25194926	4.63410074
6	Wet	4	6	150	6.971	2.296579612	4.674420388
6	Wet	4	6	0	5.74745	2.18159795	3.56585205
6	Wet	4	10	0	5.0976	1.973294326	3.124305674
6	Wet	4	10	75	5.24855	2.114462025	3.134087975
6	Wet	4	10	150	6.95685	2.326112392	4.630737608
6	Wet	4	6	75	6.37065	2.163232353	4.207417647
6	Wet	4	2	150	8.02635	2.438115634	5.588234366
6	Wet	4	6	0	6.35555	2.134372043	4.221177957
6	Wet	4	10	150	6.55775	2.286753234	4.270996766
6	Wet	4	2	0	7.58005	2.369304258	5.210745742
6	Wet	4	6	150	7.2107	2.28299449	4.92770551
6	Wet	4	2	75	7.8583	2.356437915	5.501862085
6	Wet	4	10	75	6.0667	2.195494312	3.871205688
6	Wet	4	10	0	4.9817	2.034168689	2.947531311
6	Wet	5	6	0	9.17595	2.325767057	6.850182943
6	Wet	5	2	150	13.1222	2.62026087	10.50193913
6	Wet	5	10	0	7.88415	2.184167411	5.699982589
6	Wet	5	6	75	9.70445	2.439730257	7.264719743
6	Wet	5	6	150	10.1332	2.405844946	7.727355054
6	Wet	5	2	75	11.78335	2.349041707	9.434308293
6	Wet	5	10	150	11.3785	2.607467677	8.771032323
6	Wet	5	2	0	9.95945	2.282172447	7.677277553
6	Wet	5	10	75	7.96195	2.215975223	5.745974777
6	Wet	5	6	150	11.89655	2.508052133	9.388497867
6	Wet	5	10	0	7.7414	2.16846813	5.57293187
6	Wet	5	6	0	8.66445	2.257984346	6.406465654
6	Wet	5	6	75	9.64905	2.323486111	7.325563889
6	Wet	5	2	150	11.0402	2.43119846	8.60900154
6	Wet	5	10	75	7.89655	2.236862786	5.659687214
6	Wet	5	2	75	10.3762	2.306722068	8.069477932

6	Wet	5	2	0	9.9991	2.195259615	7.803840385
6	Wet	5	10	150	7.39335	2.120668824	5.272681176
6	Wet	2	2	0	4.1568	1.675378628	2.481421372
6	Wet	2	6	75	5.4799	1.908290993	3.571609007
6	Wet	2	2	75	5.37545	2.077130841	3.298319159
6	Wet	2	2	150	5.9278	2.133057872	3.794742128
6	Wet	2	6	150	5.10295	1.904975248	3.197974752
6	Wet	2	10	150	4.75875	1.908616876	2.850133124
6	Wet	2	6	0	4.18915	1.82180787	2.36734213
6	Wet	2	10	75	4.6032	1.987100649	2.616099351
6	Wet	2	10	0	4.4806	1.853651822	2.626948178
6	Wet	2	6	150	5.4874	2.050538533	3.436861467
6	Wet	2	2	75	5.4264	2.11177114	3.31462886
6	Wet	2	10	150	4.9531	2.016920443	2.936179557
6	Wet	2	6	75	3.9696	1.795467433	2.174132567
6	Wet	2	2	150	5.6905	2.232501224	3.457998776
6	Wet	2	10	0	4.04505	1.854292576	2.190757424
6	Wet	2	10	75	4.28425	1.863861905	2.420388095
6	Wet	2	6	0	3.8744	1.69449235	2.17990765
6	Wet	2	2	0	5.15995	1.995182247	3.164767753